UNIVERSITÀ
DEGLI STUDI
FIRENZE

DOTTORATO DI RICERCA IN

Energetica e Tecnologie Industriali e Ambientali Innovative

CICLO XXX

COORDINATORE Prof. Maurizio De Lucia

TRANSIENT MODELLING OF WHOLE GAS TURBINE ENGINE: AN AERO-THERMO-MECHANICAL APPROACH

Settore Scientifico Disciplinare ING-IND/08

Dottorando
Dott. (*Sabrina Giuntini*)

Tutore
Prof. (*Bruno Facchini*)

Coordinatore
Prof. (*Maurizio De Lucia*)

Anni 2015/2017

Università degli Studi di Firenze
Scuola di Ingegneria
DIEF - Department of Industrial Engineering of Florence

PhD School: *Energetica e Tecnologie Industriali ed Ambientali Innovative*
Scientific Area: ING-IND/08 - *Macchine a Fluido*

Transient modelling of whole gas turbine engine: an aero-thermo-mechanical approach

PhD Candidate: Ing. Sabrina Giuntini

Tutor: Prof. Ing. Bruno Facchini
Academic Supervisor: Dr. Ing. Antonio Andreini
Industrial Supervisor: Ing. Marco Mantero
PhD School Coordinator: Prof. Ing. Maurizio De Lucia

XXX PhD School Cycle - 2015-2017

A mio padre.

Acknowledgements

Un ringraziamento prima di tutto al Prof. Bruno Facchini per avermi dato la possibilità di avere un posto nel suo gruppo, permettendomi di crescere umanamente e professionalmente, infondendomi fiducia e sostenendomi con preziosi consigli.

Un ringraziamento al prof. Maurizio De Lucia, per le sue indicazioni e per la sua attività come coordinatore del dottorato.

Un immenso grazie all'Ing. Antonio Andreini per esser sempre stato presente e per avermi aiutato con la sua vasta conoscenza, pazienza e disponibilità, insegnandomi molto e fornendomi un metodo. La sua attività di tutoraggio è stata fondamentale nello sviluppo e completamento di questo lavoro, nonché nella mia crescita professionale e personale.

Desidero poi ringraziare tutte le persone che lavorano in Ansaldo Energia come gli Ingg. Sven Olmes, Philippe Lott, Carlos Simon Delgado, Alessio D'Alessandro, e in particolare Marco Pirotta e Emanuele Burberi con cui ho condiviso difficoltà e traguardi di questo progetto di ricerca. A Emanuele in particolare un grazie ancora più sentito per l'amicizia e per il sostegno dimostratomi.

Un grazie particolare al mio tutor industriale, l'Ing. Marco Mantero per aver creduto in me, per avermi fatto sentire davvero parte di qualcosa di importante, per avermi trasmesso entusiasmo e avermi coinvolto in un'attività che profondamente mi ha insegnato il lavoro di squadra.

Desidero inoltre ringraziare l' Ing. Guido Dhondt per il suo tempo e i suoi preziosi consigli con cui mi ha aiutato a indirizzare il mio lavoro.

Un grazie anche a tutti coloro che per un motivo o per l'altro ho

incontrato nel mio percorso e mi hanno trasmesso conoscenza e metodo, come gli Ingg. Luca Andrei, Alessio Bonini e Luca Innocenti, nei primi periodi di attività presso il gruppo, e il Prof. Carlo Carcasci per i consigli e le dritte sul lavoro e non solo che mi hanno accompagnato durante il percorso.

Grazie anche a tutti i ragazzi di Ergon Research (Lorenzo, Riccardo, Cosimo e Mirko) e in particolare a Francesco, con cui ho condiviso le fatiche del progetto.

Un ringraziamento particolare a tutti i miei colleghi ed ex-colleghi con i quali ho condiviso tante ore, tante discussioni stimolanti e tanti momenti divertenti: tutti i ragazzi dei laboratori, Daniele M., Riccardo, Tommaso B., Giulio, Alessio e Lorenzo C., e tutti i numerici, Stefano, Davide, Daniele P., Leopoldo, Lorenzo P., Simone, Dominique, Andrea, Matteo.

Un ringraziamento speciale ai senior del gruppo, a chi c'è ancora e a chi è altrove, Lorenzo M., Tommaso F., Alessandro, che mi hanno insegnato davvero tanto, con un grazie particolare a Lorenzo W., che è stato una preziosa guida, prima e durante il dottorato, aiutandomi sempre con pazienza e professionalità.

Infine grazie a tutti i miei amici, e in particolare ad Andrea e alla mia famiglia che mi hanno sempre supportato e sopportato, nei miei alti e bassi, nei fine settimana inesistenti perché "devo finire una cosa", nelle mie indecisioni e insicurezze che sono sempre riusciti a trasformare in parole e gesti che mi hanno spinto fino a qui.

"Nothing in life is to be feared,
it is only to be understood."
Marie Curie

Abstract

In order to improve gas turbine performances, the operating temperature has been risen significantly over time. The possibility of applying more and more extreme operating conditions is mainly due to an efficient engine cooling. Secondary air system (SAS) design aims at obtaining the maximum efficiency with the minimum demand of mass flow bled from the compressor. Adequate cooling strategies have to be developed in order to guarantee suitable components lifespan and avoid failures. Anyway mass flows and pressure drops inside the secondary air system depend on the fluid-solid heat transfer itself, and in particular on the actual running clearances and gaps determined by the thermal expansion of components according to the current thermo-mechanical loads to which the engine is subjected.

Due to changes in power generation market, the relevance of these issues increased considerably for large power generation gas turbines. In recent years their operating conditions have been deeply modified since more frequent and fast startups and shutdowns are required to meet electric load requirements. In order to manage thermal and mechanical stresses encountered in these repeated transient operations, and in order to monitor a number of parameters which should remain inside the pre-established operating ranges, the capability of predicting the thermal state of the whole engine represents a crucial point in the design process.

Accurate prediction tools have to consider the strongly coupled phenomena occurring among SAS aerodynamic, metal-fluid heat transfer and deformations of the solid, in order to correctly estimate gaps and

develop adequate SAS configurations. According to this, a *Whole Engine Modelling* (WEM) approach reproducing the entire machine in the real operating conditions is necessary in order to verify secondary air system efficiency, actual clearances, temperature peaks, structural integrity and all related aspects.

It is here proposed a numerical procedure, developed in collaboration with Ansaldo Energia, aimed to perform transient thermal modelling calculations of large power generation gas turbines. The aerodynamic solution providing mass flows and pressures, and the thermo-mechanical analysis returning temperatures and material expansion are performed separately. The procedure faces the aero-thermo-mechanical problem with an iterative process with the aim of taking into consideration the mutual interaction of the different solutions, in a robust and modular analysis tool, combining secondary air system, thermal and mechanical analysis. The heat conduction in the solid and the fluid-solid heat transfer is computed by a customized version of the open source FEM solver CalculiX® . The secondary air system is modelled by a customized version of the native CalculiX® one-dimensional fluid network solver. Correlative and lower order methodologies for the fluid domain solution allows to speed up the design and analysis phase, while the presence of the iterative process allows to take into account the complex aero-thermo-mechanical interactions actually characterizing a real engine.

A detailed description of the procedure will be reported with comprehensive discussions about the main fundamental modelling features introduced to cover all the aspects of interest in the simulation of a real machine. In order to assess the physical coherence of these features the procedure has been applied to two different test cases representative of typical real engine configurations, tested in a thermal transient cycle. The first one represents a simplified gas turbine arrangement tested with the aim of a first assessment from the point of view of the thermal loads evaluation. The second one is a portion of a real engine representative geometry, tested for the assessment of the interaction between SAS properties and the geometry deformations.

Contents

Nomenclature

Acronyms		
BCs	Boundary conditions	
$CCPP$	Combined Cycle Power Plant	
CFD	Computational Fluid Dynamics	
CHT	Conjugate Heat Transfer	
FEM	Finite Element Method	
GUI	Graphical User Interface	
HPT	High Pressure Turbine	
IPT	Intermediate Pressure Turbine	
MTO	Maximum take off	
OEM	Original Equipment Manufacturer	
WEM	Whole Engine Modelling	
Greeks		
γ	Heat capacity ratio	$[-]$
ϵ	Emissivity	$[-]$
ϵ	Elastic strain tensor	$[-]$
Θ	Absolute body temperature	$[K]$
ξ	Pressure Loss Coefficient	$[-]$
ρ	Density	$[kg\ m^{-3}]$
σ	Internal stress tensor	$[kg\ m^{-3}]$
τ	Time scale	$[s]$
θ	Absolute temperature	$[K]$
ω	Rotational Speed	$[rad\ s^{-1}]$

Letters

A	Area	$[m^2]$
a	Thermal diffusivity	$[m^2\ s^{-1}]$
C	Absolute velocity magnitude	$[m\ s^{-1}]$
C_t	Tangential velocity component	$[m\ s^{-1}]$
$c_f r$	Friction factor	$[-]$
c_p	Specific heat at constant pressure	$[J\ kg^{-1}\ K^{-1}]$
d	Displacements vector	$[m]$
F	Generic force	$[N]$
f	Body force per unit of mass	$[N\ kg]$
f	Generic function	$[-]$
HTC	Heat transfer coefficient	$[W\ m^{-2}\ K^{-1}]$
h	Total enthalpy	$[J]$
h^θ	Body flux per unit of mass	$[J\ kg]$
k	Thermal conductivity	$[W\ m^{-1}\ K^{-1}]$
L	Total length	$[m]$
L	Characteristic length scale	$[m]$
M	Momentum	$[J]$
$\dot{m}$	Mass flow rate	$[kg\ s^{-1}]$
N	Number of entities	$[-]$
$P\ p$	Pressure	$[Pa]$
$\dot{Q}$	Thermal power	$[W]$
q	Heat flux	$[W\ m^{-2}]$
R	Gas constant	$[J\ kg^{-1}\ K^{-1}]$
R	Radius	$[m]$
Re	Reynolds number	$[-]$
SR	Swirl ratio	$[-]$
T	Temperature	$[K]$
t	Time	$[s]$
t	Thickness	$[m]$
$Thick$	Thickness	$[m]$
U	Circumferential velocity	$[m\ s^{-1}]$
$V,\ v$	Velocity magnitude	$[m\ s^{-1}]$

W	Relative velocity magnitude	$[m\ s^{-1}]$
Subscripts		
abs	Absolute	
$assigned$	Assigned	
axi	Axisymmetric	
$blade$	Blade	
c	Compressor	
$conv$	Convective	
$elem$	Element	
f	Fluid	
$face$	Face	
$fluid$	Fluid	
fr	Friction	
$hole$	Hole	
$i,\ j\ k$	Generic component or coefficient	
in	Inlet	
m	Average	
max	Maximum	
min	Minimum	
nd	Non dimensional	
out	Outlet	
$plane$	Plane	
R	Rotoric	
$real$	Real	
rel	Relative	
rot	Rotating	
s	Solid domain	
s	Static	
S	Statoric	
$solid$	Solid	
t	Tangential	
w	Wall	
$wind$	Windage	

0	Total quantity
1	Generic component
2	Generic component

Introduction

The quest for fuel efficient engines, besides the requirement of low emissions, has become during years the main target in the development of turbogas engines. The increase in gas turbine efficiency and specific power depends on the possibility of raising the inlet temperature when component efficiencies and pressure ratio are fixed [1], and today temperatures reach values well above those allowed by materials thermal resistance. Despite the constant development concerning materials, the possibility of raising the engine operating temperature is mostly due to the cooling system using air bled from the compressor. Effective cooling strategies are required to ensure adequate life to components but it is also important to remind that cooling has a cost on the performance of the thermodynamic cycle. A progressive reduction of the global efficiency inevitably occurs increasing the amount of coolant. So the aim is to obtain cooling systems able to ensure the required component lifespan and respect the safety standards, for a minimal amount of coolant flow. The goal of the designer is to maximize the effectiveness of the cooling system while limiting the penalty on performances.

The different cooling devices are fed by means of the internal air system, called secondary air system (SAS). The tasks of the secondary air system are manifold, mainly regarding the supply of coolant to the various critical components, the sealing in bearing chambers and flow paths, and the control of axial loads.

Apart from the typology of engine, if aero-engine or heavy duty gas turbine (Fig.1), some common features are present in both the arrange-

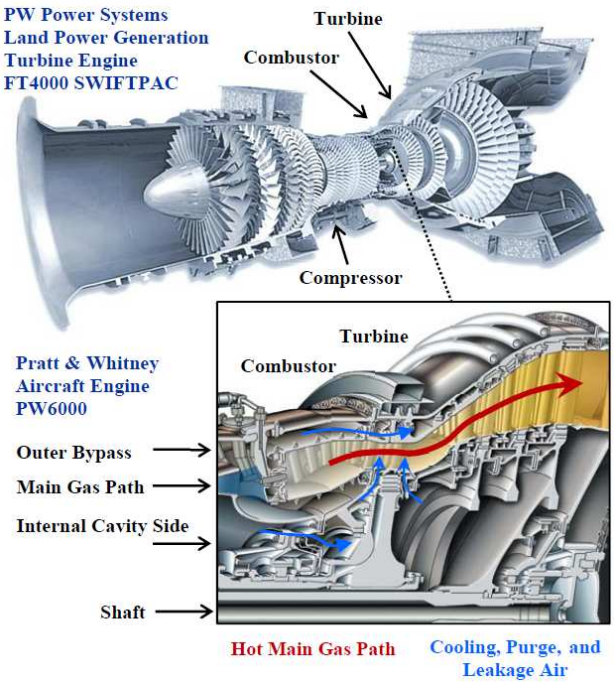

Figure 1: Example of gas turbine engines from PW Power Systems and Pratt & Whitney highlighting the turbine hot gas main flow and the secondary air system [2, 3].

ments, such as ducts, pipes, holes, seals, discs, cavities between coaxial rotating and stationary discs, or rotor-stator cavities. For each feature, various geometries and typologies have been devised, as in the case of seals used to control the branches flow rate, which differentiate in labyrinth, brush and rim seals.

The fluid-dynamics and thermal behavior of flows inside these cavities and passages is of fundamental importance to establish the performance of the secondary air system and definitively for the lifespan and integrity of the engine. In particular, an error in the assessment of cooling mass

(a) Burn-through of turbine rotor blades.

(b) Melting of a nozzle vane.

Figure 2: Characteristic gas turbine forms of failures caused by long-lasting excessive temperature of exhaust gases [5].

flow can lead to a wrong prediction of the metal temperature of turbine hot components. This is a critical safety aspect of engine design [4]. Overheating causes, at best, reduction of the lifespan of components but, at worst, can result in catastrophic failure through disk bursting and blades damage (Fig.2).

In [6], the effects of SAS pressure loss and temperature rise on blade temperature and life are investigated. As obvious the reduction of the blade cooling inlet pressure causes coolant mass flow to decrease. As a result, the amount of heat transferred to coolant decreases and blade

average temperature increases. Based on authors results, 10% SAS pressure loss can result in 14 K increase in maximum blade temperature [6]. Moreover, 5% increase in inlet coolant temperature results in 10 K rise in maximum blade temperature. Secondary air pressure reduction causes the blade temperature to increase and then blade life severely decreases. In the similar manner, blade lifetime is seriously depended upon the imposed temperature and stress level and any changes in these parameters can results in life limit. Again, in [6] authors show that the 5% augmentation of SAS temperature means 10 K increment in blade maximum temperature, causing blade creep life to decrease 40%.

Besides the necessity to properly estimate the cooling mass flow to hot component in order to guarantee their proper lifespan, another relevant topic is the evaluation of the clearances and gaps, and the function played by the secondary air sealing to prevent hot gas ingestion. Indeed, rotors are directly heated by conduction from turbine blades exposed to the hot mainstream therefore there is the need of cooling disc rims but also of sealing cavities against ingestion. This means to use a certain quantity of purge flow to maintain the cavity temperature under proper levels, considering also that the swirling motion of the air within the cavity, caused by the rotation, produces dissipation of kinetic energy, and this can lead to a rapid increase in cavity air temperature if proper purge flow is not present. Needed purge and cooling flows are bled off from compressor from a suitable stage according to the pressure levels of the zone which is necessary to feed, then it is directed toward a turbine wheel space (Fig.3) and then discharged through the rim-seal gap between rotor and stator. When the rotor blades are cooled the usual requirement is to fully seal the gap against ingestion, but in the cooler downstream stages, usually purging the space and reducing the cavity temperature to an adequate level can be enough [8].

Concerning the turbine stator well, phenomena inside this zone are very complex. Generally the coolant flow needed to seal both cavities enters in the upstream cavity and then pass to the downstream one through the labyrinth seal (Fig.4). The hot gas themselves enter the

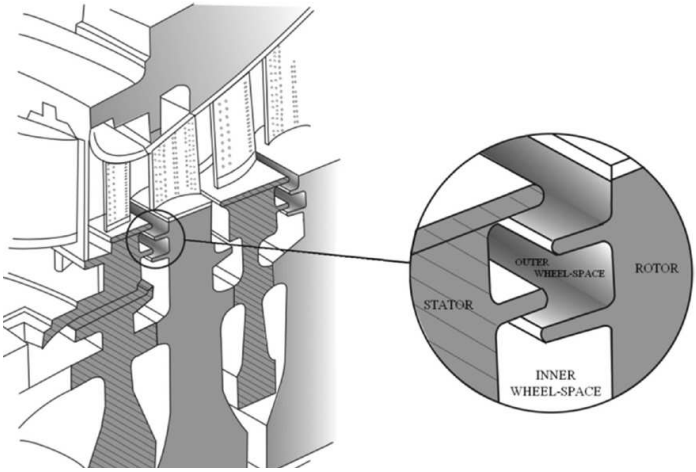

Figure 3: Rotor–stator turbine stage and double seal inset [7].

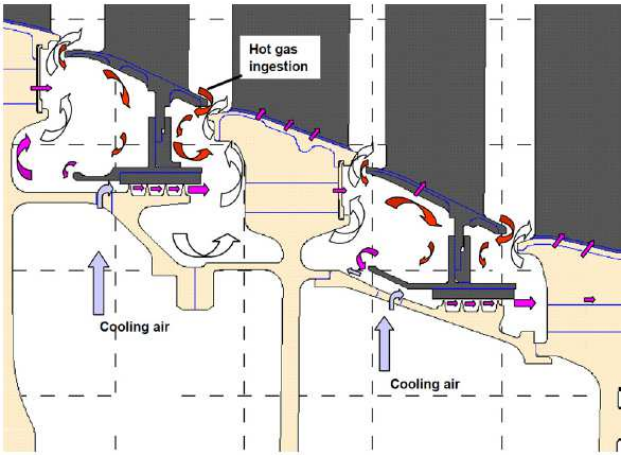

Figure 4: Typical turbine stator well [9].

cavities and the entity of ingestion is function of the swirling motion imposed by the rotating surfaces, and of the leakage flow of the seal. If seal leakage is higher than the designed one, the hot gases enter heavily the upstream cavity; on the other hand, the ingestion increases in the downstream cavity if the leakage is lower then that designed, resulting in a downstream cavity less fed by cooling air. In its turn the seal leakage depends on the gap between seal components. Studies in [10] estimate that an increased seal clearance (from 0.4 mm to 0.9 mm) produces an increase in hot gas ingestion up to more than 100 % for a constant cooling mass flow. This gives further evidence of the importance of correctly evaluate the actual seal gap in working condition due to thermal expansion and centrifugal forces too.

As temperatures in the engine raise, the relevance of these issues and in general the importance of heat transfer between structure and secondary airflow is increasing. As a matter of fact, secondary air properties heavily influence material temperatures and the consequent thermal expansion of engine parts. Redefining tip clearances and seal gaps, this modifies considerably pressure losses and mass flow rates in the air system, impacting flow and material temperatures [11].

The weight of these matters in the engine design has been always particularly marked in the aeronautical field because of the intrinsic nature of the operation of the aero engines (Fig. 5). During transient operation the quantity of cooling air to be supplied depends upon the operating point in the flight cycle. For example, at the takeoff the critical components of the engine such as high pressure turbine (HPT) and intermediate pressure turbine (IPT) blades are subjected to high temperatures and gradients which may result in thermal fatigue and at worst compromise the blade integrity. Therefore a large amount of cooling air is provided. On the contrary, in the cruise phase, the engine operating conditions reach a quasi-steady state. In this state the components are at relatively low temperatures and gradients are also reduced [13]. Such variable operations lead to very different conditions in thermal expansion of component, and maintain the geometries and gaps in fixed ranges is mandatory. As an

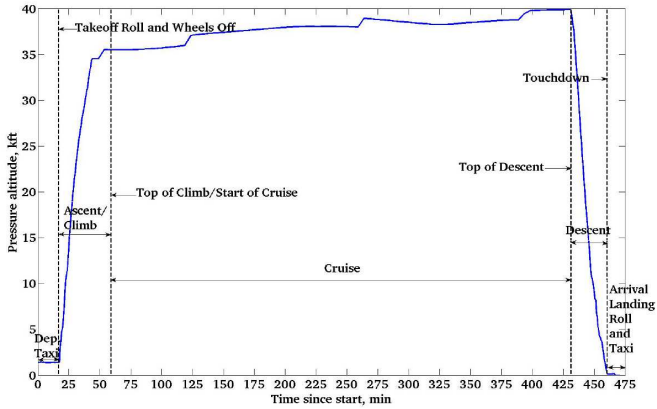

(a) Airbus A330-223 a typical profile of the pressure altitude versus time and the different flight phases.

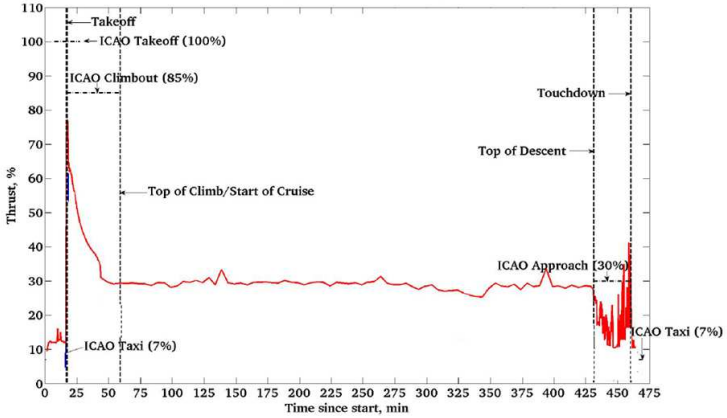

(b) Airbus A330-223 Flight Data Recorder percentage thrust versus time.

Figure 5: Flight phases and aero engine transient operation [12].

example, blade tip sealing has always been one of the major concerns in aero engine design due to the direct correlation between effective sealing and turbomachinery efficiency [14],[15]. Loss of tip sealing can occur

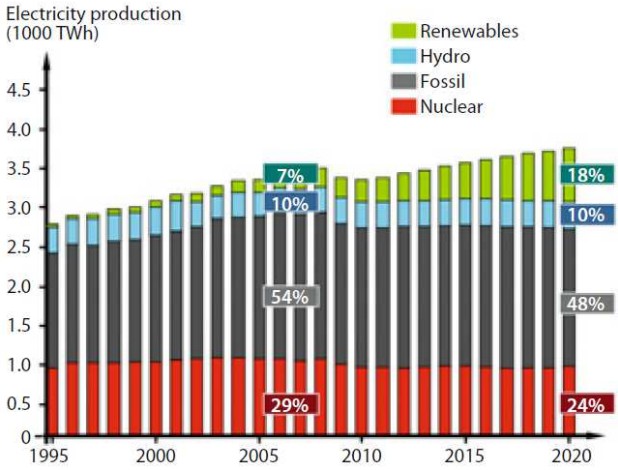

Figure 6: The rise of renewables [18].

when component sizes change due to thermal and mechanical loads during transient operation. Maintaining a tip clearance that is both small enough to effectively seal and also large enough to reduce the possibility of the rotating blade rubbing the static structure is a crucial design objective [16]. Because gaps changes during engine operation, active clearance control is a current area of research [17] and must be supported by proper aero-thermo-structural calculations.

The novelty today is that the importance of these topics increases also in heavy duty gas turbines field, considering that engines for electric power generation are nowadays subjected to very frequent transient operations, during startup, shutdown but also load adjustment, consequence of the introduction of renewable energy in the electric market.

Indeed, according to the 2016 World Energy Outlook [20], renewable energy and natural gas are the big winners in the race to meet the demand for power over the next 25 years. The rapid growth in renewables (Fig. 6) in particular wind and solar power, is changing the electricity supply landscape and how gas turbines are being called on to generate to the

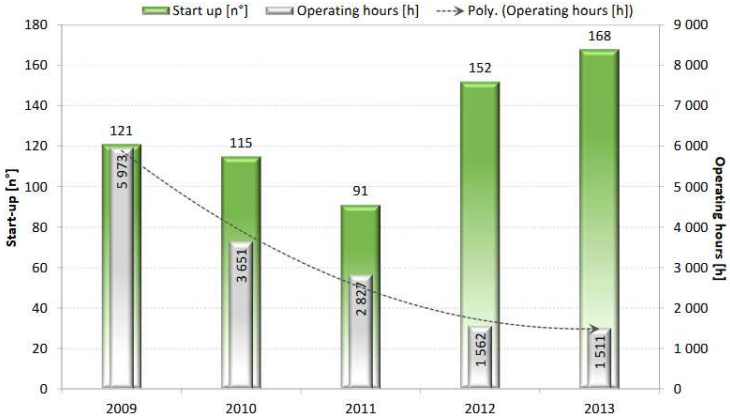

Figure 7: Flexibility operation data 2009-2013 from the Torrevaldaliga combined cycle power plant (Tirreno Power) [19].

grid. The modern power grid needs intelligent resources able to ramp up and down swiftly, efficiently, and repeatedly [21].

Due to these changes, gas turbine operators are taking on an additional new role: switching from providing baseload to providing power at times of peak demand (Fig. 7). Introduction of renewables drives the need for more flexibility, and as a consequence plants have to change load faster with daily, and even double daily, startups [19]. Gas turbine plants that can be dispatched within minutes are important assets for balancing electric system loads and maintaining grid reliability. Simple cycle gas turbines have traditionally served as peaking units because they can be started within minutes and ramped up and down quickly. They are less thermodynamically efficient than combined cycle turbine plants but can be profitably deployed during peak times when the price paid for electricity is higher [21]. Reserve turbines can be kept spinning (either without producing any energy or operating below optimum output) and brought rapidly online if required.

This has lead to important changes in the engine design and control. Gas turbines designed in the 80s were optimized for efficiency, overall

availability, and reliability; not for how fast they start up or shut down. Today, instead, a 750 MW system can reduce its power output to about 100 MW in about 6 and a half minutes and come back up again just as fast; previous facilities could only dial back to about 200 MW without fully shutting down and took several minutes longer to come back up [22]. In Fig. 8 the power output for a 430 MW combined cycle power plant is reported: an improved fast startup sequence is applied and the transient operation takes less than thirty minutes.

Even if great improvements have been achieved in high cycling and peaking, fast startups, and load ramps control, plant flexibility is critical for on-call gas turbine generation since transient operation should be very fast, in order to achieve rapidly the required load, circumstance that stresses strongly the engine [23]. Fast startups and shutdowns are very problematic from the point of view of design and control, because of the dramatic changes in temperature that components have to face, which are responsible for important deformations of geometries and thermo-mechanical stress. The new turbines are incorporating better materials for thermal handling, including nickel-based superalloys and single-crystal materials along the hot gas path. They also use better cooling systems, rely on physics-based models for combustion control, and many efforts are aimed at integrating a better understanding of the clearances involved when different parts expand and contract at different rates. This point is a very challenging one, since cooling system efficiency and structural integrity of components depend on it.

To this end, a reliable and fast method of prediction of the engine behavior in transient conditions, in terms of metal temperature and displacements distributions is necessary to monitor the overall thermo-mechanical behavior of the engine. The need to control the expansion rates of parts and ensure good seals is a crucial aspect to be investigated, and improved simulation tools are required for the prediction of the air system behaviour over a variety of operating conditions, such as those encountered during a transient cycle.

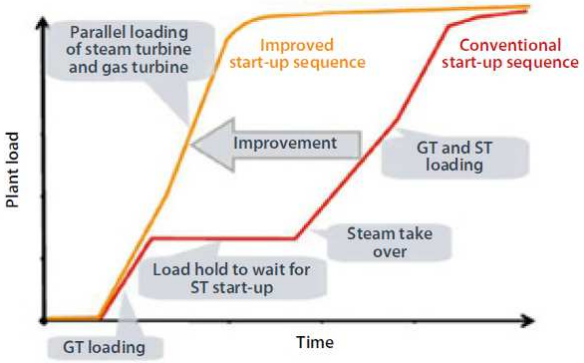

(a) "Start on the fly", an improved star-up sequence.

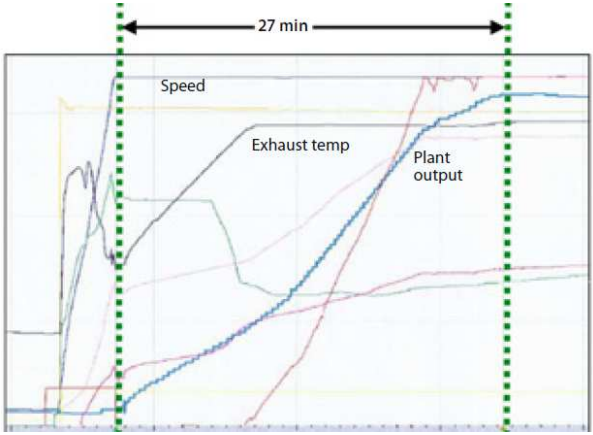

(b) The 430 MW Pont sur Sambre combined cycle plant.

Figure 8: Combined cycle power plant transient operation, [18].

Research objectives

This work presents a Transient Whole Engine Modelling procedure, developed in collaboration with *Ansaldo Energia*, aimed at predicting

metal temperatures and displacements on the entire cross section of a gas turbine engine, based on a modular and correlative approach. This procedure is thought for large heavy gas turbine for power generation for the evaluation of the aero-thermo-mechanical interaction in transient operations. A 1D fluid network of engine secondary air system is coupled with a 2D solid thermo-mechanical finite element model of engine components. The procedure is based on a customized version of the free FEM suite CalculiX® . The unsteady heat transfer calculation over the solid domain is coupled to a sequence of structural static and steady flow problems using a quasi-steady state approach. Strong coupling is accounted iterating on the solution of the whole transient operation, proceeding on the successive solution of the fluid and the thermo-mechanical problems.

Objective of this work is to present the new procedure and to assess its physical coherence, showing the modelling schemes introduced and the methodology capabilities, through its application to representative test cases. The aim is to highlight its modularity and flexibility in the design and test of different engine configurations, and its potentialities in catching the deep coupling of aero-thermo-mechanical phenomena.

Thesis outline

The present thesis is structured as follows.

Chapter 1: Whole Engine Modelling reports an overview of the aero-thermo-mechanical coupling methods and of the Whole Engine Modelling approach motivations and background, giving a literature review.

Chapter 2: Proposed methodology focuses on the description of the presented iterative coupled transient thermal WEM procedure for the prediction of gas turbine temperature distributions, thermal expansion of components and the interaction between the latter and secondary air system. The different sub-blocks of the procedure (SAS aerodynamic solution and thermo-mechanical analysis), are presented with the explanation of the coupling strategy adopted.

Chapter 3: Code customizations reports a description of the customizations introduced in the code and some examples of first assessments performed to prove the correctness of the implementations. A wide discussion about the main fundamental modelling features introduced in the methodology is provided, both for the one-dimensional fluid network solver and the FEM code.

Chapter 4: Assessment of the proposed methodology focuses on two test cases used to assess the behaviour and the physical coherence of the procedure during a transient cycle. First, a comprehensive assessment of the thermal loads evaluation capability of the procedure is presented, carried out on a simplified test case geometry, with a comparison of results with a reference FEM code. In the second part of the Chapter, the assessment of the aero-thermo-mechanical capabilities of the new methodology is performed on a geometry consisting in a portion of a real engine representative geometry, for the evaluation of the interaction between SAS properties and the geometry deformations, comparing results of the new iterative coupled methodology with the prediction of a conventional uncoupled approach.

Chapter 1

Whole engine modelling

The idea behind the concept of the *Whole Engine Modelling* (WEM) is the need to think about how the whole engine has to be designed structurally and how the individual elements will interact. Whole engine modelling looks at the behaviour of the engine during the operation with mathematical and physical models used to define how engine components must work together to achieve proper operation requirements. These data are used in detailed component design work. A WEM approach simulates the behaviour of the machine in the different phases of the operation cycle and drives decisions about how the optimum design of individual components and sub systems can be reached. But whole engine modelling can also be used to help solve problems once an engine has entered in service. The model can simulate the engine's situation at the time the problem occurred. This can help service engineers understand what happened and recommend improvements [24].

WEM methodologies can include in the simulation different phenomena and consider different levels of complexity. In the present thesis it will be referred with whole engine modelling to a procedure involving the cross section of the entire machine in which the interactions among secondary air system properties (temperature, mass flow and pressure distributions), fluid-metal heat transfer, and metal deformations are taken into account.

Thermal and mechanical stresses derive from the action of the main stream loads, rotational speed and characteristics of the secondary air system, which determine the temperature distribution on the solid. As a consequence of the thermal expansion and centrifugal strain, in their turn thermal and mechanical loads produce geometry modifications, in terms of clearances at blade tip, rotor stator rim and internal flow passages. Variation on SAS geometries affect mass flow rates and pressure losses modifying in their turn the thermal load and also affecting heat transfer coefficients too on the secondary air side.

Accurate prediction tools have to consider these strongly coupled phenomena in order to correctly estimate gaps and develop adequate SAS configurations. Controlling tip clearances involves engine efficiency and component failures. Distances between blade tip and casing determine the magnitude of clearances losses and the possibility of accidental rubbing between static and rotating components [25]. On the other hand achieving effective SAS design means to fulfil all the functionalities required to the secondary air system (cooling, sealing, purging, etc) with the minimum air consumption, in order to limit the penalty on the cycle performances. Air consumption is directly affected by mass flow splits and pressure looses, and ultimately, by sealing gaps and cross section areas of flow passages. Managing all these goals can be possible only developing a procedure that involves all the components of the engine and allows its comprehensive simulation. According to this, a WEM approach reproducing the real machine operating conditions is necessary in order to verify secondary air system efficiency, actual clearances, temperature peaks, structural integrity and all related concerns [26].

As mentioned in [11, 28], industrial practices for aero engine mostly carry out the performance of fluid network solution, thermal analysis and solid deformation assessment in a separated way. First the aerodynamic calculation is executed determining the fluid properties in the secondary air system. Then, with other data and assessments, comprehensive of the main flow behavior and the other features, they are provided as boundary conditions to the thermal analysis. From the thermal analysis

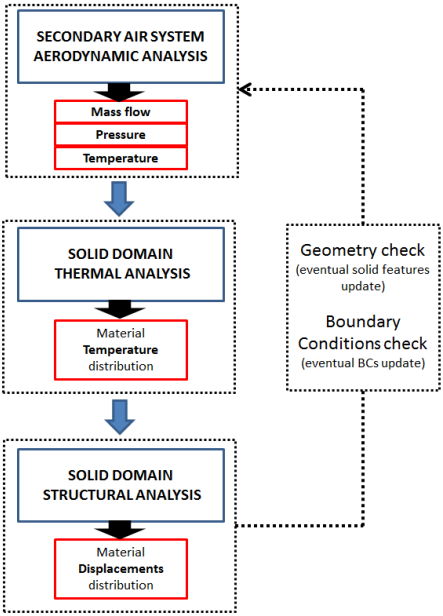

Figure 1.1: Decoupled sequential WEM approach [27].

the conditions for the mechanical solver are provided and displacements evaluated. This procedure is iterated if necessary by the user until a converged solution is reached. The acceptability criteria depend on the different best practices. Therefore the approach is decoupled and carried out in a sequential way, according to the scheme reported in Fig. 1.1. It does not take into account the coupling nature of the phenomena and proves to be a process potentially slower since outputs from one solver must be passed as boundary conditions to the other, with the necessity of managing information passage among at least three tools. In literature such kind of investigations are documented, to the author knowledge, mainly for aero-engine application since in the case of aircraft, the intrinsic nature of the operation cycle require the knowledge of the different engine conditions during the various cycle phases.

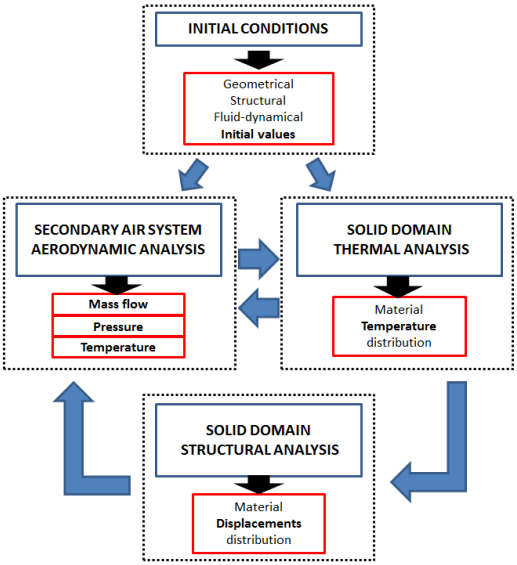

Figure 1.2: Coupled Fully Integrated WEM approach [27].

On the contrary, for heavy duty applications the evaluation of the transient operation behavior of the engine is currently performed considering calculations of the secondary air system at certain key time points (such as at the base load condition), and with a proper scaling in time of the mass flow and the other boundary conditions as functions of load and speed. No iterations on the SAS solution are generally performed, neither running gaps and clearances are considered. Design completion is often based on a single, finalizing, iteration disregarding the coupling aero-thermo-structural effects.

However due to the modified operating conditions to which have been recently subjected the new generation power plants, a new interest in the transient cylce of engine has been born. New coupling methodologies (Fig. 1.2) with an internal coupled solution and a fully automatic data

exchange among different analysis blocks totally hidden to the user, became attractive not only for the aero engine application, but also for the large power generation gas turbine. Such kind of approach would allow to:

- appreciate the strong interaction among the different problems (aerodynamic, thermal, structural);
- overcome the time consuming processes of writing output from one code to the other;
- limit the user data managing and the introduction of additional human errors.

Coupling can be introduced at various levels:

- thermal: calculation of solid-fluid heat transfer;
- thermo-mechanical: assessment of heat transfer and thermal expansion;
- aero-thermo-mechanical: evaluation of the effects of thermo-structural modification of the domain on the SAS properties and vice-versa;

and in different fashions:

- according to the manner of treating the different solid and fluid domains and solving the equations set:
  - fully coupled;
  - segregated;
- in the case of segregated methodologies, according to the way the boundary conditions are set among different domains and tools:
  - monolithic;
  - partitioned.

Below reader can find a literature review about the different approaches through which, over the years, the different levels of coupling have been faced.

1.1 Coupling approach overview

In literature, despite sub-classifications sometimes not univocal, primarily two type of methodologies are presented for the solution of the solid-fluid heat transfer problem [29]:

- fully conjugate (or fully coupled) approaches in which a single numerical simulation is carried out comprehending the solid and fluid fields in a unique domain through the application of one solver for Navier Stokes and Fourier equations;
- segregated approaches through which the different convective and conductive problems are solved separately by specific tools tailored for the fluid and solid domains, producing each one the boundary conditions to be applied to the other in an iterative way.

When using a fully conjugate approach, a direct coupling is implemented, in which different fields are solved simultaneously in one large set of equations applied to the entire domain, fluid and solid together. A single numerical simulation is run to solve the overall heat transfer problem at once. Such kind of approach has the advantage to guarantee the implicit temperature and heat flux continuity at the fluid-solid interfaces, but it could encounter a difficult convergence due to large differences in characteristic time scales of involved phenomena. This is even more evident in transient simulation since small time steps have to be applied to solve the unsteadiness in fluid domain [30]. A number of works show the application of the conjugate analysis to engine components, such as blades and vanes [31, 32], and rotor-stator systems [33]. In [33] a fully coupled conjugate heat transfer (CHT) calculation has been carried out in order to assess the three-dimensional effects that can occur in actual engine disk system because of several non-axisymmetric components which inevitably affect the local heat transfer phenomena, and which are disregarded in the standard axisymmetric calculation usually performed. As an example of a fully conjugate calculation domain, [33] grid is reported in Fig. 1.3 : solid and fluid domains are kept together and solved at the same time in one single model.

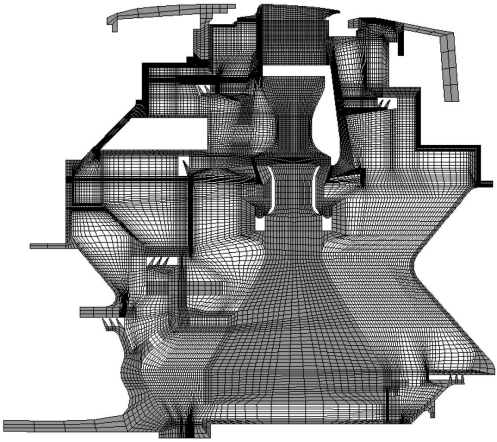

Figure 1.3: Example of a monolithic fluid-solid domain grid for fully conjugate analysis (a turbine rotor-stator system [33].)

On the other side, when using a segregated method, fluid and solid domains are solved separately: each set of field equations is solved independently, and provides boundary conditions for the other [34]. The equations are solved iteratively until the set convergence criteria are satisfied. In this kind of methodologies specific tools are used to solve each single problem. The application of separately codes tailored to the solid and fluid domains, allows to exploit the advantages of applying, through different codes, specific numerical approaches and models. This traduces in a reduction of the computational cost and makes possible, in reasonable time, simulations such as calculations of a transient operation, otherwise not feasible with a fully conjugate CFD solution.

The coupling of the different problems and domains in segregated approaches can be carried out in a monolithic or partitioned way [35] according to the method adopted for the integration of the solution of one domain in the other. In a monolithic approach one problem is actually coded as boundary condition for the other and a coupled system is solved

simultaneously. Instead in a partitioned approach, the problem is split into the sub-problems, each of which is solved by a black box solver. One model feeds the others and vice versa with appropriate information by means of averaged quantities. The solution of the original multi-domain problem is regarded as a suitable fixed point problem, based on the successive solution of the sub-problems [35].

Concrete example of coupling scheme is the FEM-CFD combined application. The idea behind is to use finite element analyses to predict the metal temperature and stress distributions with the thermal boundary conditions provided by the CFD calculations. Through an iterative process the metal temperature distribution from the FEM is imposed as temperature boundary condition to the CFD model and the heat flux distribution from CFD is imposed as heat flux boundary condition for the FEM model. Results of each analysis become the boundary conditions for the other.

FEM-CFD coupling has been adopted for various analyses of components subjected to thermal transient cycle, such as pre-swirl systems [36, 37] and cavities [38, 39]. In [36] thermal analysis of a turbine disc through a transient test cycle is demonstrated using CFD modelling for the cooling flow and 3D FEM for the disc (Fig. 1.4). Coupling is achieved through an iterative loop with smooth exchange of information between the FEM and CFD simulations at each time step. Authors report that the coupled simulation took few weeks using a PC cluster with multiple parallel CFD executions.

To speed up the CFD simulation in FEM-CFD coupling generally the flow is assumed steady. The assumption states that air flow adjusts instantly with respect to a variation in its boundary conditions corresponding to metal temperature changes. This is an acceptable approximation, as time scales involved in convective phenomena are relatively short compared to time scales typical of heat conduction [40]. Avoiding costly unsteady CFD simulation for the fluid domain, increased time steps for unsteady FEM simulation of heat conduction in solid regions can be applied.

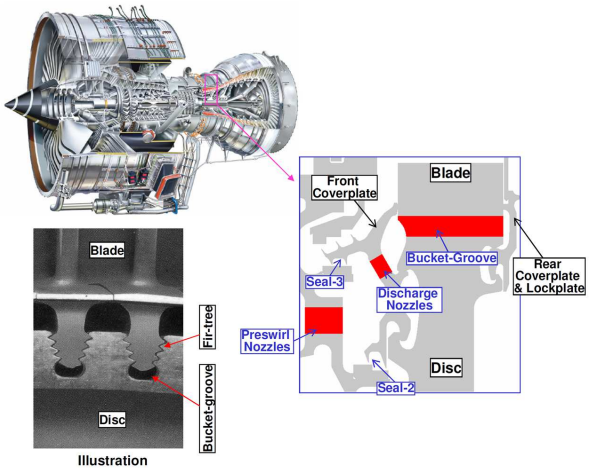

(a) The 3D FEM model and Illustration of geometry.

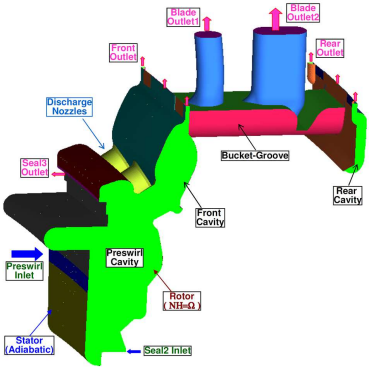

(b) The 3D CFD Model.

Figure 1.4: Example of CFD-FEM coupling application (a turbine disc system [36].)

In addition to this generic assumption, also other solutions have been developed during the years to contain computational cost. In [30] with the so called "frozen flow", in the transient calculation only the energy equation is solved, while the flow conditions are fixed in the CFD

simulation during the solution at the interface for certain time intervals. In [41] a FEM-CFD procedure inspired by the Anderson mixing method for the heat transfer coefficient evaluation is used, reducing the CFD solver invocations and improving the convergence rate. To overcome convergence difficulties due to the FEM-CFD coupling, in [42] measures were taken to control numerical instabilities. Improvements were achieved by limiting the heat transfer coefficient used, under relaxation and averaging the last few iterations for heat flux in the CFD calculations. In [43] an effort of making FEM-CFD approach more compatible with turbine design timeframes is attempted with the application of GPUs (Graphics Processing Units) for the calculation, and with a new method for the heat transfer coefficient assessment, based on a dynamic recalculation of the HTC value from current and pre-stored CFD analyses.

Despite some improvements, typically, calculations like those mentioned are applied considering parts of the SAS and not the whole system since CHT problems require considerable computational effort to resolve all nonlinearities on the fluid-solid interface. The computational cost increases as various CFD domains are involved in the analysis, with calculation time generally amounting from days till weeks for gas turbine applications [40], [42]. For these reasons the coupling of CFD tools with mechanical-structural solvers seems to be nowadays a solution of difficult application for domains of considerable dimensions and complexity such as the model of a whole engine, especially in transient conditions. This is primarily due to high computational costs of 2D and 3D CFD simulation as a consequence of the time required for the setting and calculations. Also the uncertainties that characterize the boundary conditions in a phase of design nullifies the use of such detailed and expensive tools. Consequently CFD tools find a collocation in a WEM process only as support to 1D simulation (which generally substitute the CFD analyses of the secondary air system) for the investigation of those phenomena that mono dimensional models cannot catch.

Therefore in conventional industrial practice, the CHT problem is solved using FEM analysis to evaluate metal temperatures and thermo-

mechanical stresses, coupled with relatively inexpensive one-dimensional (1D) flow network solvers. Such the coupling is quite common to predict gas turbine blade heat transfer involving coupling of 1D aero-thermal models of internal cooling passages with full 3D finite element models of the blade structure and 3D computational fluid dynamics models of surrounding flow [29, 44, 45]. But this coupling also brings up new opportunities for secondary air systems applications. Indeed, one-dimensional modelling and correlative approaches represent, in the industrial usual practice, an acceptable compromise between accuracy and computational cost for the characterization of the secondary air system in a WEM approach, both in the phase of design and analysis. The convective heat transfer coefficients are provided using literature or proprietary correlations which can be tuned on experiments and engine test data, or can be recovered like other boundary conditions from previous engine modelling, standalone CFD analyses and measurements [46]. Different levels of detail are acceptable for different aspects of the design and therefore ad hoc tools and procedures are chosen to satisfy with the minimum cost the required accuracy. So, current approaches generally determine main annulus flow conditions once and impose them at the beginning of the calculation. Variations of clearances and effects of SAS behavior during the cycle are not accounted, since their impact on the primary flow is considered of negligible relevance. Therefore no iteration on the conditions of the main flow is performed generally.

Results of the application of such conventional industrial procedures to an engine shutdown are discussed in [47]. Here, a transient thermal analysis (Fig. 1.5a) is performed on the GE frame 5 engine analysing the turning-down phase (Fig. 1.5c) starting from the steady state regime (Fig. 1.5b). The presented methodology shows to be able to adequately capture shutdown thermal behavior within the whole engine components providing results in good agreement with experimental data. Also the importance of the transient thermal results in predicting the stresses and clearances is explained inferring their behaviour from the rotor and stator bulk temperature variation obtained from the transient thermal analysis.

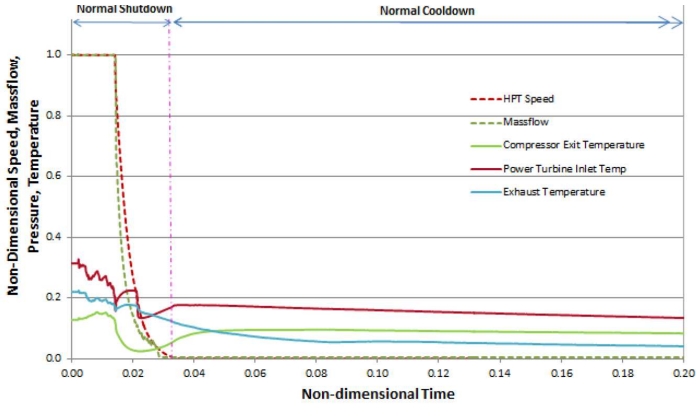

(a) Shut down mission.

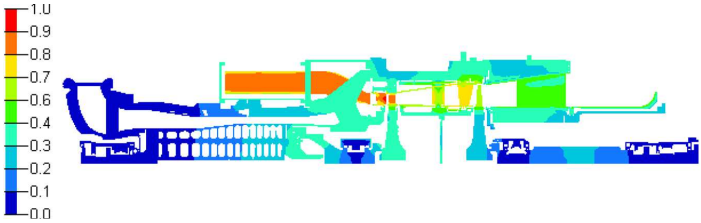

(b) Steady state thermal distribution.

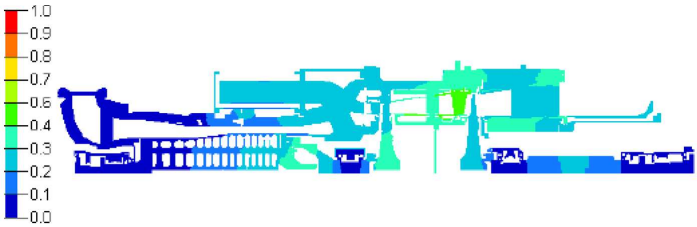

(c) Temperature at end of the shutdown phase.

Figure 1.5: Transient thermal simulation of the GE Frame 5 shutdown [47].

Therefore, displacement are here a result of the components thermal expansion but they are not included in the procedure for an update of the geometries in the thermo-mechanical analysis.

On that note, in addition to the heat transfer assessment, the other crucial point is the inclusion of hot running clearances in the fluid-thermo-mechanical transient calculation. In the aero-thermal FEM-CFD analyses the general approach is to account the effects of seal deformation by switching mass flow inlet and static pressure outlet boundary conditions between discrete levels of corresponding ramp points of the engine cycle [48]. This values can be provided by measurements ([30], [42]), or can be calculated with dedicated simulations ([43]). In [48] a fully integrated FEM-CFD aero-thermo-mechanical transient analysis through a flight cycle on an engine is applied on a sub-part of the same test-case discussed in [41]. Authors provide a comparative analysis which aims to investigate the effect of incorporating the running clearances into the analysis using "sliding boundaries" over which the nodes of the dynamic fluid mesh are free to slide during the deformation. The procedure uses an axisymmetric FEM model for the solid and a finite volume dynamic mesh for the fluid, applying proprietary solvers SC03 and Hydra, respectively. The mesh is able to accommodate the deformation with sliding boundaries over which the nodes of the fluid mesh are free to slide during the deformation. Running radial clearances of the inner and the outer labyrinth seals at MTO reach 40% and 150% of the cold levels, showing a heavy variation (Fig. 1.6). The analysis indicates that the simulation conducted on the dynamic mesh provides a better prediction of the transient thermal behaviour highlighting the benefits of including hot running clearances into a coupling FEM-CFD analysis.

On this regard also a number of commercial and open source codes have been oriented in the last years towards the inclusion of dedicated mechanical solver in order to take into consideration running clearances effects in the simulation. Often, inside the same suite different codes are present, addressed to the solution of multi-physical problems (aero-dynamic, thermal and structural). Efforts aim at taking into account

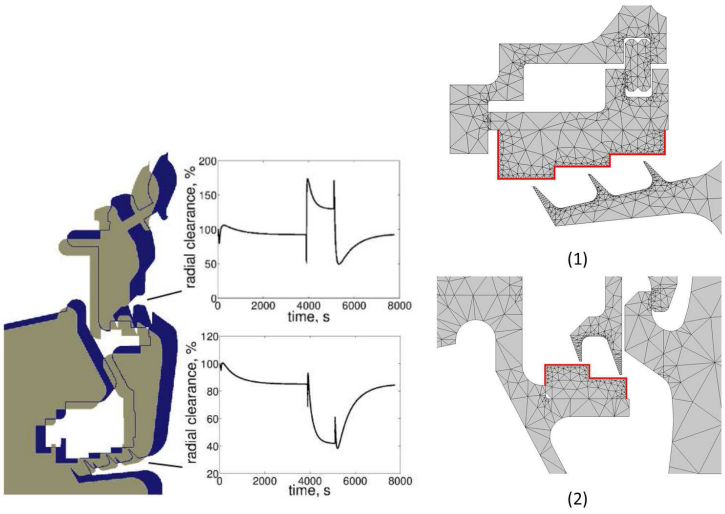

(a) Maximum take-off geometry change relative to the cold state.

(b) Inner (a) and outer (b) seals showing the coupled boundaries with the sliding interface marked in red.

Figure 1.6: Running clearances through a flight cycle on an engine representative geometry [48].

structural deformations with communication procedures among codes seamlessly to the user and requiring a unique model. In [49] a comparison of steady state metal temperature evaluation against measurements have been performed through different coupling approaches between the commercial tools ANSYS Mechanical and CFX. The study demonstrated improvements in the accuracy of thermal predictions because of the inclusion of structural displacements, but refers also to the unfeasibility of a transient approach for a fully converged solution in a reasonable time since it is necessary to set the global time-step to the small fluid time-scale.

Due to the complexity of phenomena and the consequent high computational cost, the assessment of the interactions of multi-physical multidis-

ciplinary nature, such as those treated up to now, has seen an increasing interest towards the coupling of models that are dimensionally heterogeneous, with a particular application of one-dimensional fluid network solvers for the solution of the secondary air system. As already highlighted during this review, such kind of coupling is widely used in industrial practices for the solution of the secondary air system and the fluid-solid heat transfer. This approach becomes even more attractive in the case of adding complexity to the solution as in the case of structural interaction inclusion. In [50] an aero-thermo-mechanical coupled analysis procedure is presented integrating commercial codes MSC P-Thermal and MSC MARC with the Flowmaster 1D flow solver. Coupling of thermal, structural and flow problems is demonstrated on a transient test case. The fluid domain is simulated by using a series of 1D models (Fig. 1.7) coupled with the thermal solver and with the mechanical one. The procedure is based on the capability to translate the data from one model to the others through dedicated interfaces, on an iterative loop of input and output variables coming from the different codes. This multidisciplinary approach is applied to a low pressure turbine geometry.

Also in [51] Flowmaster 1D flow solver is used. In particular authors presented a fully integrated thermal-fluid-deformation analysis methodology based on the Flowmaster solver linked to the ANSYS Mechanical code through the MpCCI coupler.

In [35] authors presented an approach based on the propetary 1D fluid network solver SPAN, providing coolant flow rates and static pressures, coupled to a the proprietary 2D/3D finite element code SC03 for the solid domain on which the thermal boundary conditions coming from the 1D fluid network are coded in a coupled way (Fig. 1.8) . Deformation predicted by the structural solver are imposed on the fluid network model, including therefore coupled effects and interactions between running clearances and flow network properties in the fluid-thermo-mechanical transient calculation.

In the procedure presented in this work the aim is to use an approach able to overcome the need of translation of the model from a solver to the

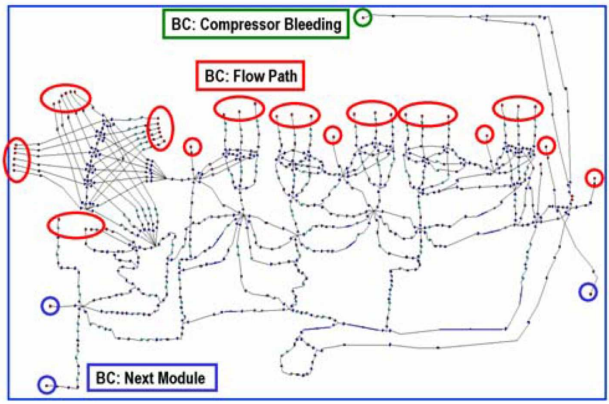

Figure 1.7: Example of low pressure turbine 1D fluid network [50].)

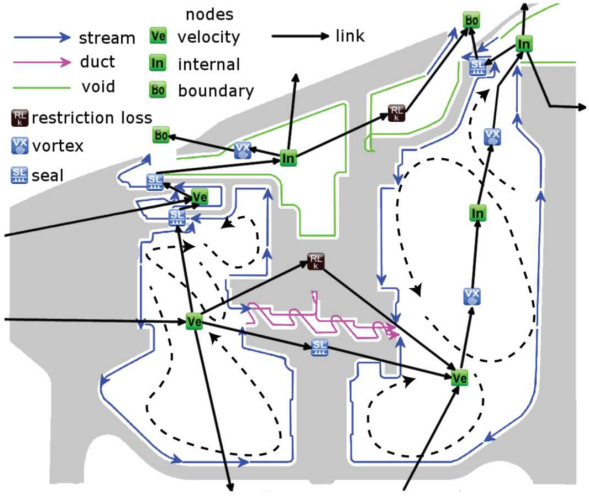

Figure 1.8: Details of 1D fluid network coupled with solid domain [35].

other in order to contain computational time and in which the different fields are linked the one to the each others in a coupled way hidden to the user. A satisfactory answer to these requirements has been found in the open source software CalculiX® . Here coupled aero-thermal and thermo-mechanical calculations can be performed. The reciprocal action in terms of heat transfer between the fluid and the structure can be taken into account in a coupled way, as well as the reciprocal action between temperature and displacements can be taken into consideration solving simultaneously the two fields [52]. Apart the great advantage of a solver thought to be able to perform in a coupled way heat transfer and displacements analysis, the presence of an integrated fluid network solver enabled the possibility of implementing in a more efficient way a system of monitoring and updating of the geometries modifications in order to achieve an integrated iterative aero-thermo-mechanical procedure. In literature other works based on CalculiX® capabilities are present. In [28] a coupled air system-thermomechanical analysis is applied to the model of a low pressure turbine general arrangement and its secondary air system has been presented as a demonstration of the fluid network tool capabilities (also given in [11]). In particular authors show the effects of solid domain gap clearances and displacements due to thermal and structural loads on the accuracy of steady state thermal predictions with satisfactory agreement with proprietary tools and experimental data.

Chapter 2

Proposed WEM procedure

It is here proposed a numerical procedure, developed in collaboration with Ansaldo Energia, for the transient finite element modelling of the whole engine for large power generation gas turbines.

The procedure aims at predicting metal temperature distributions, mass flow split and pressure levels inside the secondary air system during the entire operation of the engine, comprehending therefore regime and transient conditions. Accurate prediction of metal temperature distribution, gaps and clearances in high pressure compressor and turbine air systems, especially during transient operation, is fundamental to maintain adequate levels of overall efficiency and component lifespan.

Today these issues break into the large power generation gas turbine due to their renewed position in the energy generation landscape. The new generation turbines are designed to be able to rapidly increase or decrease power output in order to be easily applied in gas generation facilities combined with renewables or supplying their highly variable capability of feeding the grid. That's why, today, to modern gas turbine is very often demand to work at part loads and to start and shut down under very high time pressure.

These new requirements lead to a number of additional problems to be managed. From the point of view of consumption, additional

fuel is required to ramp up and operate these turbines, even if they are not synched with the grid. This increases emissions and reduces the net efficiency of the power system. OEMs are designing upgraded control technologies that improve emissions compliance in turn-down and minimize efficiency impacts at part load [21].

On the manufacturing and maintenance side, fast transients may introduce large changes in geometry between adjacent rotor and stator components. The changing dynamics in few critical seals and interfaces can affect the operation of the entire machine, compromising efficiency, integrity and components lifespan. These were topics typically concerning aero-engine design, due to the natural frequency with which these machines encounter the transient operation, as well as for more the stringent bounds on components durability and integrity due to obvious safety reasons. Today power generation gas turbine have more in common with the aero engines respect to the 80's heavy duty turbogas engine whose main requirements were efficiency and reliability. As consequence, operators will need now to leverage new turbine control, monitoring technologies, improve emissions compliance in turndown and minimize efficiency impacts at part load, in order to remain competitive long-term. Minimize efficiency detriment passes also through knowing during the design phase the actual resultant flow rates in each part of the circuit thorough the complete engine operation. Is not an easy task, but accurate assessment of them early at the design stage is a key to effective internal air system designs [35].

The new procedure is developed for the specific study of large power generation gas turbines, with the modelling of the whole cross section, and with a special attention at evaluating the thermo-mechanical behavior during transient operation and at catching the presence of coupled effects and interactions of multi-physical nature. The computational methodology shall consist of a coupled analysis of a 1D flow network model of the engine secondary air system and a 2D axisymmetric solid thermo-mechanical finite element model of engine components. Strong coupling is achieved through iteration over the transient cycle, based on the successive solutions

of the fluid and the solid sub-problems.

The procedure is based on the open source Three-Dimensional Structural Finite Element Program CalculiX® for the thermo-mechanical and fluid-dynamic solutions. Being an open source suite with interesting native feature (which will be illustrated more in detail in the second part of the present Chapter) it has been deemed as a good starting point for the new procedure. In general using an open source suite enables the possibility to customize directly the solver modifying it to add the functionalities the user wants.

A number of customizations have been introduced in the original code with the aim of being able to model all the main phenomena involved in the transient simulation of a whole engine. Customizations regarded the inclusion of some features missing in the original code and not allowing to perform some kind of evaluations, and the addition of some proprietary models aimed to get close the methodology to the industrial best practice, as well as the introduction of some improvements in the general solution handling. Modifications were addressed to both the FEM solver and the native one-dimensional fluid network solver embedded in the FEM suite (they will be presented more in details in Chapter 3).

The methodology tries to answer to a number of requirements in terms of reliability, flexibility and time saving in design and off-design analysis phases. The procedure is thought to be able to approach with low order modelling the heat transfer and secondary air system solution (mass flow splits and pressure assessment) without renouncing to an adequate accuracy level. The use of one-dimensional fluid network solver and correlative approach is imposed by the necessity to have a methodology able to provide results in a time comparable with the engine development. On the other hand, simplifications should not lead to limit the overall capabilities of the tool. The procedure must be able to mirror inside the model the engine real geometry and the related boundary conditions, without introducing arbitrary simplifications which could compromise the physics of the problem. The process must be repeatable and applicable at whatever kind of machine arrangement and guarantee the expected

accuracy. Not an easy task considering the dimension of the whole engine, the manifold components and the variety of phenomena involved. Some simplifications must necessarily be introduced and some modelling choices have been taken in order to conjugate in-time performances, generality and reliability of the procedure. Some of them are briefly commented here below and will be more deepened in the next sections. The major advantages of the proposed coupled methodology are here summarized.

- The 2D axisymmetric approach allows to reduce the dimension of the model mesh, aspect of relevance especially thinking about a whole engine model. The reduction of the model to a 2D mesh impose to operate some approximation and adjustments in order to reproduce three-dimensional features in a 2D domain, but allows to reduce computational resources.

- The low-order approach for the solution of the secondary air system, with the usage of a 1D fluid network solver, allows to speed up the design and off-design analysis phases, with respect to the application of more demanding CFD calculations, since the solution of internal cooling system is performed using best practice correlations and one-dimensional models.

- The iterative loop set to catch the aero-thermo-mechanical interactions between SAS properties and geometry deformations allows to appreciate the strong interaction among the different problems (aerodynamic, thermal, structural).

  - The aerodynamic calculations yielding mass flows and pressures, and thermo-mechanical analysis providing temperatures and the material expansion are performed separately. Maintaining separated the aerodynamic solution from the thermo-mechanical analysis allows to maintain two different level of discretization of the fluid network mesh and to satisfy different requirement of coarseness of the mesh in the two different analysis without to heavy the overall process. This type of

coupling allows to decrease computational time and permits a faster analysis without renouncing to capability of catching multi-physical interactions.

- The procedure is based on solvers belonging to the same suite, this guarantees some levels/types of coupling and shall facilitate others.
  - A native intrinsic coupling of fluid-solid thermal solution is possible, with simultaneous evaluation of the temperature in the fluid and solid nodes, saving time during iteration since only one solution matrix is solved for the two domain. Also thermo-mechanical solution is performed by the same solver, and can be carried out in a coupled or uncoupled way. Such kind of couplings (fluid-solid thermal and thermo-mechanical) reduce the number of codes to be interfaced and cuts the number of internal iterations to be solved, greatly speeding up the solution.
  - Codes of the same suites are highly compatible and interfaceable. This allows to use a light procedure for the aero-thermo-mechanical coupling, overcoming the time consuming processes of writing output from a code to the other. This also permits to limit the user data managing and the introduction of additional human errors.
- Being CalculiX® an open source code it is possible to adapt the internal solvers according to the requirements of the procedure and to free the user to insert a number of customizations, especially through the use of dedicate user subroutines, making the procedure very versatile both in design and analysis phase.
  - By way of example, boundary conditions and quantities can be set through expressions, as function of runtime variables. For WEM applications, this enables to impose real transient operation BCs and to catch also dependences of the same boundary conditions from runtime quantities, such as in the

case of heat transfer coefficient (HTC) assessment, which can be evaluated through implemented correlations depending on specific key parameters.

2.1 Procedure overview

The procedure is based on the solution of an iterative process between the thermo-structural analysis of the metal-fluid domain and the aerodynamic solution of the SAS fluid network. The simplified diagram of Fig. 2.1 shows the flow chart of the iterative scheme. The transient heat transfer problem over solid domain is coupled to a sequence of structural static and steady flow problems using a quasi-steady state approximation.

The whole engine structure is solved from a point of view of the thermal and structural fields with the application of a customized version of the open source FEM solver CalculiX® . The model is treated with a 2D axisymmetric finite element approach and it includes a dedicated thermal fluid network where fluid-metal temperatures are computed.

Fluid properties from the secondary air system in terms of mass flow splits, pressure distribution and initial temperature field are provided to the CalculiX® thermo-structural model from a previous SAS solution in terms of time series. Such SAS analyses are performed standalone with a customized version of the native open source CalculiX® one-dimensional fluid network solver.

Therefore the strong coupling and non linearity in the heat transfer process during transient thermal analyses are handled by a partly coupled scheme, as well as the interaction between the secondary air system and the geometry deformations which are evaluated through an iterative process.

As shown in Fig. 2.1 the iterative loop starts with a first solution of the secondary air system over the transient cycle, from which a mass flow and pressure distribution is obtained. Mass flow rates and pressures are imposed on the fluid network mesh in the CalculiX® whole engine model and the thermo-mechanical analysis is carried out and metal temperature

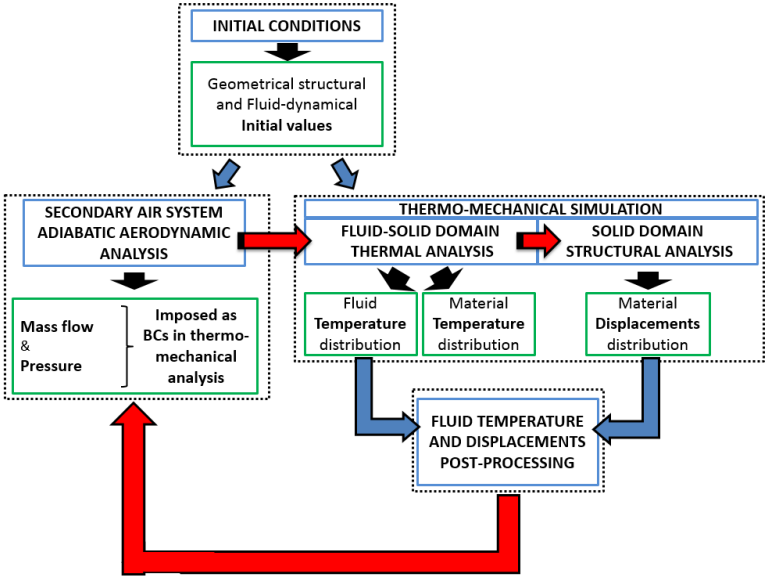

Figure 2.1: Block diagram of the iterative procedure.

distributions and displacements are obtained. These temperature distributions and displacements are post-processed and then used to update the geometries of the secondary air system and to impose new levels of temperature in the SAS standalone solution. In this way the effects of the solid-fluid heat transfer and running clearances on the mass flow splits, pressure drops and temperatures in the fluid network, are accounted: temperature distributions and new gap and clearances values calculated at the previous iteration are imposed as boundary conditions for the new one. After that, the recalculated mass flow and pressure distributions are therefore applied in the thermo-structural simulation for a new iteration, with a loop between thermo-mechanical model and aerodynamic fluid network, repeated until a converged solution is reached.

In the following sections, each sub-model and the corresponding analysis are deepened with dedicated sub-sections highlighting the peculiarities

belonging to each one. Governing equations, solution strategies and modelling schemes are illustrated for both the aerodynamic and thermo-mechanical analyses. In addition, details about the boundary conditions setting and the coupling mechanisms of the procedure are provided.

Specifically, first the fluid network solution is analysed with reference to the different phases in which it is included in the presented methodology. Since its outputs become boundary conditions for the thermo-mechanical analysis, the next section deals with the general setting of the overall amount of BCs needed for the solution of the aerodynamic analysis and of the thermo-mechanical calculation. Once clarified the conditions that are around the heat exchange between fluid and solid, the thermo-mechanical solution is presented. Finally the coupling scheme through which thermo-mechanical outputs are imposed in the fluid network aerodynamic calculation for a next iteration, is illustrated.

For the sake of clarity, the main arguments that will be deepened in the following Sections, are summarized here below:

- The secondary air system solution (Section 2.2) with details about:
  - typical fluid element typologies (Section 2.2.1);
  - fluid network governing equations (Section 2.2.2);
  - equations solution strategy (Section 2.2.3);
  - typologies of fluid network and type of calculations (Section 2.2.4);
  - application of the fluid network typologies in the presented methodology (Section 2.2.5).
- The procedure boundary conditions (Section 2.3).
- The thermo-mechanical solution (Section 2.4) with deepening about:
  - heat transfer and structural governing equations (Section 2.4.1);
  - equations solution strategy (Section 2.4.2).

- The interaction between the different multi-physical fields, thermo-mechanical and aerodynamic (Section 2.5), with details about:
  - time scales assumption (Section 2.5.1);
  - overall coupling mechanisms (Section 2.5.2).

In the two major Sections 2.2 and 2.4 about the aerodynamic standalone fluid network solution and the thermo-mechanical analysis, the two constitutive blocks in which the procedure is structured are described. The two corresponding sub-programs, with the system of boundary conditions, are organized in the iterative procedure anticipated in the present section and recalled and deepened in Section 2.5, in the view of the details of each sub-model which will be provided in the following Sections.

2.2 Secondary air system solution

Secondary Air System of modern aero engines and industrial gas turbines is made by a complex combination of flow passages, holes, ducts, pipes, seals, discs, either static or rotating, each one characterized by its own pressure loss characteristic. In order to simulate such complex system in reasonable time according to the requirements of the design process, low-order approach are in general used to solve mass flow splits and pressure drops (Fig. 2.2). This is proved by the fact that it has been in use by most of the engine manufacturers for the past 30 years [28].

It is a matter of fact that the pattern of the flow encountered is either 2D or 3D according to the heat transfer, pressure losses, rotating flows and all the other complex phenomena involved. However CFD calculation can not be applied in a systematic way. The main problem are significant computational efforts required to resolve a fully complete internal air system system, the robustness of the method, the predictive accuracy and time require for the post processing. Even quite agreement with experimental data at steady-state operating conditions has been demonstrated in literature, accurate thermal prediction during transients in gas turbine engine operation remained a very challenging problem for

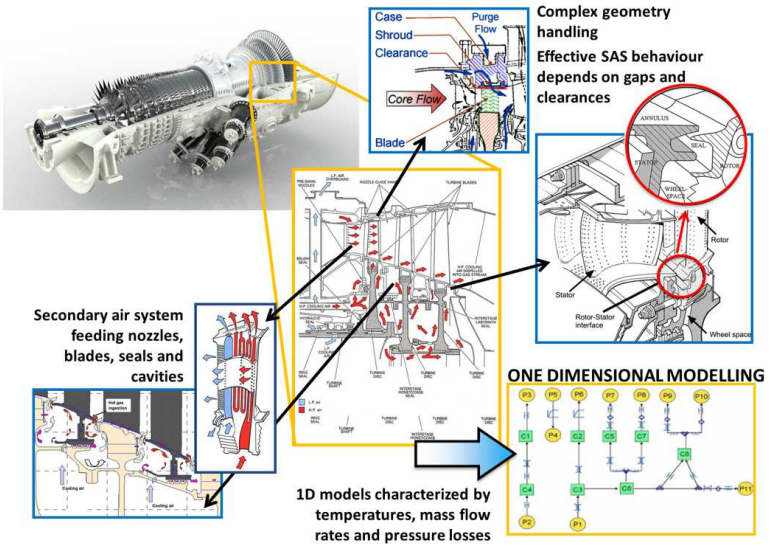

Figure 2.2: SAS solution complexity and low-order approach (Figures re-adapted from [9, 11, 16, 53, 54]).

CFD calculation, not already solved. Low-order approach for the fluid network, on the contrary, allows good flexibility and great rapidity of the simulations. For engineering purposes, simulation of such effects in a one-dimensional fashion with simplified models is enough. Moreover models can be equipped with correlations which are able to exploit and apply test and CFD results.

In a previous step of the development of the procedure, SAS analyses were performed with proprietary in-house one-dimensional fluid network solvers of Ansaldo. However, these codes developed for the analysis of specific problems or parts of the engine, were not typically able to cover all kinds of features or geometries that could be encountered in a whole engine model. In order to overcome this issue, and in order to take into account the reciprocal interactions between the different phenomena

involved in the transient operation of the engine, the integration of the native Calculix® fluid network solver has become necessary. This would allow to exploit completely the Calculix® modular features (SAS, thermal, structural solutions [11, 28]) to perform not only a coupling solution of the fluid and structure thermal fields but also to develop a method of updating and iterating on SAS geometries with an integrated coupled approach. That's why such analyses are now actually performed with a customized version of the native Calculix® one-dimensional fluid network solver, even though thanks to the modularity of the procedure, potentially a different fluid network solver could be used for the SAS solution.

In CalculiX® a one-dimensional fluid network solver is embedded and details about the approach used and its capabilities are reported in next sections.

2.2.1 Fluid element topology

In CalculiX® a special type of element dedicated to flow networks is present. This element is composed of three nodes: two corner nodes and one midside node. In the corner nodes the only active degrees of freedom are temperature and pressure. This convention is due to the fact that the total temperature or total pressure may not be known within the element, since the exact location of discontinuities (such as enlargements or orifices) is not necessarily known. Consequently, it is was chosen to define the total temperature and total pressure as unknowns in the corner nodes. These nodes are also those used to set forced convection when heat transfer with solid domain is imposed. Instead, in the middle node the only active degree of freedom is mass flow rate through the element. The mass flow is not necessarily uniquely determined at the corner nodes, since more than two branches can join together, therefore, the mass flow is set as unknown in the middle of a network element [52]. A positive mass flow rate flows from local node 1 to local node 2, a negative mass flow rate in the reverse direction (Fig. 2.3). The corner nodes play the role of crossing points in the network, whereas the midside nodes represent the flow within one element.

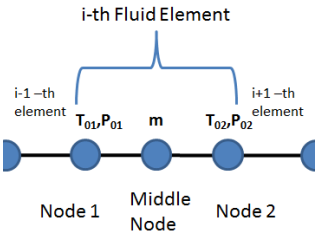

Figure 2.3: Fluid element triplet nodes [27].

According to the type of model simulated corner nodes can modify their meaning. Generally extremity nodes are assumed as big chambers in which there is a complete dissipation of the incoming flow kinetic energy. Therefore the velocity in the inlet and outlet nodes is zero and static and total parameters are identical. Nevertheless, for pipes or restrictions in series this statement no longer holds the difference between static and total values in the inlet and outlet nodes is taken into account [11].

Elements can be divided into two groups according to the role in the network:

- Boundary elements setting boundary conditions for the problem. These kind of elements constitute a special kind of network element in which one of the corner nodes, which is not connected to any other element, has no degree of freedom. The active degree of freedom is that of the midside and that of the node connected to the adjacent element. This type of element is used at those locations where mass flow enters or leaves the network for the imposition of total temperature and/or total pressures (active corned node) or mass flow rates (midside node).

- Common flow elements, for which dedicated models are present in the code, simulating a particular behaviour and modelling a specific relation between the pressure loss and the mass flow rate. Pressure, temperature and mass flow rate are determined by the solver during

the solution.

A common fluid element can belong to a specific class of models according to the phenomena it has to reproduce. Although the variety of fluid elements which can be faced in a real secondary air system, in CalculiX® there are a quite large number of flow element families implemented and available in the official internet release. The major sub-classes in which the models can be summarized are: orifices (comprehending preswirl nozzles, bleed air off takes), seals (among them labyrinth, carbon and brush seals), discrete characteristics models (for the setting of particular quantities history in time), dynamic head loss elements (comprehending branches, pipes, enlargements, contractions), vortex elements and model for the reference frame change. More details about the standard models included in the solver can be found in [11] and [52]. Additional proprietary elements have been implemented from scratch with the aim of adding a number of elements actually missing and required in the procedure, and in order to applied industrial best practice HTC correlations and pressure loss relations.

Standard and proprietary fluid elements are both characterised by a pressure loss coefficient ξ and a flow equation. In standard CalculiX® elements loss coefficients are obtained from the most known correlations which can be found in literature. In new models, loss coefficient may be experimentally obtained or determined using CFD or from proprietary correlations.

Summarizing, wherever the sub-family they belong, elements are uniquely defined by:

- the identifying number or label;
- the triplet of nodes, whose order defines the orientation of the positive/negative flow in the element;
- the type name determining the family/class of fluid element it belongs to;
- the set of properties determining the geometry and the other feature

of the element such has information about rotation, heat transfer coefficient and others.

2.2.2 Fluid network governing equations

A concatenation of network elements makes an aerodynamic fluid network. Aerodynamic network are filled with a compressible medium which can be considered as an ideal gas. As know, an ideal gas satisfies:

$$p = \rho R T \tag{2.1}$$

where p is the pressure, ρ is the density, R is the specific gas constant and T is the absolute temperature. To determine mass flow, pressure and temperature unknowns, in one-dimensional fluid model it is necessary to reduce the Navier-Stokes system to a respective quasi-one-dimensional form through the standard simplifying assumptions on a flow in a variable area duct. This can be expressed by the conservation of mass and energy in the corner nodes and conservation of momentum in the midside node. For our scopes, only stationary flow is considered.

As reported in [52] here below the formulation for the steady solution of aerodynamic network is briefly described.

The conservation of mass for compressible fluids in the stationary form can be written as:

$$\nabla \cdot (\rho v) = 0 \tag{2.2}$$

where v the velocity vector. Considering all elements connected to corner node i Eq. 2.2 becomes:

$$\sum_{j \in \text{in}} \dot{m}_{ij} = \sum_{j \in \text{out}} \dot{m}_{ij} \tag{2.3}$$

where $\dot{m}_{ij}$ is the mass flow from node i to node j or vice versa. In the above equation $\dot{m}_{ij}$ is always positive.

The conservation of momentum expresses the element equation which is specific for each type of element. Assuming an element with corner

nodes i,j it is generally of the form:

$$f(p_{0_i}, T_{0_i}, \dot{m}_{ij}, p_{0_j}) = 0 \tag{2.4}$$

(for positive $\dot{m}_{ij}$, where p_0 is the total pressure and T_0 is the total temperature), although more complex relations can be set.

Regarding the conservation of energy, the stationary form for an ideal gas can be expressed as:

$$\nabla \cdot (\rho h_0 \mathbf{v}) = -\nabla \cdot q + \rho h^{\theta} + \rho f \cdot v \tag{2.5}$$

where q is the external heat flux, h^{θ} is the body flux per unit of mass and f is the body force per unit of mass. h_0 is the total enthalpy corresponding to:

$$h_0 = c_p T + \frac{v \cdot v}{2} \tag{2.6}$$

where c_p is the specific heat at constant pressure and T is the absolute temperature. Eq. 2.6 is correct if c_p is considered to be independent of the temperature and this is widely proved for a lot of industrial applications. Just as a reminder, definitions of total temperature and total pressure are reported below:

$$T_0 = T + \frac{v \cdot v}{2c_p} \tag{2.7}$$

and

$$\frac{p_0}{p} = \left(\frac{T_0}{T}\right)^{\frac{\gamma}{\gamma-1}} \tag{2.8}$$

where $\gamma = c_p/c_v$, while T and p are the static temperature and static pressure, respectively.

In the case the corner nodes of the elements can be modelled as large chambers, the total quantities reduce to the static ones, since the velocity v is zero. Therefore considering the energy equation over all elements belonging to end node i we obtain [55]:

$$c_p(T_i)\sum_{j\in\text{in}} T_j\dot{m}_{ij} - c_p(T_i)T_i\sum_{j\in\text{out}}\dot{m}_{ij} + HTC(T-T_i) + m_i h_i^{\theta} = 0 \quad (2.9)$$

where HTC is the convection coefficient with the walls. Actually Eq. 2.9 is built so that to provide a slight temperature dependence of c_p. Indeed, since all flow entering a node must also leave, it is possible to assume for both the c_p value corresponding to the mean temperature value of the entering flow, leading to the following Eq.:

$$\sum_{j\in\text{in}} c_p(T_m)(T_j - T_i)\dot{m}_{ij} + HTC(T-T_i) + m_i h_i^{\theta} = 0 \quad (2.10)$$

where $T_m = (T_i + T_j)/2$

Notice that the quantities respect to which the equation are solved are total temperature, total pressure and mass flow rates. Static quantities have to be derived from the total ones. For example the static temperature is not a basic variable. Once the total temperature, mass flow and total pressure are known, the static temperature can be calculated and asked as an output variable to the solver.

2.2.3 Solving SAS equations

The above described system of nonlinear equations has to be therefore transformed into a set of linear equations and the method chosen is the Newton-Raphson one. The solving process is schematically presented in Fig. 2.4.

The process is started with initial values for the problem unknowns set by the user or calculated by the solver. The residuals for each equation are computed using the initial estimates. The Jacobian matrix, with the first derivatives of each equation with regard to each problem variable, is built. The linear system of equations is solved in terms of corrections used to update the current solution [28]. Checks based on the imposed

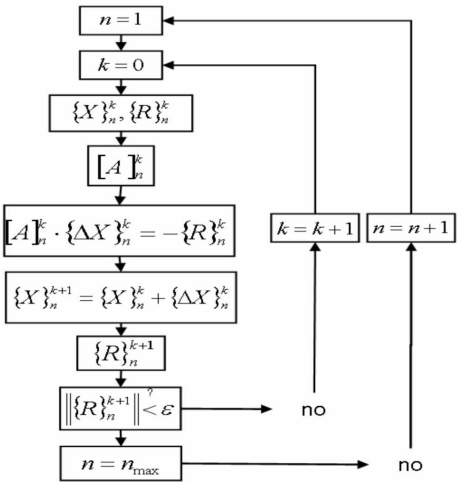

Figure 2.4: Newton-Raphson algorithm as implemented in CalculiX® [28].

convergence criteria are executed on the correction and residual size to determine whether convergence is reached for a given time increment.

2.2.3.1 Initial values

As mentioned initial values can be assigned by the user or, if no user assignation is present, the solver evaluates a first estimates of the unknown. In particular all nodes with temperature active degrees of freedom are set at an initial arbitrary temperature value of 293 K.

Concerning pressures, unknowns are evaluated by using the Laplacian law of repartition. This means that starting from the pressure boundary conditions, the pressure in a node is obtained as the average of the total pressure values of the adjacent nodes.

Once pressures and temperatures are estimated, initial mass flow rates are computed using the momentum equation, i.e. the characteristic equation of the element at stake.

At that point, all missing parameters have been obtained and therefore it is possible to assess the residuals corresponding to each equation (mass, energy and momentum equations) at each node and for each element and in this way the iterative process starts [28].

2.2.4 Fluid network typologies and type of calculations

Fluid networks in the procedure are solved and used in different fashions and analyses. Therefore, a brief summary of the modalities through which network can be run is proposed below. The two main differentiations regards if the network is solved standalone or coupled with the solid domain. Then for each one further distinction can be made.

- **Standalone**: the fluid network is executed considering only the solution of the fluid elements that compose it. Apart a number of boundary conditions imposed on boundary nodes, temperature, pressure and mass flows have to be assess by the solver in the generic nodes of the network. Equations are solved in the steady state regime. According to the typology of BCs applied, calculation can be also differentiated in:
  - **Adiabatic**: the system contains only adiabatic flow elements, the variation in temperature are due to transformations in models and mixing phenomena;
  - **Non-adiabatic**: heat transfer and discontinuities in temperature can be imposed through the use of concentrated flux applied on the desired nodes.
- **Coupled with solid domain**: the fluid network is executed coupled with the solid mesh. The advantage and novelty of the fluid network implemented in CalculiX® is the possibility to integrate the network directly in the thermal finite element model. It allows to perform thermo-mechanical calculations involving fluid-solid heat transfer without additional work in the interfacing different codes or models. Such kind of analyses can be also differentiated in one

of the following two types of calculations according to the type of equations actually solved in the network during the execution:

- **Pure thermo-mechanical**: in that case the mass flow in all elements of the network is known and the only unknowns are the temperature (in network and structure). This mode is automatically triggered if all mass flows are specified using boundary conditions. Pressures in the network are not calculated. Additionally, the type of model associated to the network element is not relevant and can be specified or not. This typology of fluid network is generally called *purely thermal network*. In the case of convection between fluid and structural walls, the convective conditions are replaced by advective elements. Network and structure are solved simultaneously. There is therefore a fully coupling in temperature assessment between fluid and solid nodes.
- **Fully coupled**: in that case the analysis involves fluid thermodynamical calculations with structural thermo-mechanical calculations. This kind of simulation is activated if the mass flow in at least one of the network elements is not known and it requires for each network element the specification of the type of the model associated to the element. Indeed, mass flow, pressure and temperature are unknown of a generic element and must be solved. This typology of network is generally called *aerodynamic network* for compressible flow. The action of the heat exchange in this case is accounted also for the mass flow and pressure assessment, the interaction between fluid properties and material temperature is complete. However the network unknowns and structural unknowns are solved in an alternating way. This leads to longer computation times, according to the strong nonlinearity of the network equations. In any case, during the transient simulation, the aerodynamic equations are solved in the steady state regime, therefore on the network side no transient effects are taken into account.

Obviously, the calculation typology depends on the physics to be modelled and on the level of coupling user wants to apply. Anyway, the choice of the typology of setting affects the calculation time and the way the phenomena are simulated. Further deepened dissertations about the topic can be recovered in [52].

To complete the overview it is important to highlight that *aerodynamic networks* can be switched into *purely thermal networks* in the case all flows and no or all pressure are given. In this case the characteristic equation of the specific model of the aerodynamic network elements are not solved and only the conservation of energy is performed in order to evaluate the temperature which constitutes the only unknown. This important feature is exploited in the procedure, as explained more in details in the next section.

2.2.5 Use of aerodynamic and purely thermal networks in the proposed procedure

In the presented methodology the SAS solution is carried out with a decoupling of the aerodynamic solution and the thermal one. As reported in Fig. 2.5, first an adiabatic standalone solution of the SAS is performed, with the assessment of mass flow splits, through the solution of the aerodynamic model of the network. The solution carried out with the proper application of the initial cold geometries, and temperature and pressure boundary conditions. The calculation is performed over the transient operation through a number of solutions discretizing the entire duration of the cycle. As already mentioned the solution is steady and no transient conditions over the fluid are taken into account.

Once the secondary air system has been solved as a sequence of steady states over the transient operation (we can consider a quasi-steady approximation) the mass flow rates and pressure distributions over the network are assigned as time variant series in thermo-mechanical analysis. This one determining temperature distribution and displacements, is performed by means of an aerodynamic fluid network switched to a purely thermal one. We talk about *aerodynamic network switched to purely*

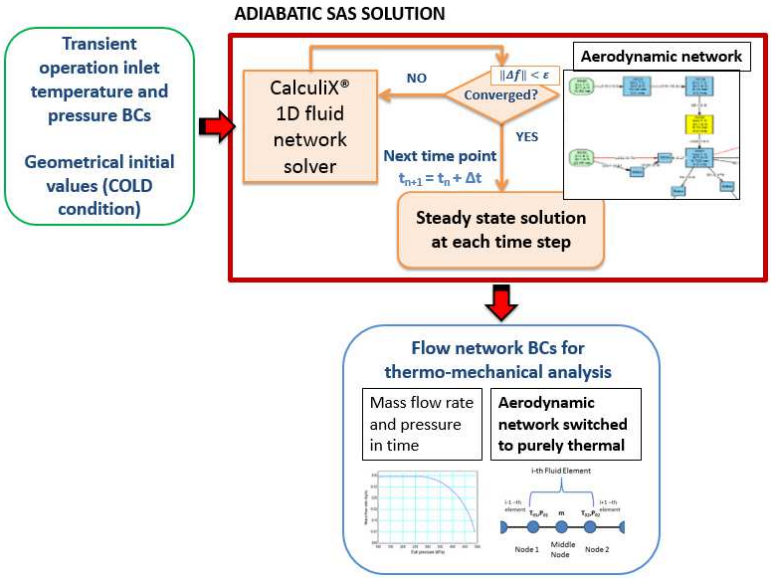

Figure 2.5: Adiabatic standalone solution of the aerodinamic fluid network (panel in red) through the transient operation (panel in green on the left). The solution is then translated in boundary conditions for the purely thermal application in the thermo-mechanical solution (panel in blue on the bottom).

thermal since in the code the state of purely thermal network prescribes the absence of a *type* or class of element identifying the fluid element: in the purely thermal network only the energy equation is solved and no element type should be defined since characteristic mass-pressure equation is not solved.

In our case we would like to use specific elements, despite the fact that only temperatures have to be calculated, in order to determine quantities like heat transfer coefficients, which are based on flow characteristics such as Prandl and Reynolds number, that requires the use of geometric parameters which are assigned in the model type. Therefore in the thermo-

mechanical model the SAS network applied is an aerodynamic network used as a purely thermal, since in this phase mass flow and pressure distribution are known and imposed, and only the energy equation is solved for the assessment of the temperature distribution over the fluid and the metal. Therefore, from now on, for the sake of simplicity and brevity, we will refer to this as *thermal network*.

The thermal network used in the thermo-mechanical model is basically different from the aerodynamic one, not only in the solution but also in the discretization and element typology. It is necessary to consider that the level of discretization required to approach the two different calculations, *aero and thermal*, is substantially different. The aero case discretization is in general more coarse than the thermal one since the crossing points of the network are mainly defined by the change in engine device typology, such as duct, pre-swirler, cavity, seals and so on. Therefore the aero discretization is mainly set by the subsequent change in typology of the elements along the SAS structure. On the contrary, in the thermal case, network has to respect the spatial discretization of the model necessary to properly catch the variation in temperature over the mesh. In this case the number of elements to be insert in the fluid network is decided by the spatial configuration of the solid mesh and by the complexity of the thermal phenomena involved.

To clarify the topic, it is proposed an example with exaggerate conditions, just to make the problem more evident. The case reported in Fig. 2.6, has two components, one rotating and one static with cooling air flowing between them, while they are subjected to the same heat flux on the respective external surfaces. A fixed HTC and swirl ratio ($SR = C_t/U$) is consider between rotoric and statoric parts.

Actually to determine the air pressure distribution along the diameter of the two discs it would be sufficient to use a vortex element solving the relation:

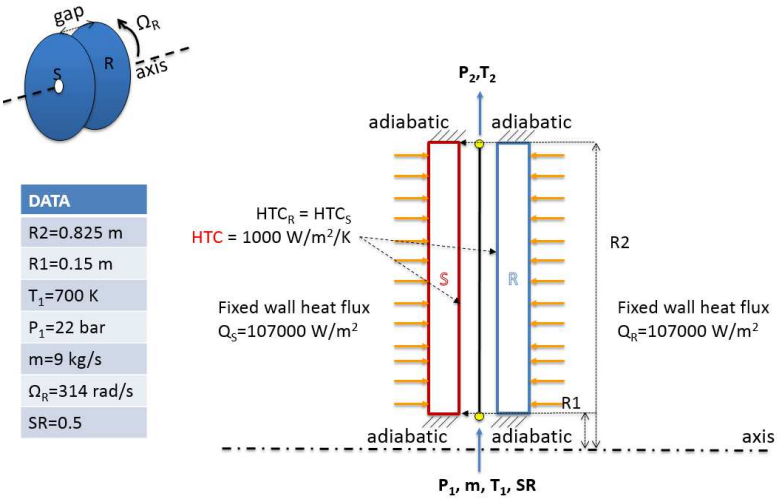

Figure 2.6: Example of thermal solution; air flowing between rotor-stator interfaces.

$$\left(\frac{p_{t_o}}{p_{t_i}}\right)_{theoretical} = \left[1 + \frac{(SR\, C_{t_i})^2}{2c_p T_{t_i}} \left(\left(\frac{r_o}{r_i}\right)^2 - 1\right)\right]^{\frac{\gamma}{\gamma-1}} \tag{2.11}$$

where p_t is the total pressure, T_t the total temperature, C_{t_i} the circumferential velocity of the rotating device, r is the radius while i and o stand for inlet and outlet.

However, if for the aerodynamic analysis a unique element could be able to describe the solution between the inlet ant outlet radius, in the case of thermal simulation, simply switching to a thermal network maintaining a unique element could lead to a very rough solution.

In Fig. 2.7 the air flowing between the two components is discritized once with a single element accommodated between inlet and outlet, once with 28 fluid elements.

As the reader can see, the solution is very different in the two cases,

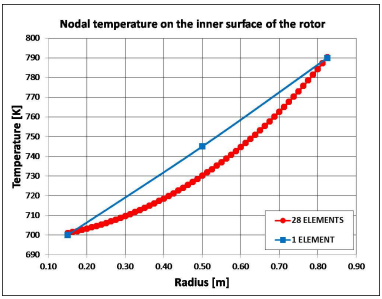

(a) Fluid temperature distributions along radius.

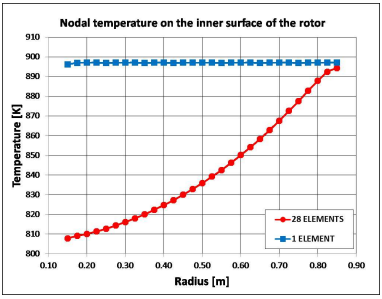

(b) Temperature predicted on the inner surface of the rotating component.

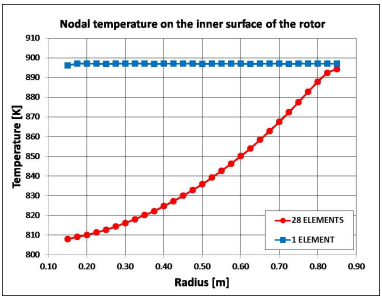

(c) Temperature predicted on the inner surface of the statoric component.

Figure 2.7: Effect of different stream discretizations on thermal distributions.

since in the first case the variation of the fluid density during the heat transfer along the edges of boundary is not caught. According to the simple boundary conditions of the case, change in fluid density makes the difference in the calculation of the rotational effect on the rotating component and in the windage evaluation, leading to very different solutions.

The other reason for which it is very probable to have different discretizations between the aerodynamic and the thermal networks, is the complexity of conditions imposed in the thermal model. Thee conditions derive not only from the solution of the aero network, but also depend on other considerations and studies about the single parts of the model and about the local phenomena involved.

For example, in the rotor cavity reported in Fig. 2.8 and Fig. 2.9, aero and thermal networks are approximated in different ways. In the aerodynamic analysis only three branches of the fluid network are accounted in that zone (Fig. 2.8a) with a number of models involved in the aerodynamic solution appropriate to simply catch the macroscopic distribution of mass flow rate in the cavity at stake and in adjacent passages (Fig. 2.8b). On the contrary, from the knowledge of the mass flow split coming from the aerodynamic solution, a more detailed thermal analysis is set (Fig. 2.9a). Considering the mass flow actually detected by the aerodynamic analysis in that zone, *secondary thermal* branches are imposed (Fig. 2.9b), providing additional splits in the cavity, obviously set respecting the conservation of the global mass assessed by the aero solution. How this mass is split inside the cavity and in its secondary passages (even not accounted in the aerodynamic simulation), can be establish with the aid of more detailed CFD solutions of the sub model, able to catch those 3D-dimensional phenomena which can not be appreciated with one-dimensional tools.

Not using an aerodynamic network fully coupled with the solid domain (i.e. solving mass flow, pressure and temperature in the same model) but maintaining separated the aerodynamic network from the thermal one, is one of the main important choice of modelling of the procedure. Certainly,

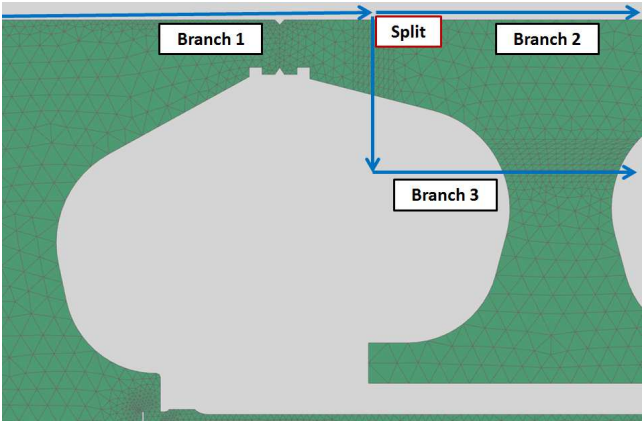

(a) Split of the flows in the aerodynamic network solution.

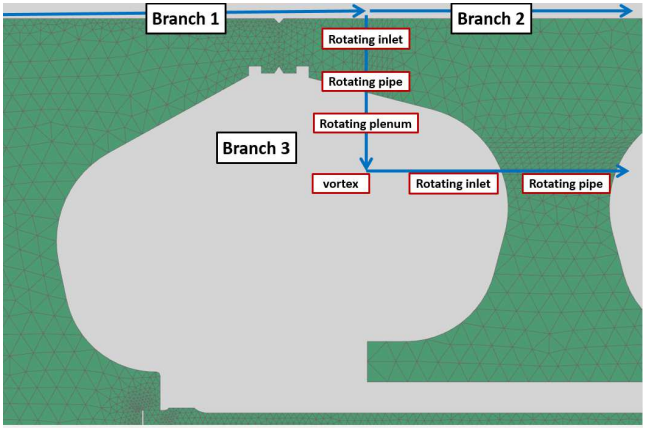

(b) Models involved in the aerodynamic network solution.

Figure 2.8: Example of aerodynamic complexity and discretizations in a rotating cavity.

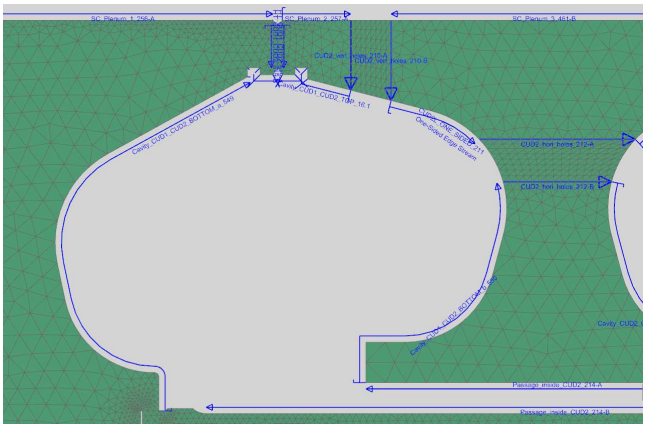

(a) Conditions actually imposed in the thermal analysis based typically on the aerodynamic network solution and other detail CFD simulations.

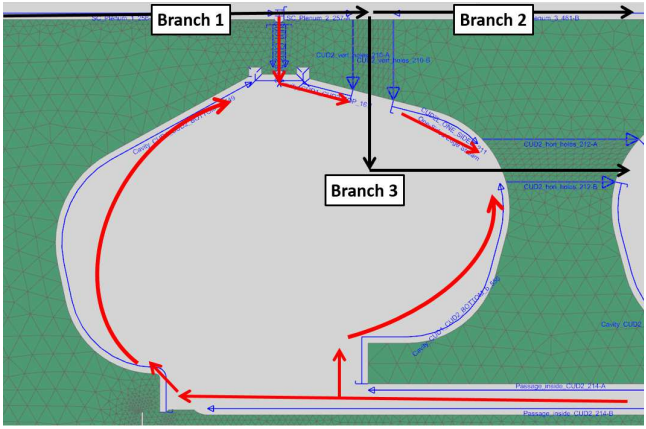

(b) Additional branches (red) respect to those of the aerodynamic setup (black).

Figure 2.9: Example of thermal complexity and discretizations in a rotating cavity.

the attempt to implement a monolithic procedure where purely thermal and aerodynamic network problems are solved simultaneously within the same model, is an attractive perspective at a first sight.

It could be thought to simply adequate the coarse mash (aerodynamic) to the finest one (thermal), adopting this latter kind of discretization for the common model. However, apart from obvious advantages of having a unique model with a fully coupled solution, this coupling scheme entails a few challenges. One is the intrinsic difficulty of merging several spatial and/or temporal scales. The temporal problem is overcome with the quasi-steady approximation of the fluid solution, calculating for each time the steady condition. But in any case this is not sufficient to have an agile solution. Indeed, the aerodynamic flow networks are notoriously difficult to solve due to the highly nonlinear equations which intrinsically have major problems to converge. Therefore, increasing the number of fluid elements in attempt to provide spatial convergence on the fluid side is not the good way, since this would cancel out any computational advantages of the same monolithic approach.

For all these reasons, in the presented procedure, two different networks are therefore adopted for the aerodynamic and thermal solutions.

2.3 Procedure boundary conditions

As highlighted in the section 2.2.5, we set two types of solution of the fluid network. In the thermal solution the secondary air thermal loads come from the standalone previous analysis of the SAS over the transient cycle and are imposed as boundary conditions in the FEM model in terms of distributions varying in time. Temperatures, set as known data on the inlet boundaries, evolve during the thermo-mechanical calculations along the fluid network extent, while the mass flow rates and the pressures are fixed. On the other side, the boundaries for the very first aerodynamic standalone adiabatic SAS solutions depend only on main flow conditions. In the subsequent iterations of the overall procedure, when the standalone aerodynamic SAS solution is subjected also on the heat transfer and metal

dilatation effects, the post-processed fluid temperature distribution and solid displacements are added as boundary conditions to the main flow BCs quantities.

Main flow conditions are based on preliminary analysis, coming from detailed CFD studies or from engine test data, when available. Based on the field/experimental information, hot gas conditions at significant flow path regions like nozzle, blades, platforms and exhaust diffuser are imposed as boundary conditions determined by aerodynamic computations. These flow boundary conditions, determined at specific time points of the operation (generally at the steady state condition), are scaled based on the standard cycle key parameters and aerodynamic data, and expressed as a function of time in order to reproduce the overall transient cycle conditions through its entire duration.

Among boundary conditions, data coming from experiment or instrumented machine or prototype are of fundamental importance in order to have physical references and real information about performances and phenomena hard to predict with numerical methods. Setting these parameters inside the calculation serves also to tune the model and to make it more verisimilar and reliable.

To this end, flow path temperatures, detected in function of time at different locations, are important boundary conditions used to estimate the thermal distribution of the gas turbine. Also in literature it is possible to find references to this practice [47], and some temperatures and pressures at key locations of gas turbine are reported as important key parameters to be measured or calculated from the experimental database system. Among them:

- Compressor inlet temperature and pressure;
- Compressor exit temperature and pressure;
- Firing Temperature;
- Exhaust Temperature.

Power and rotational speed, together with annulus mass flow, total pressure and temperature, complete the list of key parameters used to scale and set accurate boundary conditions, consistent with the engine performance data.

The same convective coefficients can be expressed through implemented correlation as function of significant parameters such as rotational speed, varying mass flow rates, fluid and wall temperatures. The possibility of catching the dependence of HTCs from the fluid properties is a crucial point, in order to reproduce a whole engine model running under real operating conditions. In the presented procedure they are calculated by the thermal solver, based on the standard and proprietary heat transfer correlations customized for gas turbine applications. This means that according to the standard industrial practice, they are tuned with the aim to match engine test data at a number of key stations with the predicted temperatures [46]. Correlations are used also to model fluid behaviour such as pumping, swirl, and windage heating effects.

In the standard industrial practice the same mass flow and pressure distributions obtained from a preliminary SAS solution are scaled through the key cycle parameters. The standard approach is based indeed on the execution of the SAS analysis at base load conditions with a subsequent scaling of the mass flow rates and pressures obtained, as a function primarily of rotational speed and power. Some few other points can be chosen for running the SAS analysis such as the point of full-speed-no load, minimum load, and so on. In any case a linear variation of the operational boundary conditions is assumed between the ramp points [41].

On the contrary, in the presented procedure differently from the conventional practice, the SAS is not solved once and scaled for all the other time steps, but there is an update of the effect of heat exchange and solid deformations. Indeed, first the standalone SAS solution is performed over the whole transient cycle according to the pressure boundary conditions assigned in time, coming from the main flow conditions. Then, through an iterative loop, standalone SAS solutions are performed taking into account the heat flux exchanged during the transient operation with the

metal, and the deformations of the solid which occur during the transient cycle and which can modify deeply the mass flow and pressure losses. These modifications can cause different mass flow splits or even inversion in the direction of the secondary air, in deep contrast with the assumption of constant mass flow splits accepted with the simple scaling in time of the mass flow rates and pressures, in the standard industrial approach.

2.3.1 BCs types

Main flow, SAS and experimental/field data can be assigned in different fashions and the main convective thermal boundary conditions can be summarized as below:

- **Heat transfer between fluid streams and solid elements**. It is required to specify fluid and solid elements involved, inlet air temperatures and heat transfer coefficients. Effects of rotations and heat pickup such as that due to windage power generation can be added. HTC and windage power are mainly based on the empirical correlations. The inlet air temperatures can be dependent on the specified performance data of the engine (key parameters). They can also be taken as exit temperatures from the upstream thermal boundary condition, without an effective physical link among branches of the fluid network (so called in the procedure *logical links*, more details will be given in Section 3.3.2.1). The fluid elements composing the fluid stream, are able to absorb or give energy and transmit it from a zone to the other. No matter the number of surfaces are involved in the heat transfer, they can be over a single edge, or two (e.g. in a duct in an axisymmetric scheme) or manifold, if more geometrical features are involved.

- **Convecting zone**. It models the convection from a solid boundary to a fluid of a known temperature. No thermal stream are necessary, the effects along the length of the boundary are accounted by specifying the number/label of the solid elements involved in the heat transfer and the value of the HTC and of the sink temperature.

- **Thermal masses**. It is used in regions where no direct heat transport by forced convection is present. Therefore it has the effect of smoothing the temperatures on coupled solid boundaries.

To complete the boundary conditions outline, radiation heat transfer is considered in all those regions where high thermal gradients are expected and thermal contacts are set between flanges and all other surfaces with contact. Structural constrains are applied on the extremities of statoric parts, centrifugal loads are imposed on rotoric components and both are subjected to the pressure loads expressed as explicit boundary conditions or coming from the SAS solution. Indeed, pressures on corner nodes of fluid elements can be applied as pressure loads of the structure.

2.4 Thermo-mechanical solution

The thermo-mechanical solution is carried out with the FEM solver CalculiX® which is able to perform in a unique code thermal and mechanical solutions addressing to a single model. In addition, fluid network can be added to the solid mesh for fluid-solid heat transfer calculation.

The procedure is developed for the solution of the behaviour of a whole engine cross section such as that reported in Figure 2.10. The solid domain is modelled with an axisymmetric approach with proper modelling for the treatment of 3D features. Axisymmetric approach has the great advantage of containing computational cost.

The axisymmetric structure is expanded by rotation about the second coordinate axis (y axis), half clockwise and half counterclockwise. The radial direction corresponds to the x-axis in the 3D expansion, the axial direction with the y-axis. The x-y plane cuts the expanded structure in half. The z-axis is perpendicular to the x-y plane such that a right-hand-side axis system is obtained. The solver is able to manage the coupling of plane and axisymmetric elements even from the point of view of the radiative calculation.

In order to include the fluid network in the thermo-mechanical FEM model, triplet of nodes are inserted in the domain, where each triplet

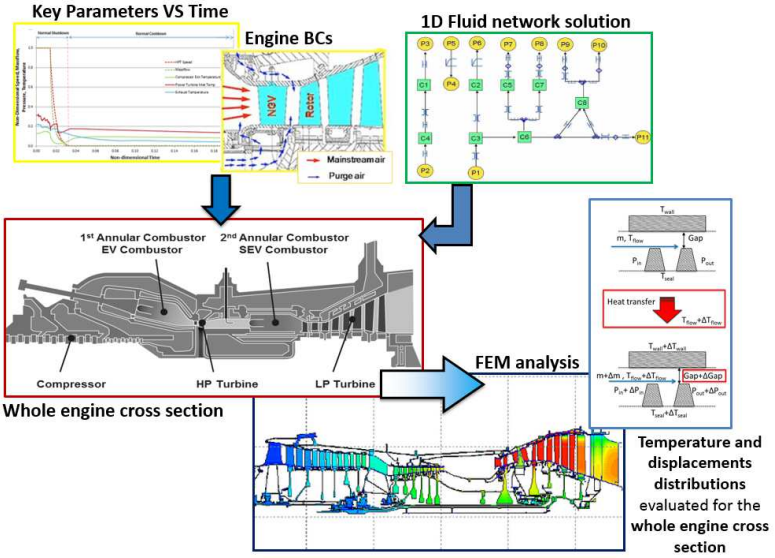

Figure 2.10: FEM inputs and solution (Figures re-adapted from [11, 47]).

represents a fluid element. In this way the fluid network is directly integrated in the finite element thermo-mechanical model. In the methodology the creation of the fluid-solid model is carried out with external tool of meshing and pre-processing (more details will be given is Section 3.3.4).

2.4.1 Thermal and structural governing equations

Concerning the heat transfer solution, the temperature is the unknown and it is estimated for both the metal and the fluid. As reported in [52], the energy equation is solved subject to temperature and flux boundary conditions ([55]). For stationary calculations, the governing equation for heat transfer becomes a Laplace-type equation which can be written as:

$$\nabla \cdot (-\kappa \cdot \nabla T) + \rho c_p \frac{\partial T}{\partial t} = \rho h \tag{2.12}$$

where κ contains the conduction coefficients, ρ is the density, h the heat generation per unit of mass and c_p is the specific heat.

Temperatures and fluxes can be imposed as boundary conditions, and in particular, possible fluxes can be:

1. Concentrated flux, applied to nodes.

2. Distributed flux, applied to surfaces or volumes.

3. Convective flux defined by the equation:

$$q = HTC(T_w - T_0) \tag{2.13}$$

where q is the flux normal to the surface, HTC is the heat transfer coefficient, T_w is the body temperature and T_0 is the environment temperature (also called sink temperature). In the specific case of forced convection calculations, as in turbomachinery applications, T_0 is fluid temperature which is an unknown too and it is determined contextually to the determination of the metal temperature. As already mentioned, it is possible to express an heat transfer coefficient from correlations or expressions inserted by the user. It can be done by compiling a dedicated user subroutine defining the HTC coefficient be provided. Different HTC coefficient patterns can be coded in the subroutine and recalled during the calculation. This allows to express the HTC as a function of variable quantities (mass flow, temperature, pressures) evolving during the same calculations and therefore to express its dependence from the transient conditions.

4. Radiative flux defined by the equation:

$$q = \epsilon(\theta^4 - \theta_0^4) \tag{2.14}$$

where q is a flux normal to the surface, ϵ is the emissivity, θ is the absolute body temperature (Kelvin) and θ_0 is the absolute

environment temperature. The emissivity takes values between 0 and 1. A zero value applies to a body with no absorption nor emission and 100 % reflection. A value of 1 applies to a black body. The radiation is assumed to be diffuse (independent of the direction of emission) and gray (independent of the emitted wave length). CalculiX® can also be used for cavity radiation, simulating the radiation interaction of several surfaces. In that case, the viewfactors are calculated, by the solver, more details about the calculation method are reported in [52]. Sometimes, it is useful to specify that the radiation is closed. In that case, the viewfactors are scaled to one exactly. For cavity radiation the sink temperature is calculated based on the interaction of the surface at stake with all other cavity radiation surfaces. If the emissivity is nonuniformthe value can be calculated runtime by means of expressions coded in dedicated user subroutine specifying the emissivity must be provided. Different nonuniform emissivity patterns can be stored and recalled during the calculation from the user subroutine.

Concerning the elastic problem in the solid domain, the governing law is:

$$\rho \frac{\partial^2 d_s}{\partial t} - \nabla \sigma_s(\epsilon_s, T_s) = 0 \tag{2.15}$$

where d_s is the displacement vector. The solid model is characterized by a constitutive law relating components of the stress tensor σ_s to the deformation gradient through a linear elastic strain tensor ϵ_s and to the thermal strain tensor due to the changes in temperature T_s modelling thermal expansion.

Different levels of coupling can be chosen in the thermo-mechanical solution:

- Coupled temperature-displacement;
- Uncoupled temperature-displacement.

In the first case the nonlinear calculation is performed with displace-

ments and temperatures simultaneously solved. In this way the reciprocal action of the temperature on the displacements and the displacements on the temperature can be taken into account. As reported in [52], the present capabilities of the solver allows to take into account the influence of the temperature on the displacements through the thermal expansion, whereas the effect of the displacements on the temperature is limited to radiation effects. In addition, the influence of the network fluid pressure on the deformation of a structure and the influence of the structural deformation on the network fluid mass flow can be considered.

In the second case, for each increment a thermal analysis is performed first. Then, the resulting temperature field is used as boundary condition for a subsequent mechanical analysis for the same increment. Consequently, there is no feedback from the mechanical deformation on the temperature field within one and the same increment. This is in general the approach used inside the procedure, due to the fact that a sequential calculations leads to a systems of equations which is smaller and faster, and execution time can be saved. Moreover, the number of iterations within the increment is determined for the thermal and mechanical analysis separately, whereas in a coupled thermo-mechanical analysis the worst converging type of analysis dictates the number of iterations [52]. It is expected that inside the single increment the effect of displacement on the view factors is negligible with respect to the other thermal phenomena occurring.

2.4.2 Solving thermo-mechanical equations

Once all the data concerning secondary air system properties an all the other boundary conditions are set, the thermo-mechanical analysis can be performed. In particular the inputs provided to the thermo-mechanical solver will be (Fig. 2.11):

- solid and fluid mesh (unique model);
- SAS properties:
  - mass flow rates,

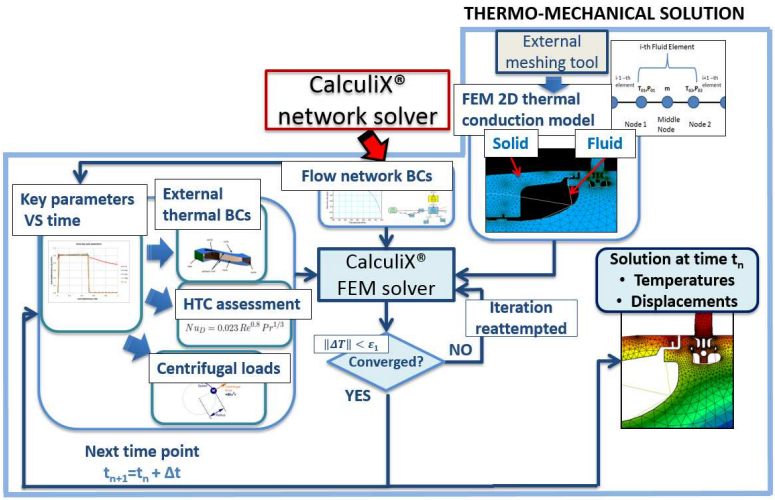

Figure 2.11: FEM thermo-mechanical iterative scheme: mesh (top right side), mass flows and pressures from the standalone aerodynamic SAS calculation (top center side) and all the other BCs (left side) are collected to the CalculiX® FEM solver, to obtain temperatures and displacements in time (bottom right side).

  - pressure distribution;

- other characteristics near the wetted walls:
  - heat transfer coefficients,
  - sink temperature (for explicit film conditions);
- key parameters varying in time;
- thermal BCs (i.e. inlet temperature of streams)
- other thermal BCs (e.g. from detailed CFD simulations);
- centrifugal loads
- displacements constrains.

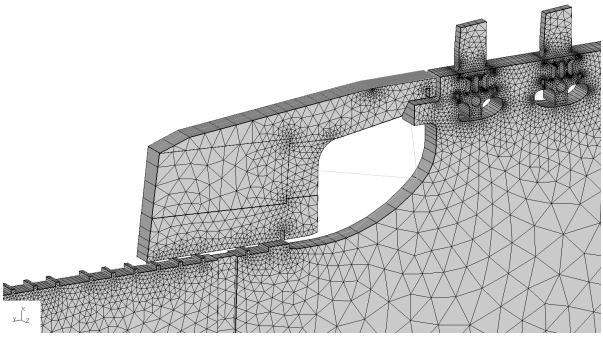

(a) Geometry at cold condition.

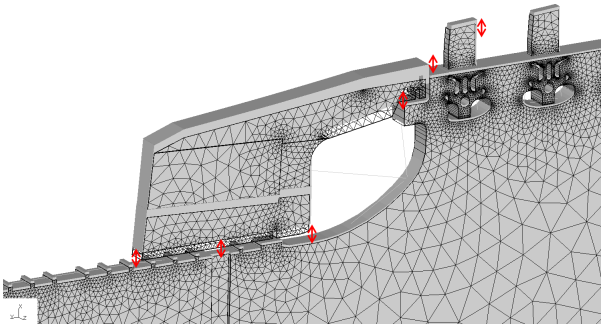

(b) Geometry displacements.

Figure 2.12: Example of geometry deformation due to thermal expansion.

The domain is solved with an expansion angle of the mesh fixed at 2° and the thickness of plane elements is properly scaled by the procedure. Transient analyses are carried out to obtain component temperatures, displacements and stresses through a real engine cycle. At each time increment the different typologies of boundaries varying in time are evaluated for the current step and applied in the thermo-mechanical solution. Thermal balance through conduction, convection, and radiation are solved in each region for each required time step. Thermal and mechanical loads are then used to the evaluation of the metal deformations (Fig. 2.12).

To find the solution at the end of a given increment, as in the case of the fluid network, the set of nonlinear equations is solved with the Newton-Raphson method, i.e. the set of equations is locally linearized and solved. If the solution does not satisfy the original nonlinear equations, the latter are again linearized at the new solution. This procedure is repeated until the solution satisfies the original nonlinear equations within a certain margin [52].

A number of convergence criteria are set, for the check of average heat flux and largest residual flux and change in solution. Convergence values can be chosen by the user and extra check can be set in addition to the standard ones. In particular for thermal transient simulation is important to set a check to limit the temperature change in two subsequent increments. This is necessary to limit the time step while advancing in the solution, with the aim of properly discretize the thermal history in time and avoid to describe the variability of temperature with too rough approximates. The risk is to obtain a converged solution with different phenomena simulated since the thermal history has been coarsely approximated missing decisive variations (peaks or falls) for the correct reproduction of the mission cycle.

As reported in Fig. 2.13, without particular check on the temperature, if convergence is stable, high time increment can be selected by the solver in advancing in the solution with the risk of missing important part of the cycle, because a linear variation of the operational boundary conditions is assumed between the two consider ramp points. An example (magnified to stress the topic) is reported in the Fig. 2.13c where for the highlighted square variation of the rotational speed it is expected a corresponding variation in temperature of main flows of the engine. Considering the green approximation a fundamental part of the transient operation is lost. Not approximating correctly the engine cycle means to apply different boundary conditions to the simulation and reach different solutions.

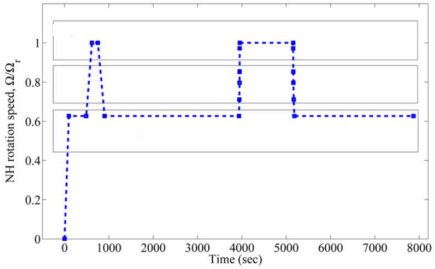

(a) Example of mission cycle. Transient cycle definition for HP rotor disk [41].

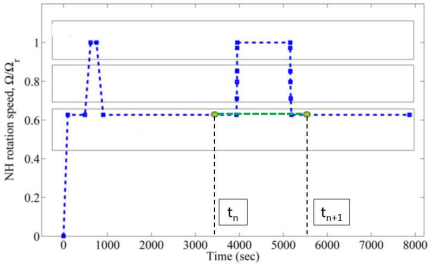

(b) Example of a possible approximation of the mission cycle; if convergence is stable, high time increment can be selected by the solver.

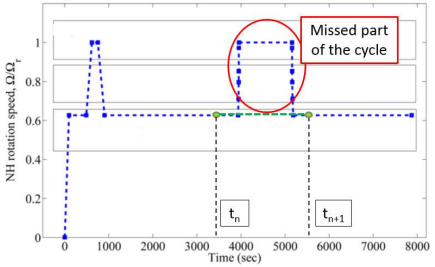

(c) Part of the cycle lost.

Figure 2.13: Example of wrong approximation of a mission cycle.

2.5 Coupled aero-thermo-mechanical analyses

The presented methodology performs the solution of the dimensionally heterogeneous analyses of the secondary air systems and engine hardware through iteration of standalone procedure sub-models and different levels of coupling. In the previous Sections 2.2 and 2.4 the sub-models and respective solutions have been illustrated. The different procedure sub-models and sub-loops are linked together by a proper imposition of additional equations and by an iterative loop handling the interactions between SAS and thermo-machanical analyses.

2.5.1 Time scales assumption

Coupling different sub-models with different characteristic time of evolution of the phenomena, imposes an issue about the proper time scale to be adopted in the overall procedure. In the presented procedure, a time-implicit approach based on the quasi-static approximation is applied. The transient thermal problem is coupled to a sequence of fluid steady and structural static problems. The dropping the time derivatives from the fluid and the solid structural sub-problems is a general practice in this type of calculation.

To this end, consider a turbomachinery application, for instance the heat transfer in a compressor diffuser (Fig. 2.14) where we assume an exit axial velocity $U = 250\,m/s$ and an average thickness of the metal $L = 0.05\,m$. Assume the thermal diffusivity of steel $a = 4.2 \cdot 10^{-6}\,m^2/s$. The convective time scale is approximately $\tau_{fluid} = L/U$, and the solid diffusive time scale may be expressed as $\tau_{solid} = L^2/a$ [56]. Hence the convective time scale results $\tau_{fluid} = 2 \cdot 10^{-4}\,s$, whereas the solid diffusive time scale results $\tau_{solid} = 595\,s$.

The very high difference in the time scale of the two different phenomena justifies the assumption that considers the time scale separation of the "fast" fluid convection and "slow" solid conduction processes [41], with the aim of decrease the cost of simulation.

Fluid transients phenomena during which the "slow" metal temper-

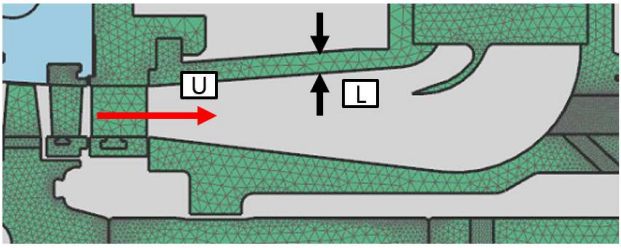

Figure 2.14: Example of heat transfer turbomachinery application.

ature state is assumed to stay constant, are neglected. Because of the low convective time scale respect solid diffusive one, the influence of unsteadiness in the fluid domain is negligible and as a result, the flow field may be considered as a sequence of steady states. That is why it is an acceptable approximation to couple steady fluid calculations with transient solid calculations.

Therefore only relatively expensive steady fluid problems are solved during the simulation, run interrogating at each time increment the boundary conditions defining the annuls flow in the transient engine cycle in terms of pressure and temperature time histories.

Concerning the solid equations simplifications, in the structural sub-problem inertial terms are not considered due to negligible effects of the small amplitude vibration around the static equilibrium on the temperature solution [41].

2.5.2 Coupling mechanisms

The objective of the procedure is to catch the transient thermo-mechanical behaviour of the engine, appreciating the coupled phenomena occurring among the different multi-physicals fields, in which the dynamics and time-dependent properties of one discipline impact the other (Fig. 2.15). The fashion used to pursue the goal provides features incorporating both monolithic and partitioned aspects (see Chapter 3).

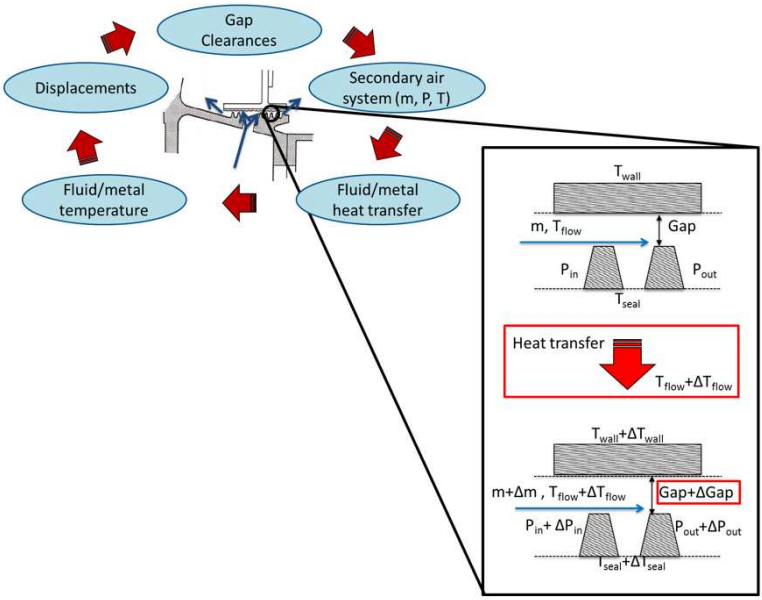

Figure 2.15: The coupled interactions among the aero-thermo-mechanical multi-physicals fields.

Standard approach up to now considered the assessment of these phenomena with a sequential approach, scaling base load mass flow splits, pressures and temperatures during the thermal transient of a whole engine mission, according to some key parameters, or interpolating between some few other operating points. In the particular case of heavy duty design, very often, no loops were performed among the three processes (SAS, thermal and structural solutions).

However the new requirements in terms of performances and hardware lifing controls have been translated into more stringent limits on the uncertainty of predicted temperatures that must not exceed a standard deviation of about 10-15 Kelvin in heavy duty turbine applications.

To meet these more demanding specifications, there is the need to over-

come the two more restrictive approximations of the standard approach to the aero-thermo-mechanical problem:

- the description of the time variant properties of the fluid network through a rescaling of base load conditions or interpolations between some few known operation point;
- the absence of a characterization of the interaction between SAS properties and geometrical deformation, intrinsic of a decoupled sequential approach.

Regarding the first point, a more accurate characterization of the time history of the fluid properties is provided in the presented procedure. Indeed the fluid network solution is taken over the entire duration of the cycle through a sequence of steady state calculations, whit a more significant number of points, respect to the standard discretization.

As explained in Section 2.2.5, in the procedure the SAS analysis is performed decoupling aerodynamic and thermal solutions. Even under the assumption of steady solution of the fluid network, the direct coupling of fluid solution with the thermo-mechanical one is notoriously a reason of slowing down of the solution. Alternating solution of the network and the structure leads to longer computational times.

Differently the way proposed allows to couple directly in the solution time step, only the temperature degree of freedom. Through the thermal network, temperatures of the fluid are solved simultaneously with the temperatures on the structural side, which is much faster than the alternating way required if also pressure and mass flow rates are involved in the coupling. Limitation in the number of solutions of aerodynamic equations is a problem also present in literature. It is possible to find different attempts tailored on the specific approaches, to speed up and interrupt the coupling of variables when the impact on the integrated simulation does not determine a significant variation on convergence [41, 50].

Separating the aerodynamic solution from the thermal one also leads to a decoupling of the network equations respect to those of the structural problems. This type of solution is to be preferred because networks

generally lead to small sets of equations which are intrinsically asymmetric. If they are solved together with the structural equations, the presence of the small network contribution would produce a complete asymmetric matrix, increasing greatly the calculation time. This is due to the fact that aerodynamic networks are characterized by highly nonlinear equations, requiring more iterations to reach convergence than structural one [52]. For this reason is more convenient to solve network and structural matrices standalone treating the solution of one as boundary conditions for the other.

Concerning the second point of the previous list, the presented methodology tries to model the multi-physical aero-thermo-mechanical interaction, through the coupling mechanisms summarized at the beginning of the Chapter and here deepened in the view of the further details given about the sub-blocks composing the procedure.

In Fig. 2.16 a more detailed representation of the process is given. The sub-block in red is related to the aerodynamic SAS solution (Section 2.2), the sub-block in blue represents the thermo-mechanical solution (Section 2.4), while the sub-block in green illustrates the coupling method which links the two others (Section 2.5.

Following the block diagram, the simulation starts with an initialization of the variables at the first instant, which in general corresponds to the cold engine conditions. Hydraulic diameter, length and gaps are set at initial cold values. These values are assumed as reference, corresponding in the thermo-mechanical model to the initial geometrical distance between 2 nodes set on either side of the diameter/gap or at the extremities of the length. During the simulation they are monitored in order to point out the variation of their position respect to the 100% of the cold feature. Monitor nodes belong to the thermo-mechanical mesh, and displacements, to which they are subjected, are related to the corresponding fluid element feature (gap, diameter, etc.) through internal post-processing seamlessly from the user point of view.

Once set the geometrical initial values, a first adiabatic solution of the standalone aerodynamic model of the SAS is performed over the transient

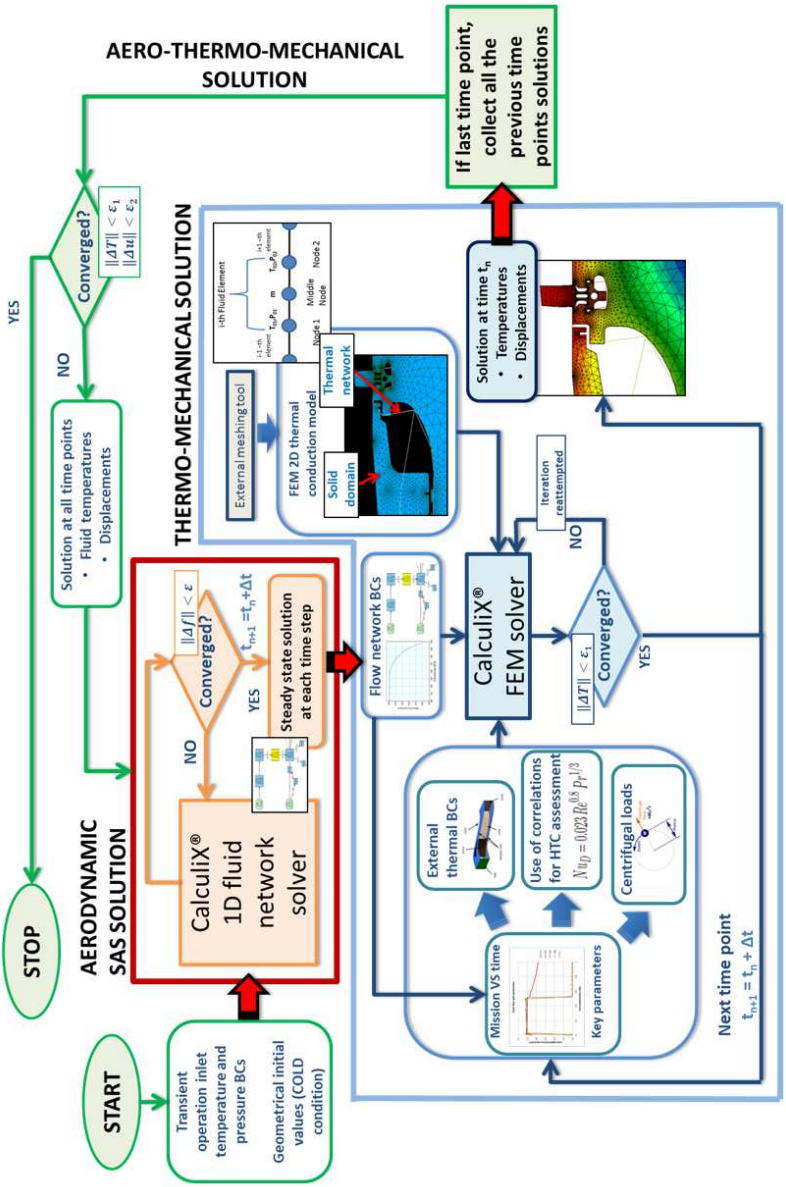

Figure 2.16: Whole iterative coupling process inside the procedure.

operation, by the knowledge of main flow annulus conditions which are impose once and for all at the beginning of the calculation. Variations on the main flow properties due to changes in clearances and SAS behaviour during the cycle are not accounted, since their impact on the primary flow is considered of negligible relevance. Therefore no iterations on the conditions of the main flow are performed.

Then first obtained fluid properties (mass flow rates, pressures and initial inlet temperature) through the SAS structure are imposed as boundary condition in the thermo-mechanical model in which a dedicated thermal network is imposed at the level of mesh for the solution of the heat transfer problem between fluid and solid domain. FEM model is also supplied with all the other boundary conditions varying in time.

The FEM model is stepped through the transient cycle according to the solution time step required by the user and by the convergence history. In particular the main execution program for each time step discretizing the transient operation, performs a nested iterative process in which the convergence in the coupled fluid network-thermomechanical fields is searched.

The coupling between the two fields is obtained through the imposition of the proper equations linking the unknowns of the fluid and solid domain. In particular, on the solid side mass flow rates and pressures from the secondary air system and boundary temperatures are used for the formulation of:

- Convective loads:

$$\dot{Q} = HTC \cdot A \cdot (T_w - T_{f,i}) \tag{2.16}$$

  where T_w is the local wall temperature and $T_{f,i}$ is the temperature of the i-th fluid element node linked to the portion of solid whose temperature is T_w. According to the Newton's law of cooling, the heat flux $\dot{Q}$ is expressed using the convective heat transfer coefficient HTC. This is a simplified engineering approach to the solution of internal flow problems [57]. Here fluid temperature represents the

bulk average energy input and the heat transfer coefficient accounts for the details of the local temperature distribution and the flow conditions. A monolithic approach is used to couple thermal fluid-solid fields through an "hard coded" convective condition which is treated as an advective boundary condition, since Eq. 2.16 is part of the Eq. 2.5. In the procedure this formulation requires the specification of the solid element or group of elements, the faces of which define the surface impacted. The fluid node or group of fluid nodes interacting with the surface must also be specified. Heat transfer coefficients are either specified directly in the model or internally accounted by the solver during calculations using a dedicated subroutine expressing correlations or other runtime quantities dependences.

- Mechanical loads referred to the action of the static fluid pressure on the material applied as a distributed load on the solid elements faces.

Meanwhile on the fluid side, temperatures are affected by the convective exchange, according to:

$$\dot{Q}_{i,j} = C_p \cdot \dot{m}_{ij} \cdot (T_{f,j} - T_{f,i}) \tag{2.17}$$

in particular the downstream extremity element node (the j-th node, supposing the i-th as the upstream) will be affected by the heat flux $\dot{Q}_{i,j}$ as in Eq. 2.17.

Using these boundary conditions to supplement the thermo-mechanical model, at each time step, temperatures and deformations are obtained from the thermo-mechanical analysis and the consequent changes in the structure and network temperatures are assumed as new conditions for the thermal solution for the next step.

Fluid/material temperature repartition and displacements are stored step by step, and post-processed at the end of the transient cycle. Once the last time step has been performed, overall temperature and displacements are compared with the values obtained from the previous run on the

transient operation.

Indeed, due to the heat transfer the predefined monitor nodes have been undergone axial and radial displacements, which have modified their relative position, along with the rest of the mesh nodes. Hence the variation of distance between the two monitor nodes is therefore estimated and compared with those recovered at the previous overall iteration. If convergence is not reach temperatures and displacements are elaborated and used to update geometries and the temperature levels through the standalone aerodynamic SAS model, in an iterative loop between the SAS analysis (block in red Fig. 2.16) and the thermo-mechanical one (block in blue Fig. 2.16), until a converged solution is reached (block in green Fig. 2.16).

Hence, the interaction and the effects of heat flux and geometry variations on the fluid-dynamic of the SAS are taken into account through this external loop. Weaker coupling through the displacements are resolved at the outer level with a simple fixed-point iteration. Iteration after iteration, the effect of fluid/solid heat transfer is taken into account through the imposition of new thermal boundary conditions on the internal nodes of the standalone aerodynamic network, as well as the effect of deformation is modelled with the application of new dimensions on significant geometric features of SAS elements, such as gaps and clearances.

Chapter 3

Code Customizations

CalculiX® original code has manifold remarkable native features, some of them already cited in the course of the procedure description and exploited in the methodology. However a number of aspects can not be faced with the original features of the code. Therefore there has been the need to modify the program in order to improve its functionalities and introduce the missing modelling features required for the whole engine simulation type.

Changes have been introduced in both the FEM and fluid network solvers. The customization, thought to cover the main aspects of interest in the modelling of a real machine, has been in some cases quite heavy, also because of the necessity to meet the requirement of the industrial practice for which the procedure have been tailored. As a consequence, reasons of confidentiality do not allow to disclose some details linked to the new models or features introduced in the procedure, as well as, about cases used for the assessment of itself.

Anyway, the more general applications and customizations will be presented in this Chapter with comprehensive discussions of the fundamental modelling aspects which are at the heart of the work and constitute the novelty of the present research. Among them, stator-rotor interface handling, pumping effects, dependence of the heat transfer coefficient

from runtime variable parameters subjected to the transient cycle and the effect of running clearances.

The new implementations have required a continuous application of debugging and testing, carried out in the first evaluation phase mostly with the usage of very simple test cases in order to assess the correctness of the implementations. The new blocks, models and features have been compared when possible with analytical solutions not requiring computer aided solutions, in all the other cases they have been compared with the solutions of some Ansaldo in house tools for the secondary air system analysis, and with some FEM reference codes for the thermo-mechanical solution. The tests have been performed with increasing levels of complexity:

- Firstly the new element/feature has been tested alone to ensure the coherence of CalculiX® computations respect to an analytical solution (if possible) or respect to a reference model, and detect therefore more easily eventual discrepancies.

- Secondly, configurations involving several elements/features of the same class have been modelled increasing the model dimension.

- Next, different class of models/features have been jointed in more complicated models in order to add complexity to the simulation: more complex networks with manifold branches have been submitted to the fluid network solver; models with higher number of feature, also interacting the one with the others, have been performed to test the new version of the FEM solver.

- Finally, real arrangements have been considered, with the aim to assess the physical coherence of the methodologies proposed and their consistency in the solutions with respect to the boundary conditions imposed.

In this Chapter some preliminary tests will be proposed just to clarify some aspects and to demonstrate how work progressed, whereas the more

complex geometries will be presented in the next Chapter 4, dedicated to the assessment of the presented procedure.

In the following Sections 3.1 and 3.2, customizations introduced in the reference original code CalculiX® version 2.11 are presented, referring respectively to implementations in the 1D fluid network solver and in the FEM code.

3.1 Fluid Network solver customizations

Actions on the fluid network solver regarded mainly:

- customizations required to meet the solution strategy of the industrial practice and the application of proprietary SAS elements (Section 3.1.1);
- some improvements in the in the solution strategy (Section 3.1.2).

Because of the nature of the above cited modifications strongly linked to the industrial proprietary knowledge, for some changes/adjustments only a general description can be provided.

3.1.1 Industrial best practice customizations and new elements library

Here below the main adjustments mostly oriented to introduce the procedure in the general industrial best practice, are presented.

3.1.1.1 New elements

Each class of elements corresponds to a given subroutine containing the loss coefficients and the flow equations of the type of element. This structure enables a greater flexibility for developments in terms of corrections, modifications or the addition of new elements. Concerning this latter aspect, a number of additional elements have been included in order to apply proprietary patterns and correlations, and model adequately some flow features not actually available in the current internet release. New elements have been mainly devised for:

- concentrated losses (inlet, contraction, enlargement and bend elements);
- effects of rotation (rotating inlet, pipe, gap, plenum and slit);
- cavity behaviour (vortex elements);
- filter effects;
- seals behaviour;
- leakage phenomena;
- impingements effects;
- efflux through vanes and blades (flow functions elements);
- imposed heat fluxes and pressure drops;
- recovery phenomena (ancillary element able to calculate the total pressure from the static one).

As already mentioned in the assessment practice, models have been firstly tested standalone and then jointed in more complex networks, up to test existing real engine SAS configurations, with a number of elements of some hundreds for whole engine configurations.

Calculation time is usually significantly below what reported by other proprietary solvers tested, e.g. on a 2.67GHz INTEL(R)Core(TM) i7 920 (Bloomfield) CPU machine, a portion of SAS network made of 338 elements including the typical elements typologies for SAS applications, runs in 6.5 seconds.

A variety of tests have been performed with the aim of stressing the solver, and ensuring a good testing campaign over the range of interest for such kind of applications. Error margin between CalculiX® and the in house reference software remained always small, with a relative error between the two systems, under the 1% for all the tests performed.

3.1.1.2 Solution with respect to static pressure

In order to meet the industrial practice and apply proprietary heat transfer and pressure libraries, it has be chosen to solve the system with respect to static pressure. All the elements included in the customized version of the fluid network solver are solved for the static pressure and the total temperature at their boundary nodes. On the contrary, the original code strategy is solving for the total pressure at the boundary nodes.

The choice of solving for the static is motivated by physical, mathematical and procedural argumentations:

- In a 1D code a unique static pressure can be associated to the outlet of e.g. a pipe or an orifice into a plenum: the static pressure at the outlet throat of a pipe is (unless choking) the same as the static pressure inside the outlet plenum, while the total pressure is different;

- Given the mass flow rate, the total temperature, the cross section and the static pressure at a given node, it is always possible to find the corresponding Mach as the positive solution of a quadratic equation: this solution always exists and can be found in explicit form. On the contrary, starting from the total pressure at a given section, an implicit equation (which may have no solution for high mass flow rates) is required to derive the Mach;

- Several correlations were already used in the static-to-static form, according to the industrial practice of matching static-to-static pressure drops with experimental data. A block with a static-to-static correlation can be fed with an inlet total pressure by inserting an appropriate upstream ancillary block which builds the total pressure from the static pressure value at that corresponding section. In this way the static-to-static correlation can be actually used as a total-to-static. An example is the flow function block which gives the mass flow rate as a function of the inlet to outlet

pressure ratio. If the ancillary element calculating the total pressure is placed upstream, the total pressure and not the static is stored at the inlet node of the flow function model, hence the flow function correlation can be used as a total-to-static.

3.1.2 Contributions to the improvement of SAS solution

The modifications reported below can be considered of common interest and oriented to the general improvements of the fluid network code. This aspects have been also shared with the CalculiX® original code developers.

3.1.2.1 Swirl variable

Preswirl devices are used to impart a tangential velocity to flow before it enters a rotating component. In this way, it is possible to reduce the loss due to the difference in circumferential velocity between the gas entering the rotating device and the rotating component itself.

An example is reported in Fig. 3.1, where v_{rot} is the rotational velocity of the orifice the preswirl nozzle is feeding, v_{abs} is the absolute velocity of the air leaving the preswirl nozzle and v_{rel} is the velocity in a reference frame rotating with the orifice (relative velocity). The tangential component v of the velocity of the rotating device as seen by the air leaving the preswirl nozzle (which is $-v_{rel}$) is the swirl component of the velocity and is a very significant quantity for the assessment of the SAS behaviour and performances.

However CalculiX® original fluid network solver performs solutions in terms of total temperature, total pressure and mass flow rate only, whereas swirling effects are taken into account in some elements such as preswirl nozzle or vortex, but the tangential velocity must be set as an imposed input of the model. A propagation of this quantity inside the system is not provided, neither equations of conservations.

Therefore, swirl has been added in the solution performed by the solver through the insertion of a new dedicate unknown to be resolved

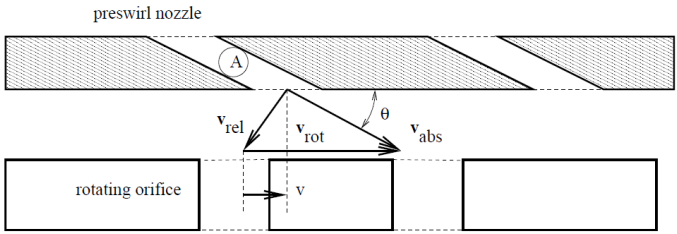

Figure 3.1: Geometry of a preswirl nozzle and the orifice it feeds [52].

together with total temperature, pressure and mass flow. In particular the new variable added in the custom library is the tangential velocity, defined at the boundary nodes of each element (as the static pressure or the total temperature).

Unlike the original CalculiX® code, where the user had to specify where a rotating cavity had to take its input swirl from, this extended library is able to automatically deal with the mix and split of tangential velocities at junctions, even in presence of reverse flow, according to the network topology. Indeed, the swirl management foresees that the circumferential velocity is propagated by mix nodes. The same approach used for temperature is applied, i.e. the swirl is determined in the mixing nodes as a weighted average with mass flow rates of the branches merging in the mix node at stake.

From the point of view of the equation solution, swirl is solved in a previous separate step. First, solver carries out the solution of swirl component at fixed mass flow rates, then in a second step it executes the standard coupled solution of pressure, temperature and mass flow rate with fixed swirl component.

The setting of the swirl value at the inlet boundaries is done with a dedicated block for the imposition of such boundary.

Equations are written in order to propagate correctly the swirl also in case of flow reversal.

3.1.2.2 Temperature and swirl at the outlet boundary nodes

In case of flow reversal it is very important to specify the exit temperature boundary condition at the outlet nodes of a network. These values are used in case flow changes direction respect to that expected by the user in the setting of the fluid network, eventually just for intermediate iterations during the calculation.

In the native code once a boundary condition is specified the corresponding node is not solved and its value (temperature) is held fixed, even if the assignation of the used could not correspond to the real solution of the node.

In the new version, therefore, the correct temperatures and the swirl values are taken from the upstream node (boundary condition on the node is therefore redundant) and overwritten after the network calculation, if the last element before an output node does not change the temperature and swirl. Otherwise a dummy argument (e.g. orifice with unitary discharge coefficient and large section area) is insert in the case a model changing temperature/swirl is linked to the output BCs node.

3.1.2.3 Convergence check

Convergence checks are very important not only for the solution accuracy but also for the execution time. Therefore adequate thresholds have to be applied, but also proper convergence verifications have to be imposed.

The native convergence check algorithm consists in the evaluation of the current Newton Raphson correction (for pressure, mass flow and temperature) with respect to the highest correction ever met from the beginning of the iterations. The former must be less than a fraction (set by the user) of the latter. In the same time the current Newton Raphson largest residual must be less than a fraction of the average of the largest residuals from the beginning of the iterations.

The original algorithm above is prone to problems in case of a series of residuals convergent to zero but never being less than its average from

the beginning: it may happen that a perfectly convergent network cannot be seen as convergent. For this reason a new convergence check algorithm, based on the simple condition that for all the nodes and all the variables (pressure, temperature, mass flow and swirl) the related correction must be less than a required tolerance, is added to the original algorithm.

Also the native algorithm of non-convergence criterion has been revised and subjected to less restrictive parameters. When the pressure (or temperature) is negative, or number of iterations is greater than a given value, or the largest correction at a given step is greater than the largest correction at the previous step, the network is detected as divergent and re-inizialized with a smaller over relaxation parameter. The default values for testing the non-convergence conditions were rather strict and might prevent the detection of convergence in a quite large number of real SAS cases. For this reason convergence parameters have been readjusted in order to guarantee effective convergence, avoiding stops due to a not real detection of divergence.

3.1.2.4 Stability of the solution - Derivative decoupling between mass flow and temperature into the Jacobian matrix

In some cases of large networks, it was detected that starting from a guessed mass flow distribution across the network (far from the correct one) CalculiX® experienced large temperature oscillations during convergence, which could not be damped by a normal under relaxation.

This behaviour has to be traced back to the fact that CalculiX® uses a full coupled approach to solve mass flow, pressure and temperature which is not usually necessary in the solution of standalone adiabatic networks. In particular the derivative with respect to the mass flow is coupled with the temperature in the enthalpy equation and with the pressure in the pressure drop definition, characteristic of each element.

As a result of the coupling, unlike reality, the mass flow rate will be very sensitive to the temperature variations. For complicate networks this coupling prevents convergence.

To overcome the problem, a decoupling between mass flow and temperature has been introduced by imposing to zero the derivative of the temperature degree of freedom respect to mass flow degree of freedom into the Jacobian matrix. This solution allowed to fix the main part of convergence issues in the the tested real SAS network.

3.1.2.5 Improved residual functions for element blocks - Square roots and multiple solutions

In CalculiX® the residue formula of a fluid element is derived from the momentum equation. Equivalent equations can be used to have a different form of the formula, and in some critical cases a particular form can be more suitable than others. Many elements have equations including square roots as:

$$\begin{aligned} f &= \dot{m} - \sqrt{(p_{in} - p_{out})} && \text{if} \quad p_{in} > p_{out} \\ f &= \dot{m} + \sqrt{(p_{out} - p_{in})} && \text{if} \quad p_{out} > p_{in} \end{aligned} \tag{3.1}$$

However the square root can lead to convergence problems due to the first derivative which van cause overshooting. In many elements of the new library, this equivalent form has been implemented:

$$f = \dot{m}|\dot{m}| - |p_{in} - p_{out}| \tag{3.2}$$

This formula avoids overshooting issues and convergence problem.

3.2 FEM solver customizations

Actions on the FEM solver regarded mostly:

- customizations introduced to meet requirements related to:
  - the proposed WEM solution approach, and among them:
    - a procedure dedicated element (Section 3.2.1);
    - a proper automatic HTC scaling according to the specific BCs typical of WEM applications (Section 3.2.2);

  - the proprietary heat transfer libraries (Section 3.2.3);

- addition of features and models for the simulation of those phenomena which was not possible to reproduce with the original code, and among them:

  - variable rotational velocity (Section 3.2.4);
  - rotational effect handling (Section 3.2.5);
  - heat pickup (Section 3.2.6).

The same considerations made for the fluid network customizations about non-disclosure agreements limiting the possibility of showing some details or tests, are still valid.

Here below the main modifications applied to the internet release version 2.11 of CalculiX® code are described.

3.2.1 Generalized element for thermal network application

As explained in Section 2.2.5, a different type of network is adopted for the aerodynamic and thermal solutions.

In the previous Section, customizations introduced at level of aerodynamic solution have been explained, referring to the introduction of new elements and some improvements/changes in the solution strategy.

Now here it is proposed a description of the customizations introduced at level of the fluid elements but in the field of the thermal network for the thermo-mechanical solution.

The customization regarded the introduction of a generalized element, with a number of new inputs, required to transfer the needed information to the procedure. We refer to a *generalized* element since in the thermal solution, no mass flows or pressures have to be solved, but only the temperature is estimated, and therefore there is no need to specify a characteristic element typology (pipe, seal etc). The fluid element for the thermal network can be interpreted as a box in which inserting some

geometrical information, and through which codifying commands for the solver.

Hence, the *generalized* element of the thermal network has been implemented with the task to transmit a number of inputs to the procedure, such as:

- geometrical information for the HTC calculation through correlations:
  - cross section area,
  - diameter,
  - length of the element,
  - grain diameter at the element surface,
  - etc.
- information for the automatic calculation of the effect of the rotation on the temperature:
  - inlet and outlet radius,
  - rotational speed,
  - swirl ratio,
  - swirl velocity (mutually exclusive with the swirl ratio),
  - etc.
- flags for the activation of the treatment of some other particular features.

This kind of customized element is applied in the procedure to each fluid branch subjected to heat transfer, therefore it is used not only for the SAS application but also for the main flow characterization (Fig. 3.2), when convective heat transfer conditions are imposed. In this case the temperature set at the inlet evolves in space and time, during the simulation due to the heat transfer with metal, and/or because of the presence of additional phenomena, such as the rise in temperature throughout the compressor annulus due to compression effects, for instance.

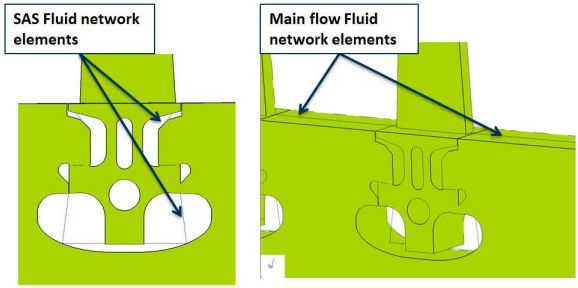

(a) Coupling of fluid elements and solid domain in SAS and main flow regions.

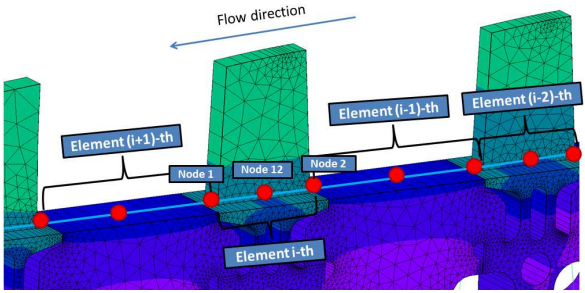

(b) Main flow fluid elements details.

Figure 3.2: Applications of the generalized fluid network element and coupling with solid domain [27].

3.2.2 Axisymmetric-plane stress elements coupling and HTC scaling

The procedure is devised for the solution of a fully featured 2D axisymmetric gas turbine models, where stator and rotor components are modelled as axisymmetric, exception for the zones of the mesh corresponding to channels, holes, bores, blades and nozzles. Indeed since the geometry is modelled in 2D, suitable area and volume multipliers are considered for all non-axisymmetric features. It is not the only possible solution, in literature also other characterizations are reported, for in-

stance components like blades can be not physically modelled and the effect of heat transfer from aerofoils hub and tip regions can be considered using experimentally validated coefficients [47].

In the proposed procedure in case of non-axisymmetric features the element type applied is the plane stress with appropriate modelling assumptions to account for 3D features. This follows the conventional industrial practice where features such as bolts, holes, etc. are modeled using an equivalent wall thickness and a proper HTC values scaling.

In addition, in case of bores, holes and channels, the thickness of elements simulating the material present in the circumferential direction between a channel and the other, must be properly shaped in order to guarantee a coherent plane stress thickness distribution along the radius. The aim is to assign a thickness not equal for all nodes in the span direction but linearly increasing with the radius respecting the correct ratio between solid and empty volumes in the circumferential direction at each radius location. The thickness calculation is performed by an in-house tool of pre-processing, devised also for a number of other functions which will be better introduced in Section 3.3.4.

In order to solve the 2D axisymmetric domain, CalculiX® uses on the 2D model solution an expansion angle fixed at 2° and plane element thickness is scaled automatically by the solver in order to consider the proper fraction of material on the expansion angle of 2°. In other words the assigned thickness ($t_{assigned}$) is divided by 180 ($Thickness = t_{assigned}$ /180, Fig. 3.3). The scaling is also automatically applied to the mass flow rate. These aspects affect in their turn the assessment of the HTC to be applied, as well as the consideration of the effective surfaces available for the loads application in the interfaces between plane and axisymmetric elements does.

Since a correspondent automatic scaling is not applied to HTC coefficients, this has required a dedicated implementation accounting:

- the 2° expansion,
- the consequent thickness and mass flow scaling,

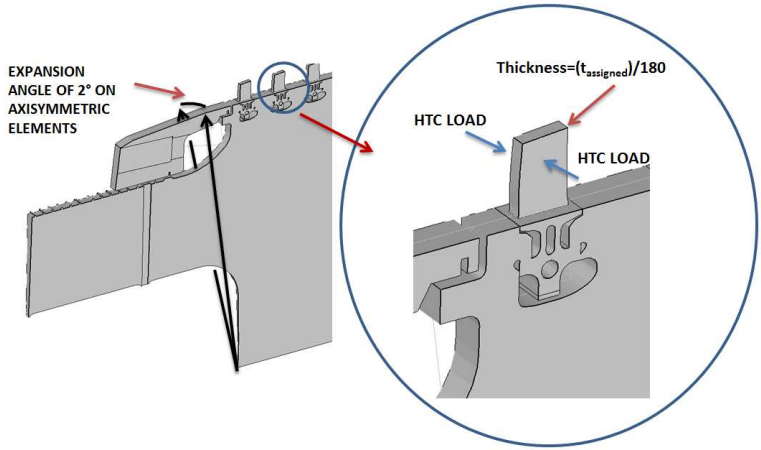

Figure 3.3: Axisymmetric-plane elements coupling and thickness handling [27].

- the typology of surfaces on which the HTCs are applied, i.e. if developed from axisymmetric elements or from the thickness of plane elements.

All these aspects are taken into account to correctly scale heat transfer coefficients assigned by the user or obtained from correlative approaches, in order to respect the energy balance in the 3D phenomena approximation with 2D modelling.

In general different cases of HTC scaling have to be faced in a WEM procedure, the main typologies are illustrated in the following sub-sections.

3.2.2.1 HTC scaling on plane elements: Blades

The simplest example of implemented scaling is that applied to the blade HTCs. First, see that on a blade row the globally assigned thickness on the corresponding plane elements is:

$$t_{assigned} = t_{blade} \cdot N_{blade} \tag{3.3}$$

where t_{blade} is the thickness of the single blade and N_{blade} is the number of blades in the row.

Considering the thickness and mass flow scaling, and considering that the surface of application of the HTC coefficient on a blade correspond to the sum of the 2D plane faces (see Fig. 3.3), the HTC to be assigned is:

$$HTC = (HTC_{bladeFace} \cdot N_{blade})/180 \tag{3.4}$$

where $HTC_{bladeFace}$ is the HTC value assigned on the blade surface on the single rear and front face of the plane element expansion on the 2°, applied by the user or obtained through the proper correlation.

3.2.2.2 HTC scaling in axisymmetric-plane elements coupling: Holes

Consider the 2D mesh of the Fig. 3.4. The region delimited by the edges in blue (Fig. 3.4a) is the region of the hole and it is modelled with plane elements with proper thickness, whereas all the others are axisymmetric elements. The thickness applied is the result of the subtraction of the empty volume from the solid. In the case of a number of holes in parallel, the empty volume will be the empty volume of the single hole, multiplied for the global number of holes.

Suppose user wants to apply an HTC coefficient for the characterization of the convective heat transfer between a fluid flowing inside the hole and the surfaces of the hole. It is possible to apply the HTC on the 2D faces of the plane elements, or on the edges in red (Fig. 3.4b), or on both. In the first case (application on the red surface in Fig. 3.5), the scaling to be applied is the same demonstrated in the case of HTC on blades in the previous sub-section. In the second case, user can apply the HTC or on the thickness of the plane (banded surface in Fig. 3.5) or on the surface of the axisymmetric element sharing the common edge (green surface in Fig. 3.5). In the third case, user could apply the heat load on the plane thickness or on the axisymmetric surface, and on the 2D normal and reverse face of the plane.

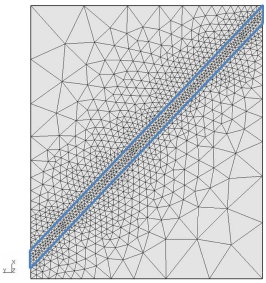

(a) Region of the holes in parallel, modelled with plane stress elements with proper thickness.

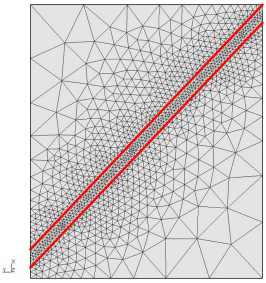

(b) Edges defining the surfaces on the axisymmetric side, on which HTC coefficients are applied.

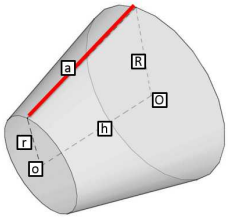

(c) Surface generated by each red edge of Fig 3.4b: lateral surface of a truncated cone with the "a" dimension corresponding to the red edge of Fig 3.4b.

Figure 3.4: HTC scaling on the interface of plane-axisymmetric elements in holes.

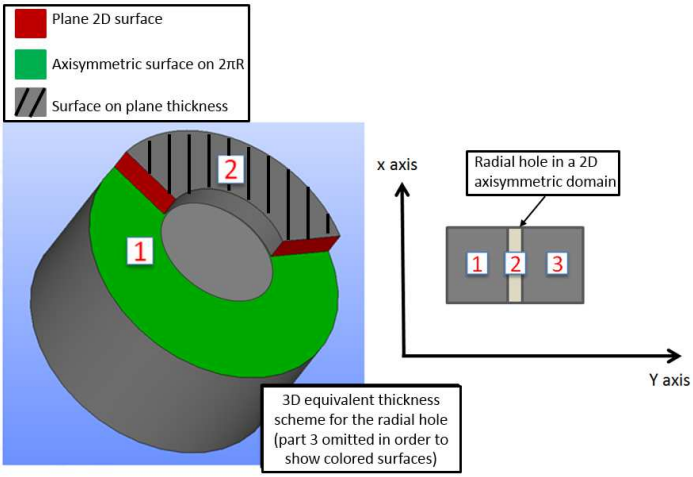

Figure 3.5: Axisymmetric approach: 3D equivalent thickness scheme for a radial hole.

In the procedure the choice of apply the heat load on the axisymmetric element surface has been made. However in CalculiX® this means that the surface on which the HTC value will be applied is the surface obtained from the revolution of the edge on the 360° (Fig. 3.4c). Obviously this surface does not coincide with the real one, which corresponds instead to the inner surface of the bore multiplied for the number of bores.

Hence, there is the need to properly scale the HTC coefficient which will be assigned on the 360° axisymmetric surface (lateral surface of a truncated cone, Fig. 3.4c) in order to maintain the correct product $A \cdot HTC$ corresponding to reality.

The scaling is provided considering the following equivalence over the single involved element of the mesh:

$$HTC_{axi} \cdot A_{Element\ on\ 2 \cdot \pi \cdot R} = HTC_{real} \cdot A_{half\ cilindrical\ portion\ of\ the\ hole} \tag{3.5}$$

where HTC_{axi} is the scaled value to be applied in the CalculiX® model

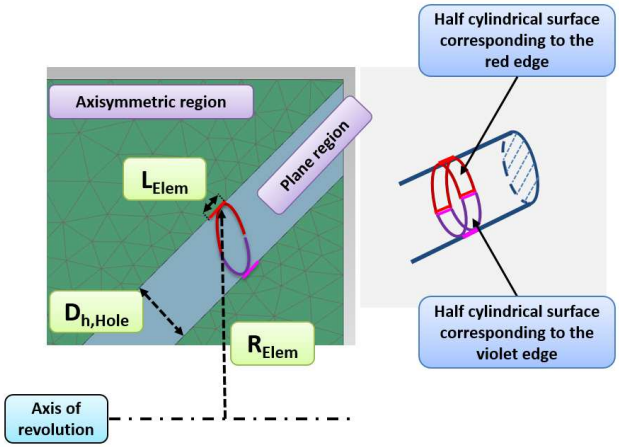

Figure 3.6: Axisymmetric-plane interface and HTC scaling on holes.

in order to account the surface of application used by the solver, while HTC_{real} is the real value which should be applied on the inner surface of the duct and which is a value provided by the user or calculated by the solver through a dedicated correlation.

The equivalence comes from the idea that each element of length L_{Elem} generates on the 360° a surface whose counterpart in reality is the half lateral surface of the cylinder of height L_{Elem} (Fig. 3.6), where L_{Elem} is a portion of the global hole of length L_{Hole}:

$$L_{Hole} = \sum_{i=1}^{n} L_{Elem,i} \tag{3.6}$$

where n is the number of elements on the single edge defining the duct (Fig. 3.6).

Eq. 3.5 in geometrical terms becomes therefore:

$$HTC_{axi} \cdot 2 \cdot \pi \cdot R_{Elem} \cdot L_{Elem} = HTC_{real} \cdot (2 \cdot \pi \cdot R_{Hole} \cdot L_{Elem})/2 \tag{3.7}$$

where R_{Elem} is the average radial quota of the element (corresponding to

the radius of the mean point of the edge), L_{Elem} is the length of the edge of the 2D element at stake (located in the interface between plane and axisymmetric domain), and R_{Hole} is half of the hydraulic diameter of the channel ($D_{h,Hole}/2$).

Then, Eq. 3.7 can be simplified and the scaling formulation of the HTC coefficient inside a hole is obtained as:

$$HTC_{axi} = HTC_{real} \cdot \frac{R_{Hole}/2}{R_{Elem}} \tag{3.8}$$

Considering the total number of holes, the value to be applied is:

$$HTC_{axi} = HTC_{real} \cdot \frac{R_{Hole}/2}{R_{Elem}} \cdot N_{Hole} \tag{3.9}$$

where N_{Hole} is the number of holes in parallel in the real model.

3.2.2.3 HTC scaling in axisymmetric-plane element coupling: Endwalls

Consider Fig. 3.7 representing a scheme of a rotor equipped with blades. If user wants to impose an HTC value in the region between a blade and the other, it is necessary to take in mind that applying the HTC on the edge delimiting the blade from the rotor in the 2D model, on the axisymmetric side, the solver will consider as area of exchange, the global surface of revolution on the $2\pi R$ (surface in green in Fig. 3.7).

Therefore, also in this case, there is the need to scale the HTC referred to the endwall of the blades row. This is due to the fact that the surface overs which the endwall HTC value effectively acts is the green surface reduced of the red surface in Fig. 3.7, multiplied for the blades number.

The necessary scaling is based on the equivalence that the $2\pi R$ surface developed by the edge of the axisymmetric element on the 360° must correspond to the real one of application through a multiplier, in order to maintain the correct product $A \cdot HTC$:

$$HTC_{axi} \cdot A_{Element\ on\ 2 \cdot \pi \cdot R} = HTC_{real} \cdot A_{real} \tag{3.10}$$

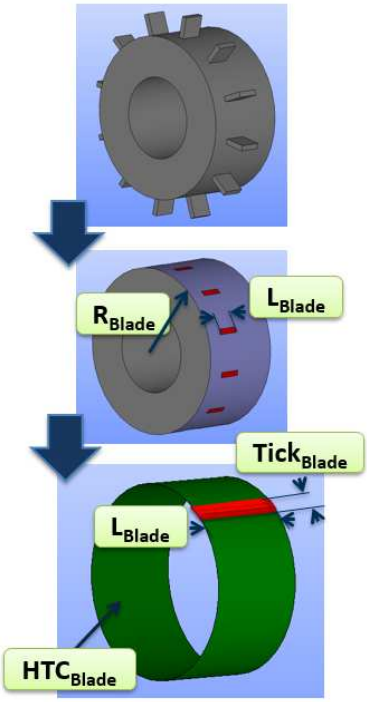

Figure 3.7: Scheme of axisymmetric-plane interface and HTC scaling on endwalls.

where:

$$A_{real} = 2 \cdot \pi \cdot R_{Elem} \cdot L_{Elem} - Thick_{Elem} \cdot L_{Elem} \tag{3.11}$$

where L_{Elem} is the length on the 2D model of the element edge delimiting axisymmetric domain from the plane one, $Thick_{Elem}$ is the thickness associated to the specific element, and R_{Elem} is the average radius of the element (Fig 3.8).

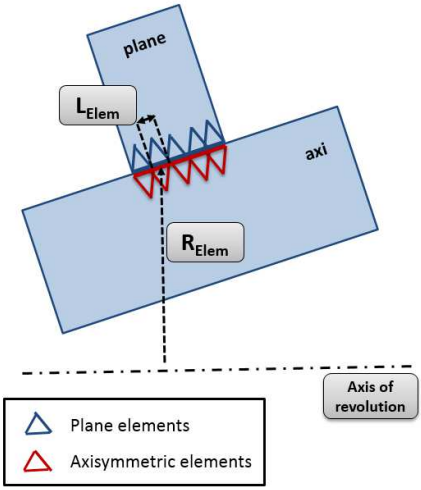

Figure 3.8: Axisymmetric-plane interface on endwalls with non-constant radius.

Therefore the equivalence becomes:

$$HTC_{axi} \cdot 2 \cdot \pi \cdot R_{Elem} \cdot L_{Elem} = HTC_{real} \cdot (2 \cdot \pi \cdot R_{Elem} \cdot L_{Elem} - Thick_{Elem} \cdot L_{Elem}) \tag{3.12}$$

The scaling formulation of the HTC coefficient on endwalls, at the interface of axisymmetric rotor elements and blades plane elements is therefore:

$$HTC_{axi} = HTC_{real} \frac{(2 \cdot \pi \cdot R_{Elem} - Thick_{Elem})}{2 \cdot \pi \cdot R_{Elem}} \tag{3.13}$$

Considering the total number of blades, the value to be applied is:

$$HTC_{axi} = HTC_{real} \frac{(2 \cdot \pi \cdot R_{Elem} - Thick_{Elem} \cdot N_{Blade})}{2 \cdot \pi \cdot R_{Elem}} \tag{3.14}$$

where N_{Blade} is the number of blades in the simulated row.

The proposed scaling is the general scaling to be adopted in presence

of axisymmetric-plane interface, with the exception for the simulation of a hole, for which the implementation illustrated in the previous sub-section is required. In the other generic case the scaling to be applied must simply take into account that at each radius the real exchange surface is that generated by the axisymmetric element on the $2\pi R$, minus the surface occupied on the $2\pi R$ by the thickness of the correspondent plane element, according to the relation in Eq. 3.13.

3.2.2.4 HTC scaling for plane-plane interfaces

Consider Fig. 3.9 and suppose to have plane elements with different thicknesses on the solid geometry, and a fluid element exchanging heat with the 2D plane elements of component 2 (yellow surface in Fig. 3.9b-c) and on purple surfaces of components 1 and 3 (Fig. 3.9b-c).

For the heat transfer on the yellow surface, there is no scaling to be performed since CalculiX® will apply the HTC on the yellow surface which corresponds exactly to the real one, therefore user has simply to indicate the convection coefficient on the normal faces of plane elements. Instead, for the application of the HTC on the purple surfaces, it is necessary in the 2D model to impose the HTCs on the purple edges (Fig. 3.9a) considering elements on the purple sides of components with higher thickness (1 and 3 in Fig.3.9).

Considering that the real surfaces of exchange for the purple sides is the difference between the different thicknesses of components, the HTC scaling for the sides should consider that CalculiX® will apply the HTC on the global thickness of elements of components 1 and 3, while the real surface for sides is the difference between thicknesses 1-2 and 3-2.

Hence, the implemented strategy foresees the application of the HTC on the thicker element and an automatic scaling obtained from the equivalence:

$$\begin{aligned} HTC_{plane} \cdot Thick_{max,Elem} \cdot L_{Elem} = \\ HTC_{real} \cdot (Thick_{max,Elem} - Thick_{min,Elem}) \cdot L_{Elem} \end{aligned} \tag{3.15}$$

where HTC_{plane} is the HTC value applied on the thicker element and

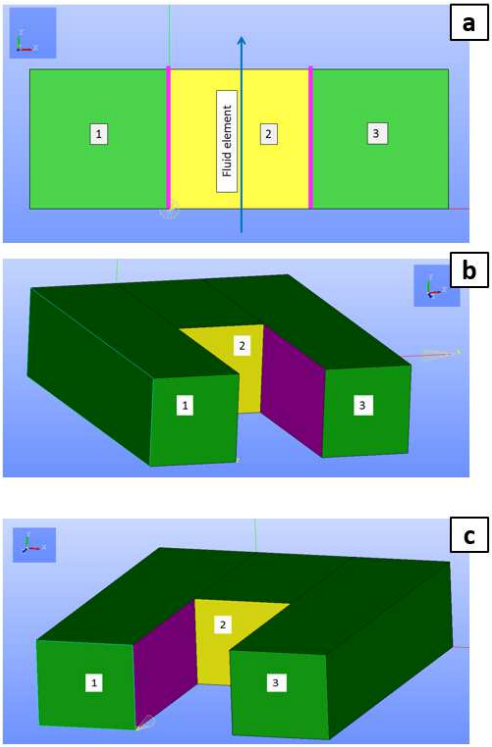

Figure 3.9: Plane-plane interface and HTC scaling.

scaled to take into account the difference between the real surface of application and that used by the solver; $Thick_{max,Elem}$ and $Thick_{min,Elem}$ represent the higher and smaller thickness on the element edge at the interface between the two domains characterized by different thicknesses.

The scaling formulation of the HTC coefficient on interfaces between plane elements with different thickness can be written therefore as:

$$HTC_{plane} = HTC_{real} \frac{(Thick_{max,Elem} - Thick_{min,Elem})}{Thick_{max,Elem}} \tag{3.16}$$

3.2.3 HTC customized library

As mentioned on several occasions, in CalculiX® there is the possibility to implement in a dedicated user subroutine the HTC correlations the user wants. User can provide the HTC value as a fixed constant one, by simply assigning it in the file of the model, or he can let the solver compute runtime the HTC value according to the relation chosen. Indeed he can call in the file the proper label of the correlation desired, taken from those implemented in the library. In the user subroutine, information about both fluid and solid elements are available and usable to compose customized expressions. Information regards:

- geometrical features and all the other inputs (flags, rotational speed etc.) of the fluid element involved in the convective heat transfer,
- fluid proprieties (heat capacity, viscosity, conductivity)
- geometrical information of the element exchanging heat with the fluid (radial location, area),
- solution at the previous iteration, if user wants to establish a dependence on runtime variables.

This is a very important feature since free the user to apply the correlations he deems appropriated for the the specific case and allows to impose a dependence of the heat transfer coefficient from the variable quantities of the calculation, being them boundary conditions varying in time or runtime calculated quantities.

A number of correlations have been implemented in the procedure, most of them derived from customized relations coming from the industrial best practice. They regard the calculation of HTC in the different zones of the machine, readapting (in a number of cases) literature correlations, such as those for internal flow, flat plate, free disk, rotating hole, stator-rotor cavity, natural buoyancy and others.

They are customized in terms of applied multipliers and coefficients coming from the best practice, in order to fit more complicated real cases

such as heat transfer in compressor disk internal cavity and holes, plena for bleeds, middle hollow shaft and shaft cover, turbine disk and casing, stator-rotor cavities. These coefficients result from tuning activities in order to match data coming from measurements, and hence with the aim to calibrate the model.

In order to allow the insertion of such coefficients, the code has been further modified allowing the insertion in the model setting of factors multiplying the runtime correlations results without the need to modify the correlation formulation and recompile the code.

3.2.4 Variable Rotational velocity

A variable rotational speed in the original code can be applied only in the case of centrifugal loads (which can be set variable in time), but not on fluid elements. For a number of native standard fluid models, a velocity can be set, but it is considered constant in time and no variation can be imposed.

Anyway in a WEM approach for the simulation of variable conditions of the engine, having a variable rotation velocity is a mandatory requirement, especially for the execution of transient phases. Therefore a dedicated modification of the code has been necessary.

According to the new implementation, a time history must be defined in the model according to variable rotational speed of components. The variable rotational velocity is imposed as any other boundary condition changing in time. Then, according to a specific codification of the name used for the identification of the rotational speed inside the code in the dedicated subroutine, the actual value of the speed is detected and stored for the current time. The information is used where required, specifically it is utilized in the subroutine called for the calculation of the rotational effects on the total temperature of fluid elements and for the evaluation of rotation effects on the heat transfer.

3.2.5 Rotational effects handling

Rotation introduces effects both on the solid and fluid domain.

Concerning the metal, centrifugal distributed loading can be applied to rotating components. The centrifugal load is characterized by its magnitude (defined as the rotational speed square ω^2) and two points on the rotation axis.

Other effects must be consider with respect to the variation in temperature in fluid elements and with respect to the effect on the heat transfer between solid and fluid domain. They have to be accounted by managing properly the effect of rotation on the total temperature of nodes and elements.

3.2.5.1 Pumping effects

Temperature increment due to rotation is considered in the original reference code in case of aerodynamic network, but it is not treated at all in the case of purely thermal network properly said.

Using aerodynamic network switched to purely thermal (see Section 2.2.5), we use the network as a thermal, but we inherit some features of the aerodynamic one, in this case the capability of accounting pumping effects on the total temperature. Therefore the generalized element (Section 3.2.1) has been included among those elements of the network for which effects of pumping are calculated on the corner nodes.

The formulation is derived from the conservation of the rothalpy, and serves to simulate the action of rotation on the fluid domain, i.e. the pumping effects acting on flows along channels and cavities. They are taken into account providing concentrated heat fluxes on the outlet fluid node of each i-th fluid element involved in the phenomenon (Fig. 3.10).

Assuming a relative frame of reference, these heat fluxes are a function of the radius R through the radial variation of temperature$\triangle T_{0,rel}\,(R)$, according to:

$$\dot{Q} = \dot{m} \cdot c_p \cdot \triangle T_{0,rel}\,(R) \tag{3.17}$$

The term $\triangle T_{0,rel}\,(R)$ for a rotating channel can be derived from the

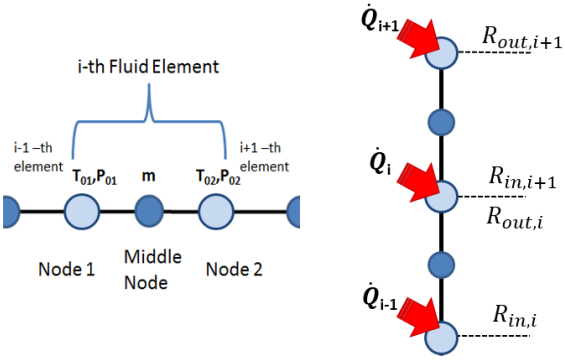

(a) $\dot{Q}_i$ to the exit corner fluid nodes, topological scheme.

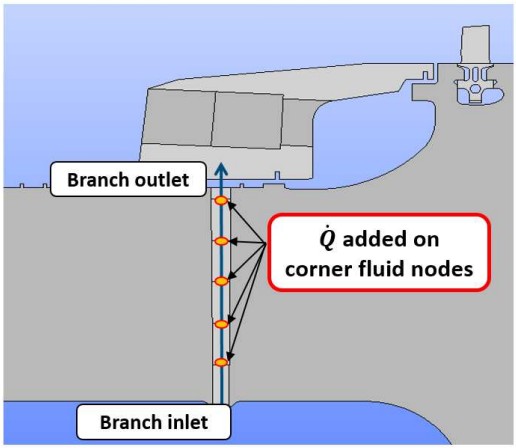

(b) $\dot{Q}_i$ to the exit corner fluid nodes of a network branch inside a rotating channel.

Figure 3.10: Pumping effects: concentrated heat fluxes on fluid nodes.

rothalpy conservation expressed in the following form (with the assumption of a constant c_p):

$$c_p T_s + \frac{W^2}{2} - \frac{U^2}{2} = const \tag{3.18}$$

considering:

$$T_{0,rel} = T_s + \frac{W^2}{2c_p} \tag{3.19}$$

where U is the circumferential velocity of the rotating device at the selected radius, C is the velocity of the gas at the same location, C_t its circumferential component and W is the relative velocity of the gas.

Hence, $\triangle T_{0,rel}$ for the i-th fluid element can be written as:

$$\triangle T_{0,rel,i} = \omega^2 \cdot \frac{\left(R^2_{out,i} - R^2_{in,i}\right)}{2c_p} \tag{3.20}$$

Therefore assuming the heat transfer solution is carried out in a relative frame of reference, for the case of generalized pipes, if rotation occurs, the outlet node temperature will change according to the Eq. 3.20, where ω is the rotational speed and R_{in} and R_{out} are the radius of the inlet and outlet corner nodes of the i-th element.

Finally, to implement the temperature changes generated by the pumping effect, the additional artificial heat flux specified in Eq. 3.17 is added to the outlet node energy balance of the i-th element (see Eq. 2.5).

3.2.5.2 Change of reference system

When fluid passes from a stationary device to an other rotating (and vice-versa), the need to account the change in temperature due to the value transition from the absolute frame of reference to the rotating frame (and vice versa), arises.

This capability is implemented in the *reference change* models included with the *generalized* element, in the thermal network adopted by the procedure. The transformation takes place at a given radius and the element has a physical length of zero. The formulation is derived from the consideration of the relations existing among components in the velocity triangle.

Again, consider U to be the circumferential velocity of the rotating device at the selected radius, C the velocity of the gas at the same location and C_t its circumferential component (Fig. 3.11a). The velocity of the

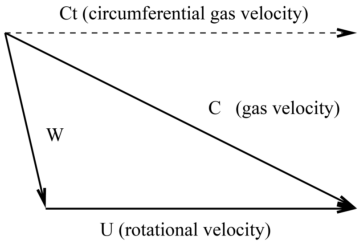

(a) Velocity triangle.

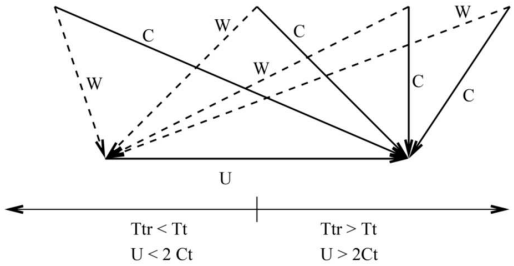

(b) Total temperature dependence on the circumferential component of the incoming flow.

Figure 3.11: Change of reference frame: dependences between stationary and rotating frames [52].

gas W in the rotating system satisfies [52]:

$$W = C - U \tag{3.21}$$

The total temperature in the absolute system is:

$$T_{0,abs} = T_s + \frac{C^2}{2c_p} \tag{3.22}$$

whereas in the relative system it amounts to:

$$T_{0,rel} = T_s + \frac{W^2}{2c_p} \tag{3.23}$$

Combining these equations and using the relationship between the length of the sides of an irregular triangle (cosine rule) one arrives at:

$$T_{0,rel} = T_{0,abs}\left(1 + \frac{U^2 - 2UC_t}{2c_p T_{0,abs}}\right) \tag{3.24}$$

therefore the change in temperature is:

$$T_{0,abs} - T_{0,rel} = -\frac{U^2 - 2UC_t}{2c_p} \tag{3.25}$$

and it is implemented through the same method of the previous subsection, applying an additional heat flux (see Fig. 3.10a) on the energy balance equation of the fluid node modelling the reference frame passage at the considered radius.

According to the size of $2C_t$ compared to the size of U, the relative total temperature will exceed the absolute total temperature or vice versa, as reported in Fig. 3.11b.

3.2.5.3 Correction for wall rotation

An other important topic regarding rotational effects managing is the evaluation of the effect of the surface rotation on the heat transfer.

This type of estimation was totally absent and a specific implementation has been added inside the original code. In particular it regards the issue of considering the fluid network in an absolute reference frame while it is exchanging heat also with a rotating surface, therefore belonging to a relative reference frame. A typical example is the case of air flowing in the interface between statoric and rotoric components (Fig. 3.12).

The fluid network located between rotor and stator exchanges heat with both rotor and stator components at its own total temperature. Each node of this stream is characterized by only one value of total temperature. There is therefore the necessity to chose in which reference frame (absolute or relative) consider the fluid branch. The issue regard the fact that the stator surface exchanges with the fluid at its own total absolute temperature ($T_{0,abs,fluid}$), while the rotor, due to its rotation,

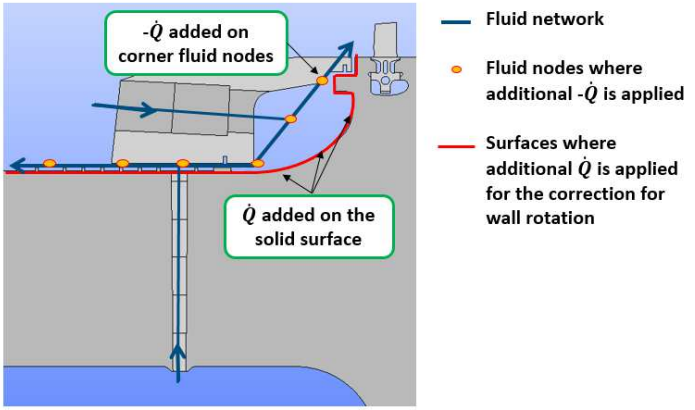

Figure 3.12: Example of a rotor-stator interface.

exchanges with the fluid at its own total relative temperature ($T_{0,rel,fluid}$).

Considering the stream in the absolute frame of reference, a correction in terms of an additional distributed heat flux is applied to the rotor side on the rotor elements facing the fluid, and with opposite sign on the fluid nodes of the stream. In a reference frame build-in with the rotor the heat exchange between fluid and rotor wall surface is:

$$\dot{Q} = HTC \cdot A \cdot (T_w - T_{0,rel,f}) \tag{3.26}$$

Eq. 3.26 can be rewritten as:

$$\dot{Q} = HTC \cdot A \cdot (T_w - T_{0,abs,f} + T_{0,abs,f} - T_{0,rel,f}) \tag{3.27}$$

then:

$$\dot{Q} = HTC \cdot A \cdot (T_w - T_{0,abs,f}) + HTC \cdot A \cdot (T_{0,abs,f} - T_{0,rel,f}) \tag{3.28}$$

defining:

$$\dot{Q_{conv,1}} = HTC \cdot A \cdot (T_w - T_{0,abs,f}) \tag{3.29}$$

$$\dot{Q}_{conv,2} = HTC \cdot A \cdot (T_{0,abs,f} - T_{0,rel,f}) \tag{3.30}$$

we obtain:

$$\dot{Q} = \dot{Q}_{conv,1} + \dot{Q}_{conv,2} \tag{3.31}$$

Notice that $\dot{Q}_{conv,1}$ is already calculated by CalculiX® in the convective heat exchange between rotor walls, considered in the absolute frame of reference, and the fluid network. It is applied automatically with the proper sign to the wall element and to the fluid node. On the contrary $\dot{Q}_{conv,2}$ is a correction for the wall rotation and it has been imposed through a distributed heat flux on each mesh element involved. According to Eqs. 3.25 and 3.30, and to the solver flux sign convention, referring to a single k-th element on the solid mesh exchanging heat with the j-th node of the fluid network, the $\dot{Q}_{conv,2,k}$ is:

$$\dot{Q}_{conv,2,k} = HTC_k \cdot A_k \cdot \left(\frac{U_k^2 - 2U_k C_{t,j}}{2c_p} \right) \tag{3.32}$$

Considering the radius of the k-th element R_k and the swirl ratio $SR = C_t/U$, Eq. 3.32 can be written as:

$$\dot{Q}_{conv,2,k} = HTC_k \cdot A_k \cdot (1 - 2SR_j) \cdot \left(\frac{(\omega R_k)^2}{2c_p} \right) \tag{3.33}$$

Finally, as mentioned, $\dot{Q}_{conv,2,k}$ is applied with opposite sign to the j-th fluid node, as the energy conservation prescribes. From the point of view of the implementation $\dot{Q}_{conv,2,k}$ is calculated in a dedicated subroutine and applied as an additional heat flux (see Fig. 3.10a) in the energy balance equation of the fluid node and in that of the solid element at stake.

3.2.5.4 Example of the evaluation process of implementations: Assessment of the rotational effects handling

The complexity of the phenomena summarized in Fig. 3.13 have been first validated on a simple case and compared with the solution of a reference FEM solver. This intermediate validation is reported as an

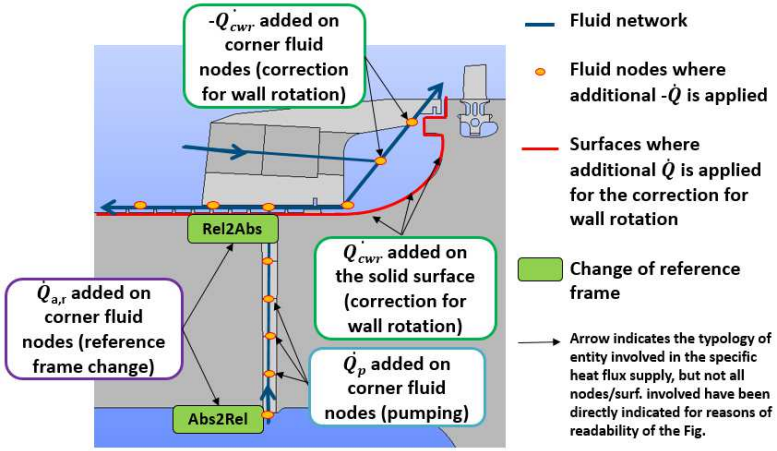

Figure 3.13: Rotational effects handling.

example of the method adopted for the assessment of the various features added in the course of the procedure development.

The case (call it *TE1*, Fig. 3.14), presents rotoric and statoric components facing each other, and for its solution the following new features have been exploited:

- thermal fluid network made of generalized and change reference frame models (Section 3.2.1),
- proper HTC scaling on hole region (Section 3.2.2),
- customized HTC correlations (Section 3.2.3),
- variable rotational velocity (Section 3.2.4),
- pumping in fluid network (Section 3.2.5),
- rotor stator handling (Section 3.2.5),
- rotation of free surfaces (Section 3.2.5).

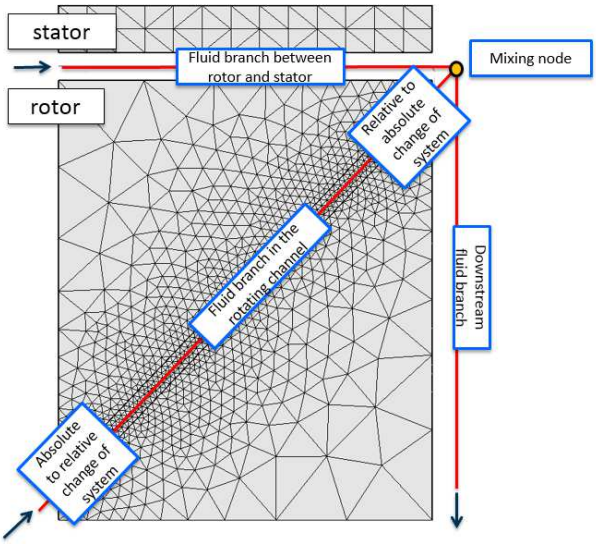

Figure 3.14: Example of TE1 case for the testing of the new features implemented.

As in Fig. 3.14, fluid branches are involve in the heat transfer with metal in the stator-rotor interface, in the hole through the rotor (actually 7 holes in parallel are simulated) and on the right side of the rotor. The solution reported is obtained from a purely thermal calculation, and inlet temperature and mass flows have been imposed as boundary conditions varying in time as well as explicit convective conditions applied on the top of the statoric component (convecting zone). Mass flow, pressure and temperature in the rotating duct are expressed as a function of the branch in the stator-rotor interface, therefore only stator-rotor interface stream BCs are reported in Fig. 3.15 where $W1$, $T1$, $Pr1$ are respectively mass flow rate, temperature and pressure in the stator-rotor annulus, whereas RPM is the rotational speed. In Fig. 3.15 quantities and time are scaled respect to the corresponding maximum value. The imposed

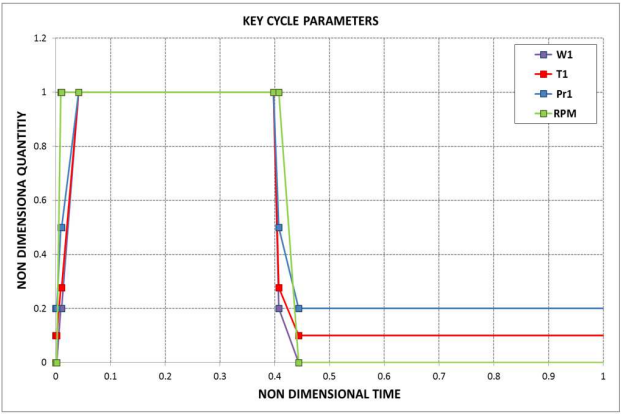

Figure 3.15: TE1 cycle parameters: trends in time of rotational speed, and temperature, pressure and mass flow rate for the main ducts.

cycle has a duration of 50300 s, and it is composed of transient ramp of acceleration and deceleration staggered by a "steady ramp", referring to the fact that in that phase the rotational speed is constant (Fig. 3.15). As in a real cycle the operational environmental parameters, such as mass flow rates, pressures and temperatures, are scaled as a function of the rotational speeds (Fig. 3.15). A linear variation of the operational boundary condition is assumed between ramp points. HTC coefficients on the top statoric component and right side of the rotor are imposed as time variable boundary conditions, whereas HTCs in the annulus and inside the rotating channels are calculated runtime by the solver according to a proprietary correlation for internal flow, function of the geometrical features of the passage, mass flow, fluid temperature and wall temperature, specifying therefore also a dependence from quantities varying in time and calculated runtime by the solver.

The simple model has been first run in sub-cases with the aim of testing the single features. These sub-cases can be summarized as reported below:

- run with the single branch in the stator-rotor interface (test of the

rotor-stator handling);

- run with the single branch in the rotor hole (test of the pumping effects and change of reference frame)

- run with the branch in the stator-rotor interface and the branch in the rotor hole and convecting zone on the top of the statoric component

- complete case, adding to the features listed above, the downstream branch exchanging heat on the rotor side (test of correction for wall rotation of a generic surface).

For reasons of synthesis, here the results of the sole complete case are proposed, compared with the solution of a reference FEM code set in an equivalent manner. Contours of the whole model and temperature profiles on some characteristic edges are plotted for three time step, respectively on the starting ramp, on the steady conditions and in the decelerating ramp.

As can be appreciate from temperature contours of Figs. 3.16, 3.17, 3.18 and from temperature plots of Figs. 3.19, 3.20, 3.21, 3.22, the agreement between the two solution is proved. Slight differences can be observed at inlet and outlet radius of the duct in the rotor (Fig. 3.19), and at the higher radius in the temperature distribution on the right side of the rotor (Fig. 3.22); these effects are due to a proved incorrect thickness distribution in those zones in the case of the FEM reference solver, which assigns an overestimated thickness. Differences at lower radius in temperature distribution on the right side of the model (Fig. 3.22) are due to the effect of the coarse mesh and different interpolating behaviour of the reference code.

Excepted the above highlighted differences, disalignments in all cases do not exceed the 5%, and well above the 5% on average. The general agreement between the two models is assumed as an indication of the coherence of the implementations introduced in the code.

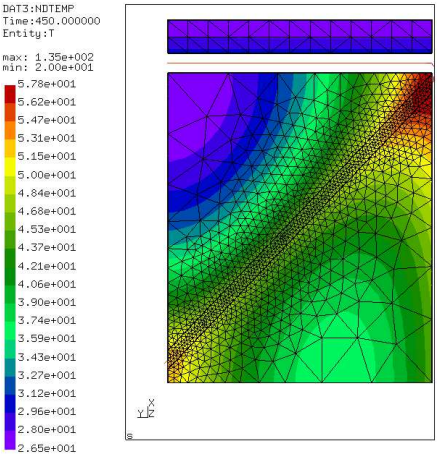

(a) CalculiX® solution.

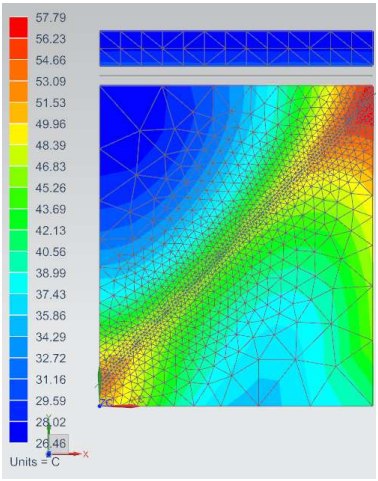

(b) Reference FEM solver solution.

Figure 3.16: TE1 metal temperature distributions in CalculiX® and reference FEM solver models at non-dimensional time 0.01 (450 s).

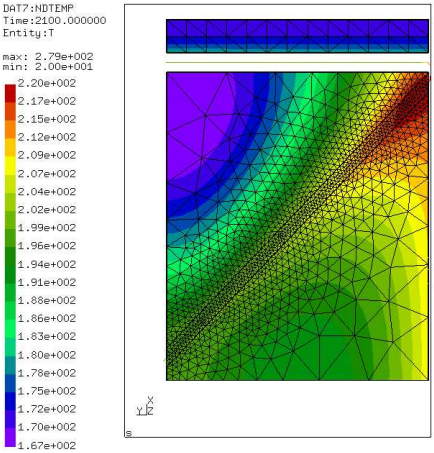

(a) CalculiX® solution.

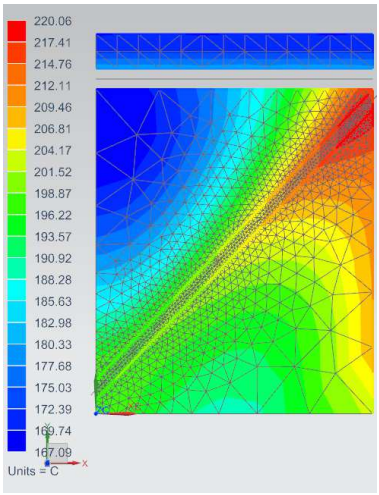

(b) Reference FEM solver solution.

Figure 3.17: TE1 metal temperature distributions in CalculiX® and reference FEM solver models at non-dimensional time 0.04 (2100 s).

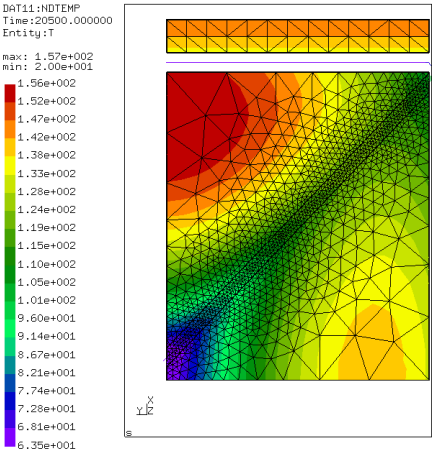

(a) CalculiX® solution.

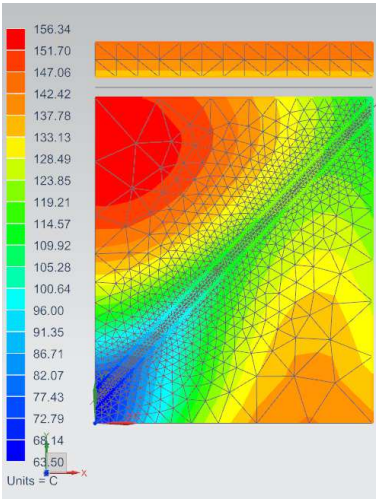

(b) Reference FEM solver solution.

Figure 3.18: TE1 metal temperature distributions in CalculiX® and reference FEM solver models at non-dimensional time 0.4 (20500 s).

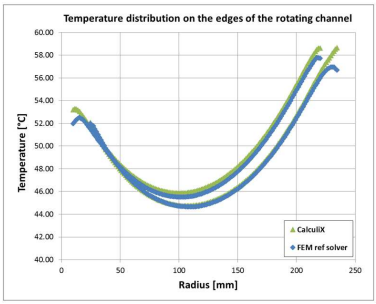

(a) Non-dimensional time 0.01 (450 s).

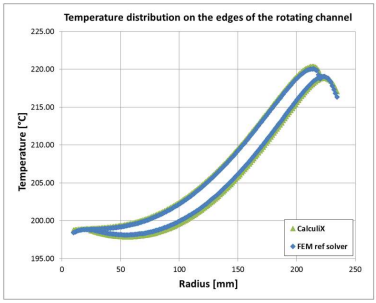

(b) Non-dimensional time 0.04 (2100 s).

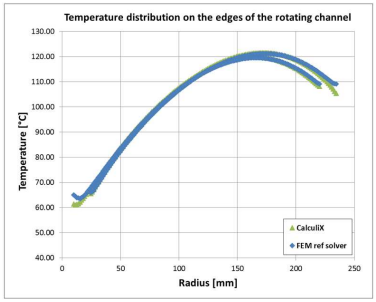

(c) Non-dimensional time 0.4 (20500 s).

Figure 3.19: TE1 nodal metal temperature distributions along edges defining the rotor internal duct.

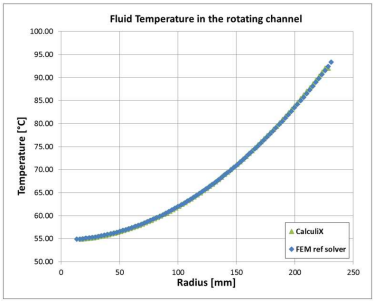

(a) Non-dimensional time 0.01 (450 s).

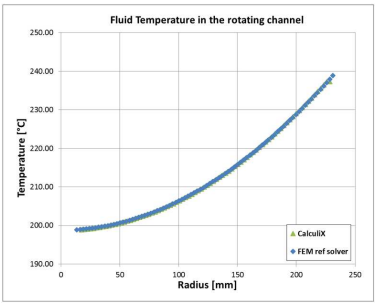

(b) Non-dimensional time 0.04 (2100 s).

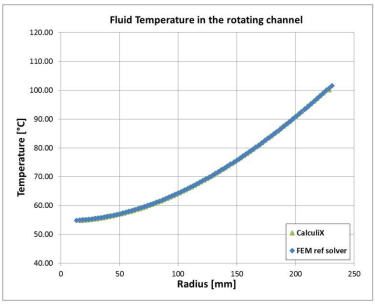

(c) Non-dimensional time 0.4 (20500 s).

Figure 3.20: TE1 nodal fluid temperature distribution along the rotor internal duct.

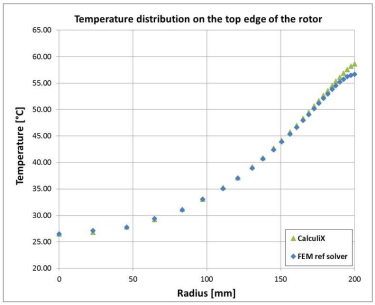

(a) Non-dimensional time 0.01 (450 s).

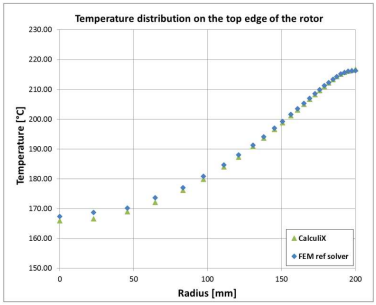

(b) Non-dimensional time 0.04 (2100 s).

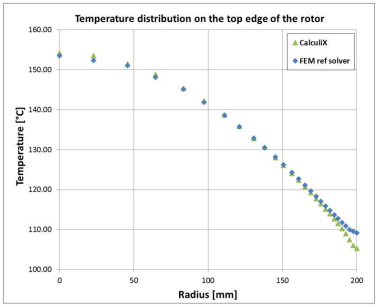

(c) Non-dimensional time 0.4 (20500 s).

Figure 3.21: TE1 nodal metal temperature distributions along the edge defining the rotor top.

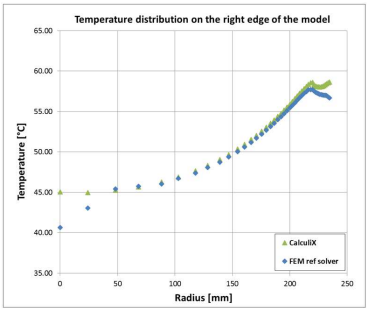

(a) Non-dimensional time 0.01 (450 s).

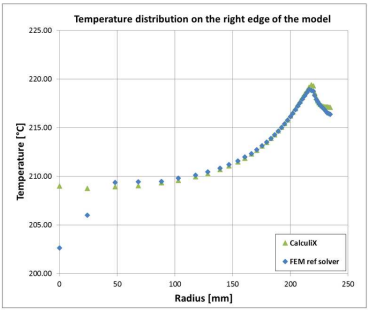

(b) Non-dimensional time 0.04 (2100 s).

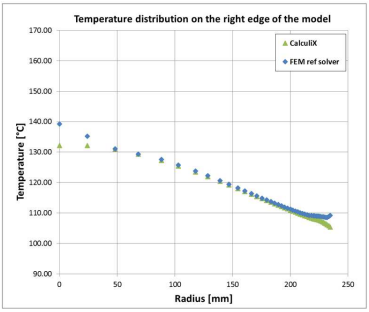

(c) Non-dimensional time 0.4 (20500 s).

Figure 3.22: TE1 nodal metal temperature distributions along the edge defining the right side of the model.

3.2.6 Heat pickup

Heat pickup effect is modelled with the subtraction/addition of an heat flux on the fluid node/solid element energy balance, in a totally similar way to what done for the models accounting the effects of rotation. This functionality was not present in the original version of the code and it has been included with a dedicated implementation.

The model has to be fed by some information analogous to that provided to the rotational effect handling block. Among them:

- geometrical details about the fluid model and/or solid element,
- fluid properties,
- swirl ratio,
- rotational speed,
- etc.

A dedicated flag, among the gas pipe model inputs, controls the way the heat pickup is taken into account, and where it has to be applied, if it has to be added in the energy balance of the fluid node or in the energy balance of the solid element.

The heat pickup is therefore an additional energy source on the fluid-solid interface, used for a number of modelling aspects in a WEM approach. Among them we can cite the effects of temperature rise due to air compression in the fluid network simulating the main flow in the compressor region.

In this case the power to be split spatially along the annulus on the fluid elements of the network is determined by the knowledge of the temperature at certain stations of the compressor. Knowing the mass flow evolving and the temperatures in two monitor locations it is possible to determine:

$$Q_c = \dot{m} \cdot c_p \cdot (T_{c,2} - T_{c,1}) \tag{3.34}$$

i.e. the power to be redistributed on fluid elements to reach temperature $T_{c,2}$ at the second station with an inlet temperature $T_{c,1}$ at the previous

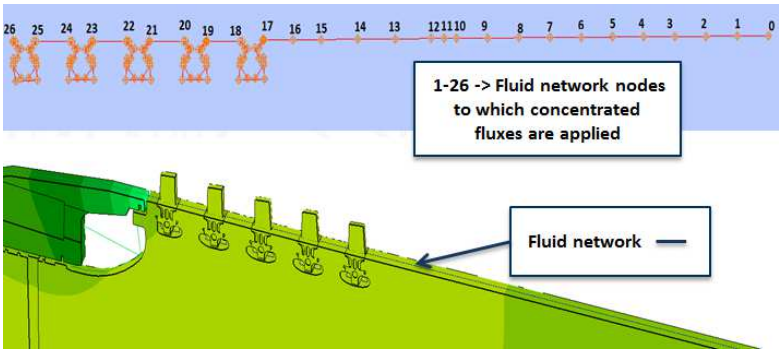

Figure 3.23: Example of heat pickup application for the simulation of compression of the fluid along the meridian channel [27].

station. Therefore to simulate the effect of the compression of the fluid along the meridian channel, concentrated heat fluxes are provided on the fluid nodes of the fluid network simulating the main flow, with an analogous approach used for pumping power and stator-rotor handling (Fig. 3.23).

Another typical application is the windage estimation. Windage is caused by the surfaces rotation, producing a temperature increase of the air that flows through rotor-stator interfaces such as labyrinth seals. The effect is more important, smaller the radial clearance of the seal is, due to the lower mass flow passing through it. As a result, this can lead to large temperature increase, whose magnitude is higher in long labyrinth seal with many fins. Therefore the effect of windage heating may become an important design variable to correctly simulate leakage phenomena and seals behaviour.

Hence, the windage term $Q_{wind}(R)$ which is the responsible for the fluid temperature augmentation due to the action of the solid walls on the fluid, has been included in the rotor-stator handling in the user library. It can be therefore easily applied to a situation such as that in Fig. 3.24, on the fluid at the interface between the stationary and rotating surfaces.

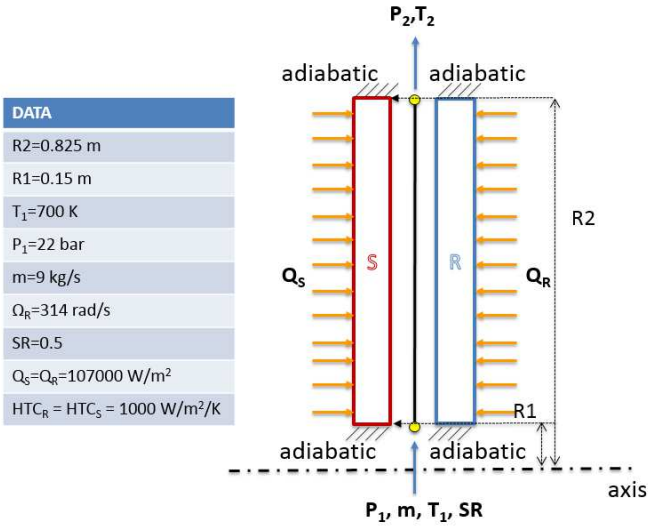

Figure 3.24: Summary of the rotor-stator reference case show in Section 2.2.5.

Considering the formulation of the friction force $F_{fr}(R)$:

$$F_{fr}(R) = \frac{c_{fr}\rho}{2}(1 - SR(R))^2 \cdot R^2 \cdot \omega^2 \cdot A \tag{3.35}$$

and the corresponding momentum equation $M_{fr}(R)$, i.e. the work exercised on the fluid by the rotor friction force:

$$M_{fr}(R) = F_{fr}(R) \cdot R \tag{3.36}$$

in an absolute reference of frame the corresponding power expression is:

$$Q_{wind}(R) = M_{fr}(R) \cdot \omega = \frac{c_{fr}\rho}{2}(1 - SR(R))^2 \cdot R^3 \cdot \omega^3 \cdot A \tag{3.37}$$

where R, A and c_f are respectively the radius location, the area of the solid element and the friction factor over the area, while SR and ω are

the swirl ratio at the corresponding radius and the rotation velocity , and ρ is the density of the fluid element involved.

The change in temperature on the fluid element temperature will be therefore:

$$T_{0,f,out} = T_{0,f,in} + \frac{\triangle Q_{wind}(R)}{\dot{m} \cdot c_p} \tag{3.38}$$

In the implemented feature, $Q_{wind}(R)$ term is added to the fluid node as an additional heat in the dedicated subroutine and this is done with a "per element" approach, i.e $Q_{wind}(R)$ is evaluated singly for each mesh element involved, with quantities of formulation referring to the specific element at stake during the calculation.

3.2.6.1 Example of the evaluation process of implementations: Assessment of the heat pickup modelling

The formulation presented above has been compared with the solution of a reference FEM code.

The case of reference is that already presented in Section 2.2.5 and a summary is reported in Fig. 3.24.

The overall behaviour of the two models is the same but some differences in the temperature distributions arose due to a different application of the heat pickup (Fig. 3.25). Indeed, differently from the proposed "per element" implementation, the code of reference calculates the total windage after integration of the windage expression per element, over the global surface on which the heat pickup has been imposed.

Therefore even though the final temperature on the fluid branch is the same, expect differences in the radial distribution of fluid temperatures are confirmed (Fig. 3.25a). This have slight influence on the metal distribution (Fig. 3.25b and Fig. 3.25c) with differences not exceeding the 0.5%.

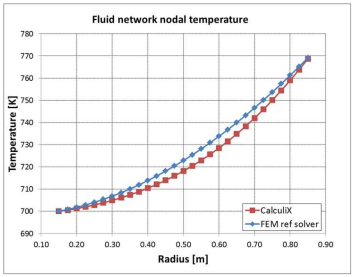

(a) Fluid temperature distributions along radius (indicating points on curves represent the corner nodes of fluid elements).

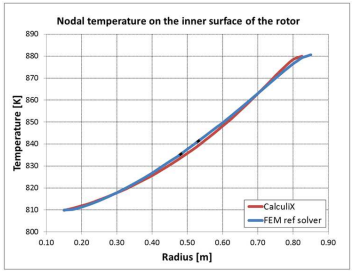

(b) Temperature predicted on the inner surface of the rotating component.

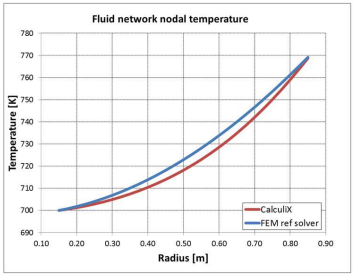

(c) Temperature predicted on the inner surface of the statoric component.

Figure 3.25: Windage effects on temperature distributions predicted by the customized version of CalculiX® and a reference FEM code.

3.3 Procedure development

An important point in the procedure development was how boundary conditions had to be interpreted from the pre-processing tools and how they had to be set in the CalculiX® model. The matter was how to meet all the requirements of a WEM setting, how to free user to set all needed boundary conditions, with the means offered by the code.

These kinds of topics have not necessary implicated modifications of the original code, but mostly they have introduce the necessity to use pre-existent features in non-conventional ways.

Indeed, procedure implementations regarded not only direct customizations of the official release of the core code CalculiX® , but also the development of:

- new methods for the correct imposition of boundary conditions (Sections 3.3.1 and 3.3.2);
- a strategy for the communications of the different aerodynamic and thermo-mechanical models (Section 3.3.3) in the iterative procedure illustrated in Chapter 2;
- a dedicated pre-processing tools for the correct translation of the user settings in the CalculiX® proper syntax, in a fast, general and replicable way (Section 3.3.4).

Main solutions to meet requirements of the global procedure setting are summarized in the following Sections.

3.3.1 Enclosed thermal masses

A non conventional use of the fluid element in thermal network is represented by the simulation of enclosed thermal masses. Generally, rotor structure is characterized by the presence of manifold cavities. Some of them are completely closed, not fed by secondary air system branches. In these entirely closed gas-filled rotating annulus, the predominant convective phenomenon is the natural convection [58]. This convection is caused

by different phenomena, among them buoyancy force, centrifugal acceleration and different temperatures of the cavity surfaces. Free convection increases the heat transfer throughout the cavities considerably.

This effect is particularly important during the whole operation cycle but it becomes one of the predominant phenomena in the shutdown phase. Indeed once the machine is turned off there is no active flow of cooling air. During the cold down, hot components give back heat to the air surrounding them through convection and radiation. This leads to increase in temperature of air surrounding the metal and decreases the pressure. Because of the buoyancy effect due to the lower density of the the heated air, flows establish inside the cavity and bring heavier cold air near to hot surface at bottom half of the shaft. This leads to a more efficient cooling of the bottom region of the shaft, while metal in the top half results to be less cooled [47]. Due to this phenomenon also the bottom portion of the casing becomes colder than the top portion. This establishes thermal and strain gradients within the components metal which is very important to evaluate in order to avoid failures, especially in machine hot restart.

Being the natural convection effect, one of the most complex phenomena to be handle, it requires specific studies and simulations to catch those three-dimensional effects that 1D models cannot appreciate. Anyway the presence of this thermal masses must be provided in a WEM procedure, eventually instructing the model with those additional information coming from more detailed analyses.

The presence of those enclosed thermal masses exchanging heat through natural convection with the metal surfaces, and contributing to mediate the temperature over the same walls, is simulated in the procedure through a disjointed fluid element with a very small flow rate at its inlet (Fig. 3.26a). This overcomes the problem of which values of inlet temperature and mass flow rate have to be imposed in the convective fluid element of CalculiX® to simulate a phenomenon for which actually no mass flow efflux is defined neither the temperature is known.

Considering the heat balance between the fluid element ans the a

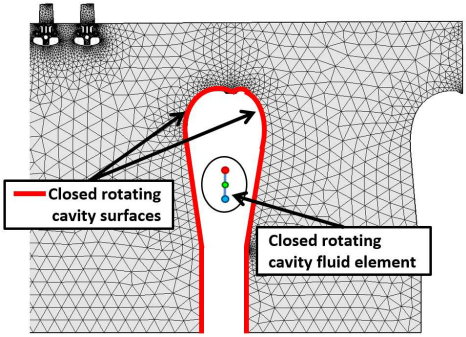

(a) Example of a closed cavity region.

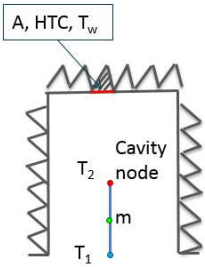

(b) Scheme of the element modelling the enclosed thermal mass and heat transfer inside the cavity.

Figure 3.26: Rotor cavity and enclosed thermal masses modelling.

single solid element (Fig. 3.26b):

$$\dot{m} \cdot c_p \cdot (T_{2,f} - T_{1,f}) = A \cdot HTC \cdot (T_w - T_{2,f}) \tag{3.39}$$

the outlet temperature of the fluid element results:

$$T_{2,f} = \frac{A \cdot HTC \cdot T_w + \dot{m} \cdot c_p \cdot T_{1,f}}{A \cdot HTC + \dot{m} \cdot c_p} \tag{3.40}$$

The flow rate very small (not actually simulating an efflux but the very low thermal inertia) will guarantee that ultimately the outlet temperature

becomes an average of those of the solid walls with which exchanges heat, leading to a process of homogenization on the walls temperatures since mass flow contributions factors can be neglected:

$$\lim_{\dot{m}\to 0} \frac{A \cdot HTC \cdot T_w + \dot{m} \cdot c_p \cdot T_{1,f}}{A \cdot HTC + \dot{m} \cdot c_p} = T_w \tag{3.41}$$

For n surface contributions, outlet temperature becomes an average of those of the solid walls:

$$\lim_{\dot{m}\to 0} T_{2,f} = \frac{\sum_{i=1}^{n} A_i \cdot HTC_i \cdot T_{w,i}}{\sum_{i=1}^{n} A_i \cdot HTC_i} \tag{3.42}$$

3.3.2 User expressions handling

In the boundary conditions setting of the thermo-mechanical calculation (e.g. we are talking about temperature and displacements solution), frequently there is the necessity to insert linear and non linear expressions. They can be dependent on key cycle parameters (i.e. quantities assigned, varying in time) or dependent on calculation quantities such as mass flow rate and temperatures taken, for instance, as exit quantities from the upstream thermal boundary condition.

Satisfying this kind of requirements imposes a particular treatment of the user expressions in the pre-processing phase. Here below the strategies chosen to meet the necessities of this boundary conditions setting are presented.

3.3.2.1 Link among branches

The logic of the CalculiX® fluid network solution would impose to connect elements when an effective link exists among them and to leave to the solver the solution of the mixing flows in term of temperature. For example, in the case of Fig. 3.14, if inlet conditions of the downstream branch refer to the outlet conditions of the upstream branches through a mixing process, the more suitable solution is to link the branches with a mixing node (Fig. 3.27a). Nevertheless, if the conditions imposed on the downstream branch are subjected to conditions rearranging in any

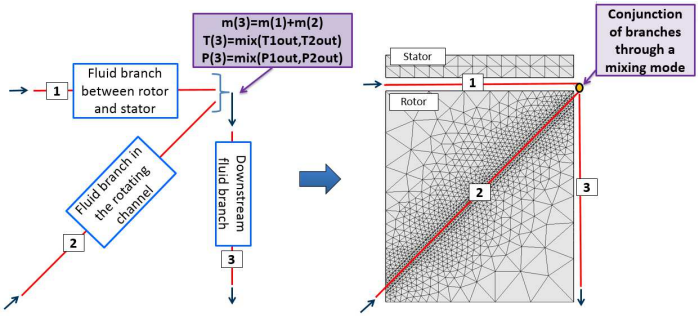

(a) Physical link among fluid network branches.

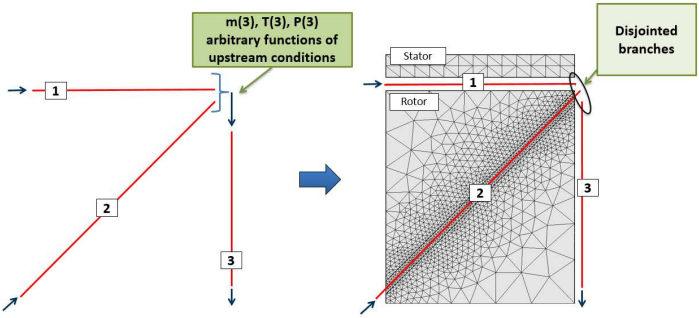

(b) Logical link among fluid network branches.

Figure 3.27: Possible link among fluid network branches.

arbitrary way the outlet conditions of the upstream elements, the mixing node cannot be adopted any more. In this case, branches must be taken separated and conditions on the downstream branch must be imposed in an alternative way (Fig. 3.27b).

This necessity can arise in a WEM procedure, for example, because of the application of parameters and coefficients of tuning, used to calibrate the model. For instance, the inlet temperature of a stream can be increase with a proper $\triangle T$ to take into account of some other upstream temperature rise phenomena, not modelled in other way.

This imposes to maintain disjointed some branches which would result

linked from an examination of the fluid network topology, but which have to be kept separated because of customizing relations expressing boundary conditions. This does not allow the standard BCs assignation in which simply the nodes and the bounding parameter are expressed, but it needs of the applications of user expressions by means of specific user subroutines in which boundary conditions can be set as relations and the dependence of a boundary value from cycle parameters or runtime quantities can be set.

These aspects complicate the automatic construction of the thermal network and the handling of the code, which should be implemented with the devised user expressions and recompiled each time a different model is run. This actually does not occur because of the design of an overcoming solution, but it constituted a field for further work and code modifications. More details about the solution of these issues will be given in the Section 3.3.4.

3.3.2.2 Cycle parameters handling

Cycle parameters are used in conventional practice to scale boundary conditions, or can be used as pure input values for boundaries, or can be combined among them and other runtime quantities to set more complicated relations defying BCs.

In general, user could want to use them as quantities to be manipulated and combined in the boundary conditions without to be directly applied as pure boundary. Again, very often this can be a consequence of the tuning practice according to which, for example, user could want to impose at the inlet of a fluid branch, a temperature given by a measurement versus time data, plus a tuning $\triangle T$. This could lead to have in the model a number of key parameters not actually used as pure boundary conditions but combined inside functions written to set them.

Since in CalculiX® boundary conditions user subroutines, calculation quantities are available in the routine only if they are a result of the calculation (at the previous step) or BCs values imposed on boundaries nodes, a generalized method to make available in the user subroutines these

key parameters even when they are not applied as boundary conditions, has been devised.

This consists in the association of the key parameters to a number of fake nodes inside the model not actually belonging to any element of the fluid network or of the solid domain in thermo-mechanical applications. Key parameters are assigned as boundary conditions, constraining a degree of freedom of the fake nodes. An automatic procedure establish and manage during the calculation the link between the cycle parameter at stake and the degree of freedom of the corresponding fake node to which it has been assigned.

In this way the key parameters in user subroutine can be recalled as any other boundary value for the formulations of arbitrary relations, even if they are not actually assigned to a real boundary of the model.

3.3.3 Iterative procedure

The iterative procedure between SAS standalone execution block and the transient thermo-mechanical calculation is performed through Python scripts. A reference to the simplified structure of the iterative procedure is reported in Fig. 3.28, and below the main passages excuted by the scripts are reported:

- First the sequence of steady state solutions of the SAS is launched and properties of fluid network are determined in a number of time steps, characterizing the transient operation in terms of mass flow rates and pressure distributions over the SAS.

- Distributions are then post-processed by a script that reduces these solutions in a tabular form in which the quantity is expressed as a function of time, in order to be inserted inside the themo-mechanical model as mass flow, pressures and inlet temperature conditions to be applied on the thermal network.

- Once the model file has been properly modified with the insertion of the mass flows, pressures and inlet temperatures for the thermal

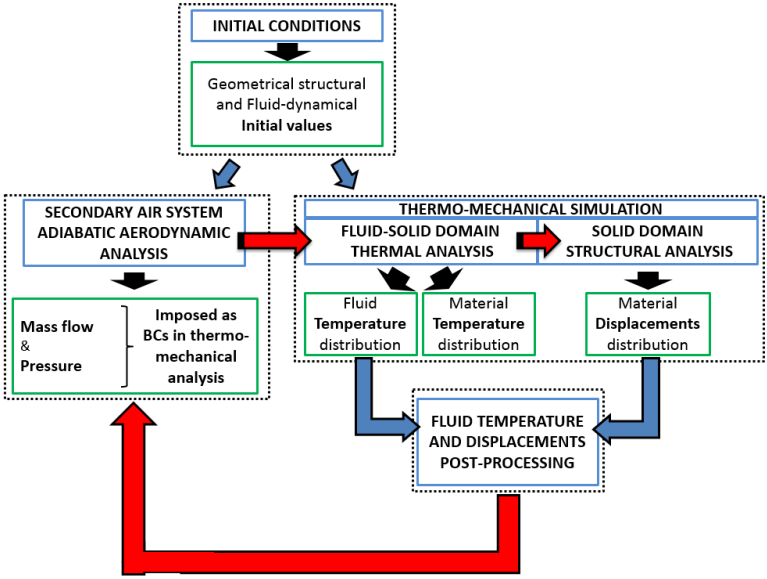

Figure 3.28: Simplified scheme of the iterative procedure.

network, the thermo-mechanical calculation is launched and the transient operation performed.

- At the end of the simulation, a file containing the solution in terms of fluid and solid nodal temperature and displacements is obtained. A script post-processes the solution file and determines from displacements the new value of geometrical features in terms of gap, diameter, and length, according to the typology of element corresponding in the aerodynamic network of the SAS standalone execution block. The same is done for temperatures which are post-processed and imposed as boundary conditions on the corresponding nodes of the SAS aerodynamic network.

The correspondence between elements of the thermal and aerodynamic fluid networks is fixed in some flags and inputs in the generalized element

of the thermal network, set in the pre-processing phase of the thermo-mechanical calculation setting. A script launched at the beginning of the procedure:

- maps the correspondence between element of the two typology of networks,
- stores the nodes on which temperatures and displacements will be monitored on the thermal network,
- stores the corresponding nodes of the aerodynamic network on which temperatures coming from the thermal solution will be reimposed,
- stores the corresponding number (label) of the aerodynamic fluid element whose geometrical feature (gaps, diameter, etc.) is associated to the displacement of the mesh node at stake.

This kind of information is than used in the post-processing of the thermo-mechanical solution and in its re-imposition as new temperature and geometrical boundary conditions for the new analysis of the SAS over the transient operation. The update of geometrical information is also carried out in the thermo-mechical model for a correct estimation of HTC values and all the other phenomena for which expressions depending on geometrical details are set.

At the end of each transient thermo-mechanical analysis the solution on the monitored points is compared with the solution at the previous iteration of the global procedure, and if differences are below an imposed threshold value the procedure stops, otherwise script impose new temperature levels and geometrical features values in the aerodynamic network for the subsequent iteration.

3.3.4 Pre-processing tools

In the procedure the pre-processing phase is carried out with the graphical user interface of a the commercial code Siemens NX® .

Although CalculiX® package possesses a graphical interface, this results to much rough for a WEM application. Indeed, a variety of

conditions have to be imposed, different in typology and in a number of the order of hundreds of user expressions and conventional BCs.

In addition, not being contemplated in the original solver a number of features implemented later in the presented procedure, an appropriated treatment of the same was obviously missing in the logic of BCs application of the native GUI.

For these reasons a GUI more suitable for this type of application has been chosen, and in the procedure the setting file containing the solid mesh and all the boundary condition is produced through Siemens NX® in an *xml* format and then traduced by an in house translator in the *inp* format read by the CalculiX® FEM solver.

Since in the pre-processing environment of NX® the fluid network is not generated since the convective heat transfer is set as a boundary conditions not based on a graphical definition of a network, the translator produces also the thermal fluid nodes inserted inside the inp file containing the traduced mesh of the solid and the BCs of the case. The criteria of refinement is linked to the solid mesh in order to provide a proper spatial characterization and it is automatically leaded by the translator with the opportunity of an user intervention where it is deemed that the refinement criteria must be corrected mainly in reason of the complexity of the thermal phenomena involved.

The different way to interpret and set the presence of a fluid network is only one of the numerous differences between the manner through which a boundary is imposed in NX® and the the fashion in which it has to be passed to the procedure solver. The interposition of the NX® GUI imposes an additional level of difficulty in the process development since the calculation is set by the user according to the conventions of the specific GUI used, and the logic behind the GUI must be translated in the CalculiX® logic. Therefore in between the user and the solver, there is not only the human intention of setting a boundary in a determined way, but also the convention in doing this imposed by the adopted GUI. All this aspects must be contemplated and managed by the translator.

Hence, the development of this tool has been a long and heavy phase

of the procedure progression. It has a great importance in the entirety of the method since it represents the link between the user requirements and the instruction of the customized CalculiX® solver. In this pre-processing phase the procedure must be general, versatile, replicable and able to mirror the geometry of the engine and the BCs imposed without arbitrary exemplifications potentially compromising the physic of the problem.

To the translator is also commit the dynamic compilation of code when user subroutines are needed for the calculation setting. This is the case when user imposes relations and expressions which have to be included in specific user subroutines, such as boundary conditions including expressions and dependences on key parameters or runtime quantities, or expressions for heat transfer coefficient calculation not included in the custom library. This is carried out with a preliminary parsing of the expression and the subsequent reconstruction in the specific user subroutine with the proper syntax required by CalculiX® . This part of the code is compiled and stored in a dynamic-link library (*dll*), enabling the procedure to load dynamically during the execution the part of the code regarding the user subroutine modified ad hoc for the inclusion of the user expressions used in the specific case.

3.4 Open issues and future developments

Development is not concluded, but still running. New implementations and customizations additional to those produced up to now are still needed to improve the capabilities of the procedure.

Among them it is planned an improvement in the expressions handling. The idea is to move from the actual managing through dedicated user subroutines in which the different quantities and runtime values are present but referred to the previous iteration, to an approach able to code the expression inside the solution matrix. Indeed the present approach decouples the solution making the parameter dependent on the solution at the previous iteration. This has an impact on the speed of calculation requiring in general more iterations, whereas the coding of expression

directly in the solution matrix will replicate the complete coupling such as that imposed for the convective heat transfer, speeding up the solution.

3.5 Contribution to CalculiX® project

The procedure has been developed mostly referring to the 2.11 version of CalculiX® . Internet official releases in the meanwhile have been continued to be produced. Some of the more general implementations/improvements introduced in the code during this research work, have been shared with the CalculiX® developers.

Some of them, deemed of common utility, have been included in the subsequent official releases. Among them it is possible to find customizable user fluid elements, variable rotational speed, heat pickup, more generalized user subroutines and others.

The idea is to share the more general aspects of innovation and to remain aligned as much as possible with the official releases for a profitable overall improvement of the code.

Chapter 4

Assessment of the proposed methodology

In Chapter 3 new functionalities and dedicated customizations applied to the reference original code CalculiX® have been illustrated. Those modifications have been introduced in the program with the aim of improving original capabilities of the solver, introducing new features and models, and customizing the code to meet the needs of the industrial practice. As mentioned in the previous Chapter, new implementations have required a continuous activity of debugging and testing, carried out in the first evaluation phase mostly with the application of very simple test cases in order to assess the correctness of the implementations, with comparisons with other validated tools or using mathematical closed form solution when possible. Some of these tests have been also reported in Chapter 3.

Anyhow, after having prove the coherence of each feature, some more complex geometry have been tested during the procedure development, in order to asses the physical consistence of the proposed methodology in a more general and solid way. In this Chapter therefore, two applications used to test the overall coherence of the procedure will be presented. They consist in two different test cases representative of typical real

engine configurations, tested through a transient thermal cycle. One represents a simplified gas turbine arrangement tested with the aim of a first assessment of the methodology from the point of view of the thermal loads evaluation. The second one is a part of a real engine, chosen to test the complete procedure also from the point of view of the interaction between secondary air system properties and geometry deformations.

A brief introduction about the issues linked to the validation of multi-physical WEM methodologies, precedes.

4.1 Validation issues

Because of model dimensions and phenomena complexity, the kind of approach proposed is based on a number of simplifications which respond to the need to have an instrument:

- able to fulfil the design requirements in terms of time compatible with the design process,
- coherent with the level of uncertainties that normally characterized the engine development phase.

The first evident type of simplification is the use of a low order approach for the fluid-network simulation. This is proved by the fact that thermo-mechanical analysis is the most demanding part of a WEM procedure from a computational point of view. Solving the 1D network does not represent any cost at all if compared with the cost in terms of time and resources of the thermo-mechanical application.

The convenience of the use of 1D network modelling is however paid in terms of magnitude of the simplification introduced, and therefore when considering the accuracy of a WEM procedure it is important to keep in mind that the accuracy of the analysis performed cannot exceed the accuracy of the SAS solution [28].

The same applies for other kinds of simplifications, such as the adoption of equivalent slots in the axysimmetric domain filled with plane elements with proper thickness in order to represent 3D feature in 2D axysimmetric

models, much more convenient to solve from a computational point of view.

These and other simplifications allow to simulate the overall process but can not catch the specificity in local solution. Therefore available prototype test results are used to improve the thermal prediction.

Sophisticated wireless instrumentation can be deployed to collect a variety of new data sets for rotating machinery. For instance, retrofitted networks and sensors can measure temperature, pressure, vibration, and flow data details. Collecting and analysing big data about equipment health especially at specialist remote data centres allows for early fault detection and maintenance, but also to acquire important data for models tuning [21].

Mission parameters are recorded to define the normal cycle behaviour. Hundreds of direct measurements points covering the complete engine structure are used, especially to improve the hot gas temperature components prediction. From the comparison among these field measurements and results of simulations (in general agreement is considered satisfying if the analytical and experimental results variation does not exceed +/- 10°C), a subsequent work is made to understand the mismatch between the two set of data [47]. Then model is consequently update to improve and refine analytical capability of evaluation and modelling practice, to capture region specific physics.

Anyhow, data collected during testing are used not only in order to tune the model but they are used (as illustrated in Section 2.3) also in the direct setting of the model, as boundary conditions with the aim of having a better match between the model and the real behaviour of the engine. In order to capture the right thermal behaviour it is necessary to have accurate mission cycle parameters.

It is told that more engine design and validation is performed by computer, the more we reduce the need for doing some of the large and expensive tests that are done today. Anyway, the role of measurements for this type of model remains of fundamental importance and testing remains a central activity in helping engineers to develop and assess this

kind of methods, which strictly depend on tuning and data from field. The purpose of the tuning phase is to make the model more reliable, in order to apply it to products and variants of the same (i.e. in design and off-design phases), reducing the costs and time needed to develop new products [21].

It is therefore a matter of fact that such procedure cannot be validated in the strict sense, but they need actually of calibrations on field data. In order to run a model and make it reproducing as much as possible the the real behaviour of the engine, there is therefore the strong need of experimental data, tuned correlations, and the general knowledge that only a company with its own libraries and field database can boast.

Therefore in the present work the purpose is not to validate the accuracy of a model, but to assess the physical consistency of the procedure and its coherence in the response to variations in boundary conditions. With this aim, applications that attest these aspects are proposed in the following Sections.

4.2 Transient thermal modelling assessment

The transient thermo-mechanical analysis produces in itself important analytical results that allows the designer to have a survey of the behaviour of the engine under various working conditions. Starting from this kind of analysis, the designer can appreciate components temperature variations over the cycle and infer a number of information about, for instance, the behaviour of thermal gradients within engine parts and clearances modifications, and up to now, deriving this information from the thermal transient results is the practice most widely used.

Thermal gradient could set up within components because of material properties, difference in heating/cooling, and contact with components having different temperatures. The entity of these gradients is higher in components that are directly exposed to main flow path or in components that come in contact with components that face main flows. These gradients lead to thermal and mechanical loading of the components,

which needs to be analysed in order to avoid consequent failures risks [47].

Temperature variation, similarly, is an important factor to be evaluated since it determines thermal expansion. If these thermal expansion behaviors are not captured accurately during the design phase, a clearance lower than that required could be imposed between stator and rotors, with the risk of rubbing at some point during transient phases. Hence, the practice is to estimate the rate of linear expansion of these components using component temperatures and arrive at cold clearances that avoids rubbing during startup or shutdown [47].

It is clear that the knowledge of the transient thermal behaviour of the engine helps designers to maintain the adequate distance between rotating and statoric components, to improve machine performance and avoid the interference failures. Therefore, having a numerical model able to adequately capture the thermal frame characterizing components represents in itself an important goal in the development of such kind of design and analysis tools.

The following application has been carried out with the aim to assess the transient thermal modelling capability of the procedure, testing therefore the capacity of the solver to properly simulate the transient operation in terms of temperature distributions and thermo-mechanical loads evaluation, according to the new features implemented in the code.

4.2.1 Test case description and model setting

In this application the procedure has been applied in a partially coupled version, i.e. not accounting the effect of displacements on fluid properties, and assigning mass flow rates and pressures to the thermal network nodes of the fluid mesh incorporated in the CalculiX® model, obtained from a previous solution of the SAS. Coupling is therefore present only at the level of fluid-metal heat transfer solution.

This form of the procedure allows at the end the comparison of the transient thermal capabilities of the methodology with a reference FEM code, whereas an equivalent comparison cannot be performed for the aero-thermo-mechanical application (as will be better explained in Section

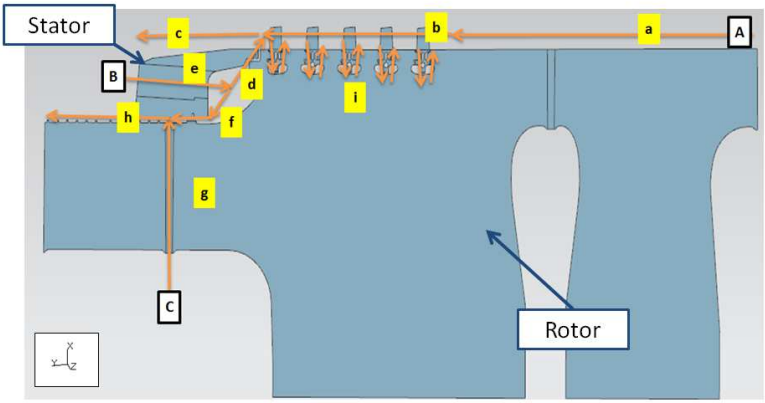

Figure 4.1: TE2 2D scheme of the test case and flows splits [27].

4.3) since a similar comparative aero-thermo-mechanical procedure is not available. We can consider therefore the application deepened in this Section as a first stage of the assessment process of the overall procedure.

The test case taken into account (call it *TE2*), consists in a 2D axisymmetric gas turbine representative geometry (as described in [27, 59]), with stator and rotor components. In particular it refers to a compressor arrangement with typical secondary air system elements such as rotating cavities, holes, air fulfilled rotating annulus, stator-rotor interface cavities and passages (Fig. 4.1).

Stator and rotor components have been modeled as axisymmetric exception for the zones of the mesh corresponding to channels and blades (Fig. 4.2). The 2D axisimmetric model has been discretized with 17973 linear triangular element with 10318 nodes. Due to the 2D modelling, proper area and volume scaling have been considered for all non-axisymmetric features like compressor blades and holes. In these cases the element type applied has been the plane stress with the appropriate modelling assumptions to account for 3D features.

Heat transfer coefficients on blades and meridian channels surfaces and

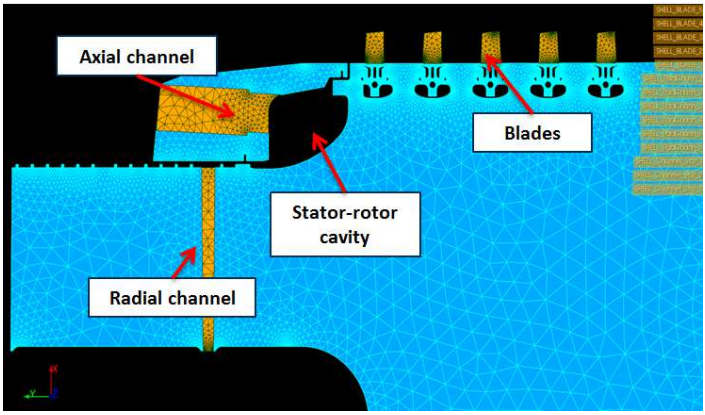

Figure 4.2: TE2 model features: axisymmetric (blue) and plane (orange) elements [27].

inside the secondary air system have been estimated through correlations customized for gas turbine applications.

Mass flow splits and pressure distributions along the main flow have been provided from external tools and want to reproduce a realistic engine behaviour. Also boundary inlet flow temperatures are assigned both for the main flow and secondary air. As conventional industrial practice, all these boundary conditions are scaled based on some key cycle parameters (some trends are shown in Fig. 4.3).

As realistic engine behaviour prescribes, the cycle is composed of a first startup phase, followed by the base load condition. The subsequent shutdown phase is normally simulated till the time instant in which temperature of all components reaches near ambient temperature. This occupies half of the time duration simulated and can be divided in gas turbine into two phases: the phase from start of shutdown to time when rotor reaches zero rpm and a second phase extending from the moment in which rotor reaches zero rpm to time when temperature of all components reaches near ambient temperature.

The presented new implementations have been used to predict metal

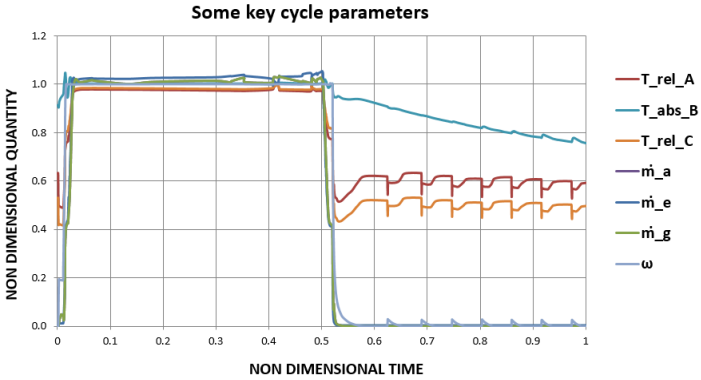

Figure 4.3: TE2 cycle parameters: trends in time of rotational speed, and temperatures and mass flow rates for the main ducts [27].

Name	Description
T_{rel_A}	Inlet relative temperature of the main flow at the compressor entry (**inlet A** Fig. 4.1)
T_{abs_B}	Inlet absolute temperature of the flow at the entry of the stator axial channel (**inlet B** Fig. 4.1)
T_{rel_C}	Inlet relative temperature of flow at the entry of the rotor radial channel (**inlet C** Fig. 4.1)
$\dot{m}_a$	Mass flow rate at the entry of the compressor (fluid network **branch a** Fig. 4.1)
$\dot{m}_e$	Mass flow rate at the entry of the stator axial channel (fluid network **branch e** Fig. 4.1)
$\dot{m}_g$	Mass flow rate at the entry of the rotor radial channel (fluid network **branch g** Fig. 4.1)
ω	Rotational speed (Fig. 4.1)

Table 4.1: TE2 cycle parameters legend.

and fluid temperatures in case of pumping, meridian channel compression, stator-rotor interface and natural convection effects in closed cavity.

Concerning mechanical loads, centrifugal distributed loading has been

applied to rotating components. Centrifugal loads have been actually the unique applied forces since fluid acting on the solid e.g. the aerodynamic blade load or the pressure gradient between cavities and main annulus can be neglected since prevailing deformations are those caused ultimately by centrifugal forces due to the rotational speed and the thermal expansion.

The effect of the compression of the fluid along the meridian channel has been also evaluated. In particular, since main flow temperature and pressure profile variations in the span-wise (radial) direction of the compressor region are in general negligible, only temperature and pressure variations in the axial direction of compressor have been accounted.

Concerning the radiation heat transfer, it has been set so that the sink temperature has been calculated automatically by the solver based on the interaction of the surface at stake with all other cavity radiation surfaces. This approach has been used in the case of the closed central cavity of the model and in the approximately closed cavity at the stator rotor interface.

Finally, natural convection has been considered in the central rotor cavity.

4.2.2 Discussion of results

The 2D axisimmetric model has been run with the presented customized version of CalculiX® and with a reference FEM solver. Some points in the solid domain have been monitored in time (Fig. 4.4) and comparisons have been made in order to have a preliminary assessment of the consistency of the transient thermal modelling adopted in the procedure.

In both cases the model setup follows the same guidelines in terms of boundary conditions, loads and modeled phenomena. The CalculiX® model setting was based on the application of 313 boundary conditions, comprehending explicit convective conditions, forced convection with fluid elements, heat fluxes and boundary temperature, pressure and mass flow rates. Differently, the model setup of the reference code was based on the imposition of 60 boundary conditions. The reference code allows the

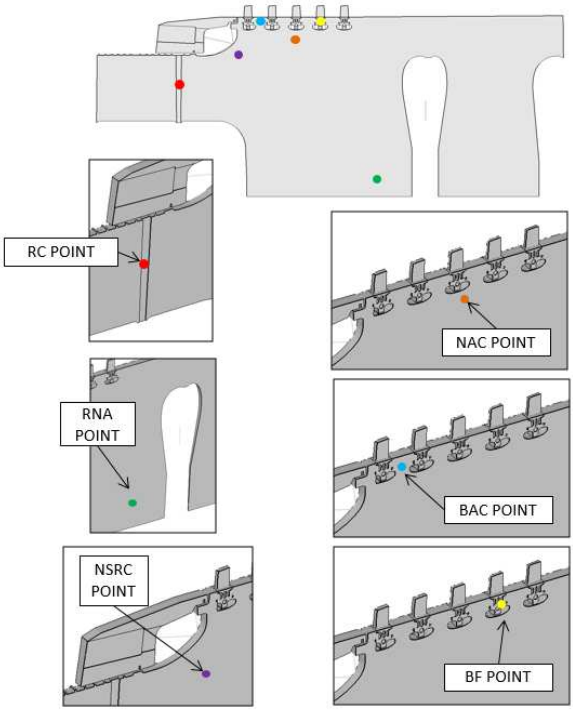

Figure 4.4: TE2 monitor points locations.

loads application on the geometric edges and a sub-discretization of the boundary in terms of corresponding forced convection conditions through automatic criteria, is carried out independently by the solver.

The transient cycle was simulated for a time duration of about 70000 s with the same condition sequence for both setups in terms of time points discretizing the complete extension of the simulation and describing the time history of the quantities amplitudes during the transient cycle.

The procedure demonstrated to be able to follow the transient operation, catching coherent behavior of the thermal model according to the engine cycle and the physic of the problem. As shown in Fig. 4.5, points

closer to the main flow are subjected to sudden rise in temperature in the startup phase and to higher temperature levels in general. Similarly, due to their exposition to the main flow, the shutdown phase is characterized by a quick temperature reduction during the firing cut off. During this phase temperatures across main channel, rotor speed and mass flow drops significantly (Fig. 4.3). Since the mass flow entering into the turbine region is very small a slight increase in temperatures across components stations is generally observed due to heat soak effect, phenomenon causing fluid temperature and pressures increase due to heat received from metal, after the engine is turned off. The effect of the rotor thermal inertia also affects components like blades which are involved in a temporary increase of the temperature: while flows are quite exhausted the predominant phenomenon is the conduction of the heat accumulated in the rotor till that moment, as it can be observed around the halfway point of the cycle in Fig. 4.5a and 4.5c. After that phase, a gradual decrease in temperatures follows. Other points like those located in zone fed by cooling and purge flows (Fig. 4.6a and 4.6b) or those located in more internal zone of the rotor (Fig. 4.6c) where the thermal inertia is higher, experience more moderately the above cited temperature variations, showing smoother trends.

As reported in Fig. 4.5 and 4.6 the agreement with the prediction of the reference FEM solver is generally good and differences not exceed the 6.5 %. Reported temperatures are scaled with respect to a reference temperature T_{ref} (approximately the maximum value detected on the observed points). Observed differences are probably due to a not fully equivalent level of discritization in the two model settings. In CalculiX® the fluid network setup has been led by considerations about the spatial discretization of the solid domain and the expected complexity of the heat transfer. In the reference solver the fluid network definition has been carried out by an automatic algorithm of discretization which can differ from that set in CalculiX® . Fluid properties generally are evaluated at a film temperature defined by the mean of the flow and wall temperature, while in CalculiX® properties are evaluated at the fluid temperature.

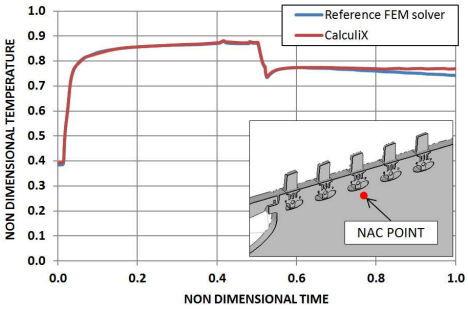

(a) Near anchoring cavity thermal response.

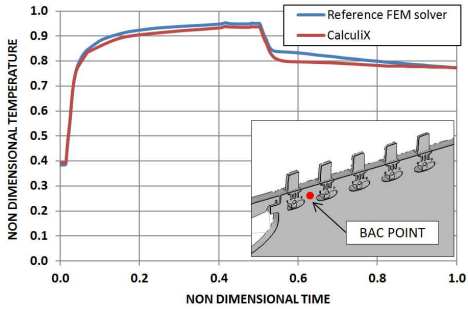

(b) Between anchoring cavities thermal response.

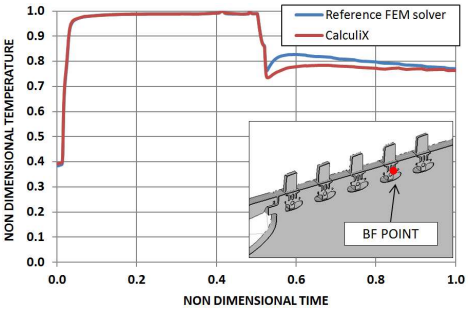

(c) Blade foot thermal response.

Figure 4.5: Non dimensional temperature trend versus non dimensional time - Points close to the meridian channel region [27].

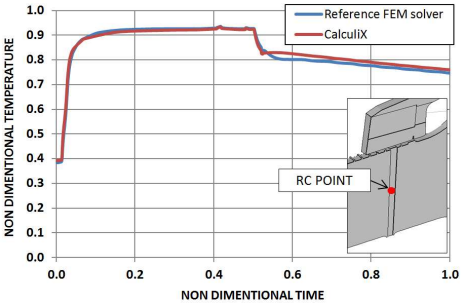

(a) Radial channel thermal response.

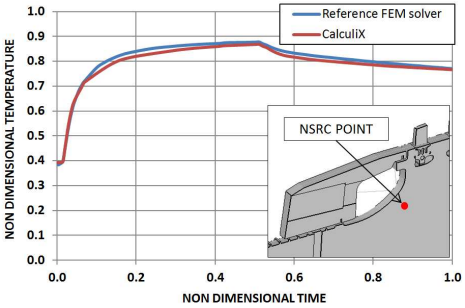

(b) Near stator-rotor cavity thermal response - Rotor side.

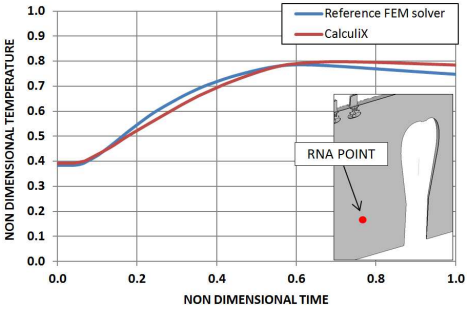

(c) Rotor near axis thermal response.

Figure 4.6: Non dimensional temperature trend versus non dimensional time - Other significant points [27].

For non-axisymmetric features like blades and holes, convective loads on plane elements and at the interfaces of the latter with the axisymmetric ones have been applied in CalculiX® with the proper scaling of the heat transfer coefficient, which can in general differ from that used by the reference code. Indeed, in the reference FEM solver the definition of the load is made on the geometric edge representing the boundary between the axisymmetric and the plane domains, making the actual exchange surface used by the solver of difficult definition, as well as the assertion if the scaling adopted by the two solvers are effectively equivalent.

Such kind of set-up misalignments can justify the differences in predictions, considered however acceptable for the goal of these preliminary comparisons aimed at assessing the customized solver capabilities and the consistency of the non native modelling features introduced.

4.3 Aero-thermo-mechanical modelling assessment

Differently from the industrial standard methodology, an aero-thermo-mechanical approach avoids the need to infer gaps and clearances from the transient thermal analytical results, but the procedure is able to provide thermal and mechanical loads, in one overall simulation. Moreover an aero-thermo-mechanical approach comprised of both SAS and thermo-mechanical models can be profitably used to predict the impact of coupling between the multi-physical disciplines involved.

An example of such application consisting in a portion of the internal air system general arrangement of a large power generation gas turbine engine (call it *TE3*, Fig. 4.7), in its structure and its corresponding air fluid network, is here presented as a demonstration of the new tool capabilities.

Unlike the assessment of the solver features for the transient thermal calculation (Section 4.2), no reference codes analogous to the developed procedure are available for comparisons, since to the author knowledge similar procedure have been developed up to now only from OEMs in proprietary codes (reader can refer to the review in Chapter 1).

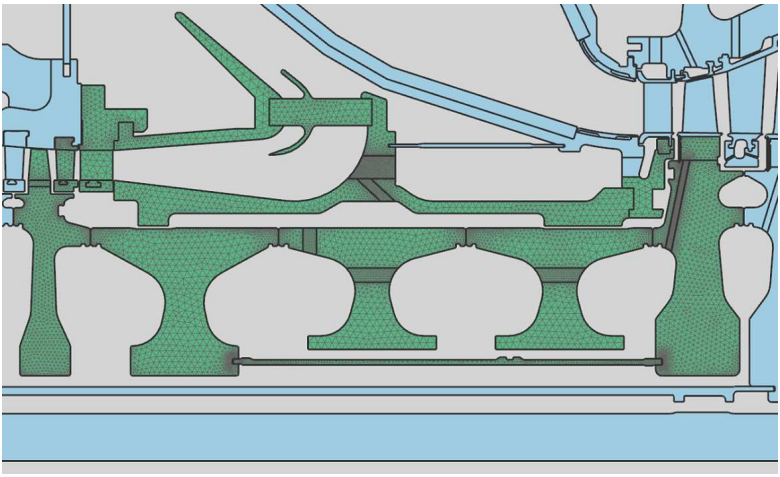

Figure 4.7: Location of the TE3 geometry in the FEM WEM arrangement.

Therefore two computations have been performed on the same model applying the uncoupled process based on one finalizing iteration and the methodology presented in this research activity. In the uncoupled approach, the gaps definition is set constant during the simulation and referring to cold geometry in order to stress in comparisons the effects of deformations, and mass flows and pressure conditions on the SAS side during the transient cycle are obtained from a previous solution of the corresponding fluid network. No iterations are performed between the SAS solution and the thermo-mechanical one, i.e. one finalizing iteration is applied. Differently, in the case run with the proposed methodology, computation monitor nodes are defined, with the aim to follow the clearances variation and define geometrical displacements which are then used to update the gaps values on the SAS model through the presented iterative approach.

This application has been proposed with the aim of assess the effect of incorporating the running clearances into the analysis, and the comparison

with the uncoupled methodology wants to emphasize the need for an integrated coupled approach by presenting the effect of mutual interactions between the air system and thermo-mechanical solution.

4.3.1 Test case description and model setting

A portion of the solid domain is extracted from the finite element model of a turbine engine (Fig. 4.7) and Fig. 4.8 shows the general arrangement used, composed of the part of the engine extending from the last stage of the compressor to the first stage rotor disk of the turbine, along the single shaft. The single-shaft configuration of the case is a disc-type rotor held up with a pre-stressed central tierod. Rotor discs are splinted together by radial facial serrations named hirth-couplings, which connect adjacent discs allowing the transmission of turbine torque to the compressor. As reader can see in Fig. 4.8b, the cooling air for the first stage vanes and blades is directly extracted at the compressor exit, specifically from the diffuser outlet and from a leakage flow from the last compressor stage.

As a representative case, the presented one has been chosen because of the presence of the main SAS devices (seals, preswirl components, cavities, channels) and a complete flow path of cooling/sealing air. From compressor seal regions, where the cooling flow is extracted for cooling of wheel spaces and for internal cooling of hot gas path components, the flow path along the shaft stops at the first turbine stage.

Between compressor exit and the first turbine stage, four seals are present (Fig. 4.8a). Monitoring the running behaviour of these parts is very important since higher the clearance value in these regions more is the cooling flow, and this can affect considerably the performance of the machine. On the other side, lower clearance values may cause interferences during the transient operation and may damage the seals, or reduce cooling flow with a detriment of the cooling system efficiency.

Although hydraulic diameter/gap and length of all SAS elements may be subject to variation due to heat transfer, however thermo-mechanical phenomena affect some elements more than others. Labyrinth seals are

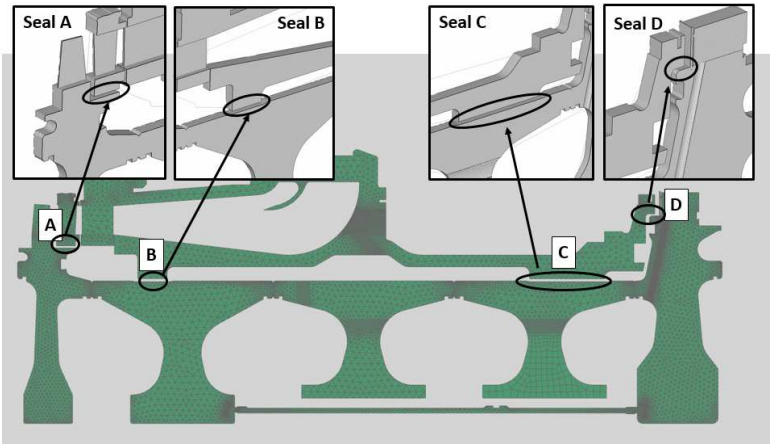

(a) Test case geometry.

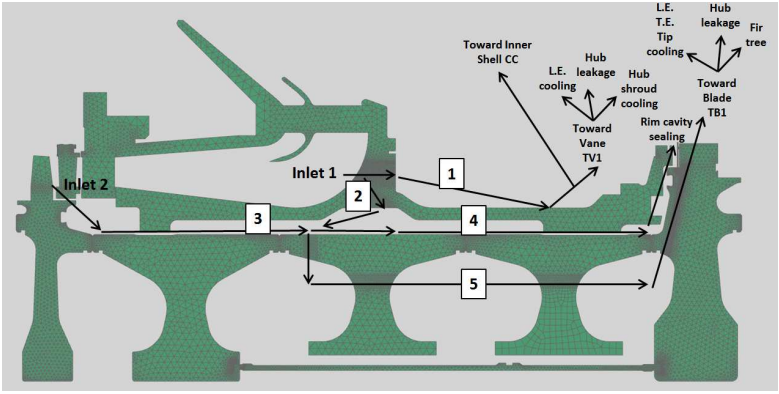

(b) Main flows repartition.

Figure 4.8: TE3 model features: geometry and SAS main flows.

in general especially impacted since seal gaps/clearances and material displacements are generally about the same order of magnitude [28]. The impact of thermal expansion on labyrinth seals is in general greater than on any other element, with a significant coupling effect. Seals control the amount of flow going in and out of the SAS circuit and therefore secondary air consumption. The accurate determination of the labyrinth geometrical definition as well as its evolution during engine operation for different load cases is crucial. Therefore, nevertheless the coupling method described is not to be restricted to labyrinth seals only and can be applied to other loss elements, the current application focuses specifically on labyrinth seals.

Therefore, in the test case, monitor points are placed in correspondence of the seals. The four seals regulating the flows are labelled with letter A,B,C,D moving from the left to the right of the model (Fig. 4.8a).

Regarding the SAS arrangement, a cross section of the main hardware components showing major cooling flow paths is given in Fig. 4.8b. Referring to that figure, cooling air from the compressor is bleed in its major amount from the diffuser (Inlet 1) and it is then spitted in one branch (1) collected towards the combustor (for the cooling of the inner shell), and towards the first stage nozzle of the turbine, for vane cooling; the other (2) is addressed to the preswirler through which enters the plenum between the shaft and the shaft cover, joining the leakage flow (3) from the last stage of the compressor (Inlet 2). The flows (2 and 3) merge and split again in one branch providing coolant to the rim cavity between rotor and stator (4), and the other (5) entering the shaft cavities and feeding the first stage blade of the turbine, providing cooling air to the bucket groove and further into the turbine blade.

The above described split characterize the main flows of the SAS aerodynamic model, but more complex distributions of flows are assigned in the thermal network (distinct from the previous one as explained in Section 2.2.5), by adopting in the thermal boundaries splits percentages of the main flows detected in the SAS aerodynamic network (Fig. 4.9).

Concerning the FEM setup, the solid model is axisymmetric and has

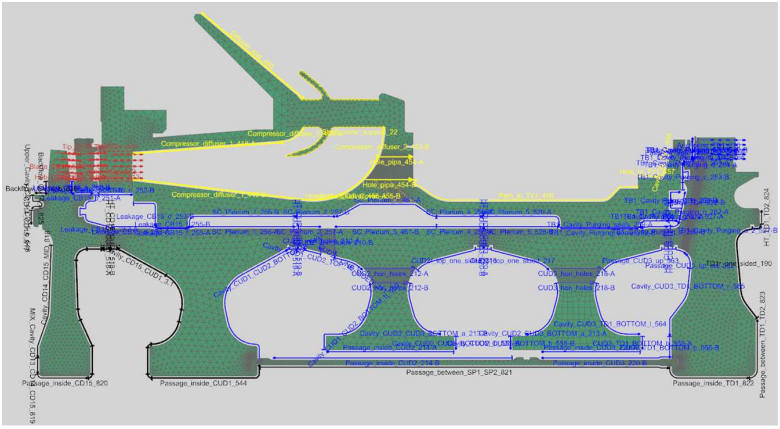

Figure 4.9: TE3 overall convective conditions whose mass flows are derived from the SAS aerodynamic solution.

been discretized into 14942 six nodes triangular elements with a total of 32133 nodes. Non-axisymmetric features such as holes and the blade are modelled using an equivalent thickness of plane elements. Structural constraints have been applied to the stator and rotor part, centrifugal loads have been imposed on the rotating one.

As a portion of solid domain extracted from the finite element model, it has been subjected to movements of the adjacent parts through the imposition of displacements boundary conditions, in particular for the inclusion of the axial trust of the adjacent components.

From the point of view of the conduction effects on the contact zones between the model and the rest of the FEM model, on the compressor side and on the turbine contacts between disks, the effect can be considered negligible since the adjacent part can be considered in each time step of the simulation at temperature levels very close the ones with the others. On the contrary, on the turbine interface between the first stage blade (not modelled) and the corresponding disk, explicit film conditions have been imposed such as to realize a realistic temperature trend on the blade

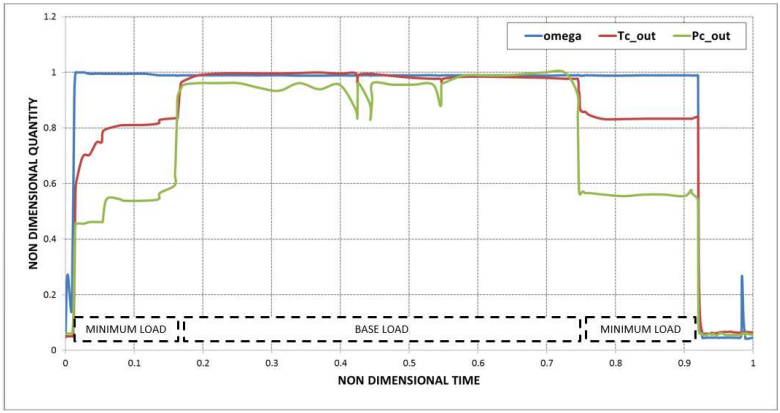

Figure 4.10: TE3 trends in time of rotational speed, temperature and pressure at the compressor exit. The extension in time of the main phases of the operation is highlighted in Figure.

anchoring during the entire operation.

The transient engine cycle is defined by specifying time evolution of a set of environmental parameters, such as annulus mass flow rate, annulus total pressure and temperature. In this application, we consider a representative cycle with two distinct regimes, minimum load and base load, separated by two couples of fast ramps of acceleration and deceleration, to reach the minimum load from the zero speed condition, and to pass from the minimum load to the base load, and vice versa in the descending phase toward the shutdown of the engine. Fig. 4.10 illustrates the engine cycle in terms of the angular speed and outlet temperature and pressure conditions of the compressor.

4.3.2 Discussion of results

The proposed assessment is focused on the effects of coupling of different physical disciplines on the transient prediction. As already explained, the aim is not the evaluation of the accuracy of the model

(requiring the availability of proprietary field data necessary for the model tuning and comparisons), but the purpose is to highlight the capability of the procedure of catching multi-physical interactions in the determination of the complex aero-thermo-mechanical phenomena inside the engine. Here below the main evidences in the comparison of the uncoupled and iterative coupled approaches are reported, considering displacements, mass flow rates and temperature variations.

Concerning the displacements analysis, in order to understand the deformations it is necessary to consider that rotating and stationary components are subjected to loads of different nature. The largest radial displacements are a result of the thermal distortions and centrifugal forces, whereas engine pressure and thrust are mainly responsible for axial translation. The uncoupled model assumes the dimension of the cold geometry constant during the calculation, whereas the iterative coupled process detects a significant variability of the gaps during the simulation, as shown in Fig. 4.11, where the differences in radial seals clearances predicted by the coupled approach are expressed as a percentage of the cold built clearances levels. In particular the major variation in radial clearance regards the seal D, located at the stator rotor interface of the first turbine stage, ranging from -16% to 24% of the cold conditions. Time histories of displacements together with related temperature predictions at the rotating and non-rotating sides of the seals, are also given in Figs. 4.12 and 4.13.

Fig. 4.11, 4.12 and 4.13 show that during the acceleration, there is an initial closure of the seals due to the fast centrifugal expansion of the rotor. Immediately after this, the seal reopens primarily because of the thermal growth (see details in Fig. 4.11b). This leads to the rapid under/overshot observed at the transition ramps. Specifically this behaviour occurs in each ramp of acceleration/deceleration, i.e. between zero velocity and minimum load, and between minimum load and base load, both in the startup and shutdown phases. When conditions tend to stabilize, the clearance gradually reduces reaching the stabilized value typical of each phase, at approximately non dimensional time $t_{nd} = 0.15$ (minimum load,

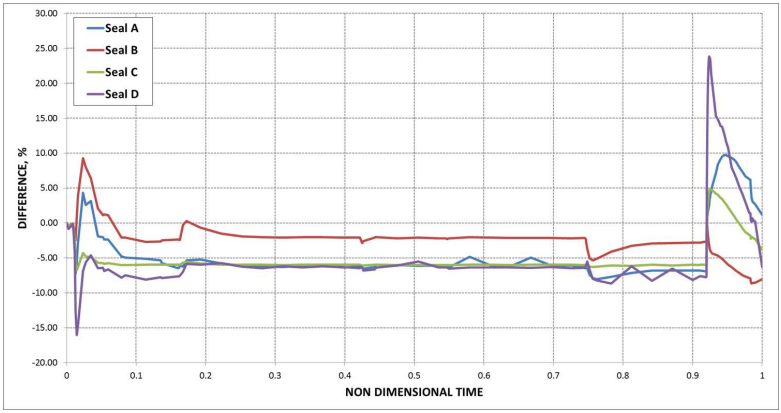

(a) Difference between cold built conditions and iterative coupled approach predictions of radial seal clearances in seals A, B, C, D in the whole time duration.

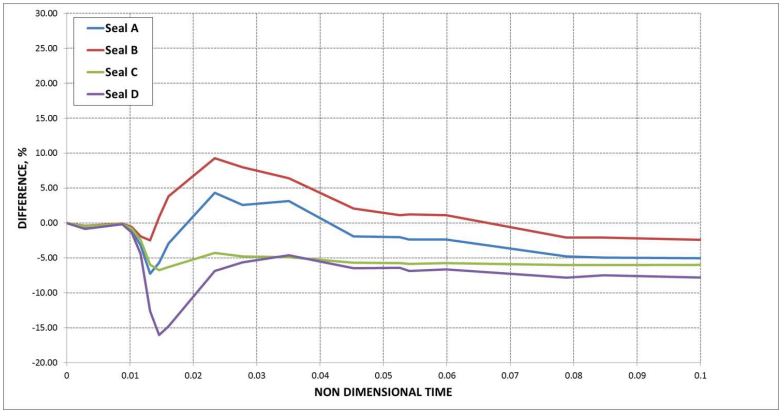

(b) Difference between cold built conditions and iterative coupled approach predictions of radial seal clearances in seals A, B, C, D - details of the startup phase.

Figure 4.11: Iterative coupled approach predictions of the radial seal clearances expressed as a percentage of the cold built levels.

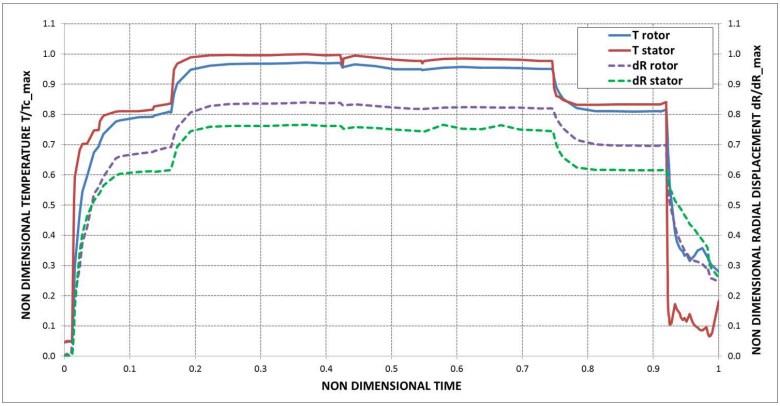

(a) Non dimensional temperature and displacement at seal A.

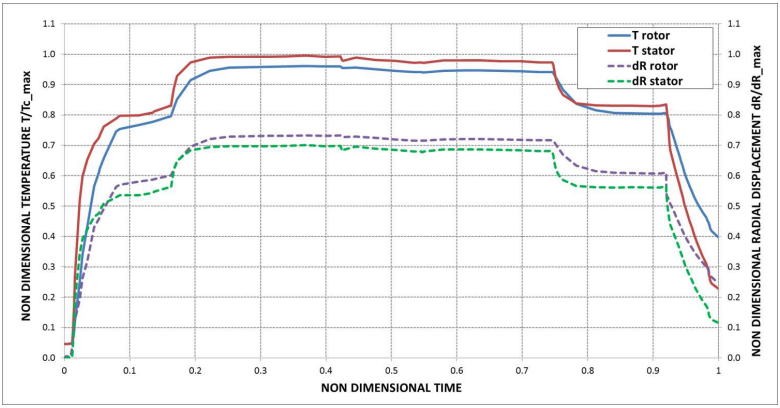

(b) Non dimensional temperature and displacement at seal B.

Figure 4.12: Temperature and displacement predictions on the rotor and stator walls normalized by maximum levels of outlet compressor temperature ($T_{c,max}$) and maximum radial displacements in seals (dR), respectively at inlet of the inner seal A (a) and at inlet of seal B (b).

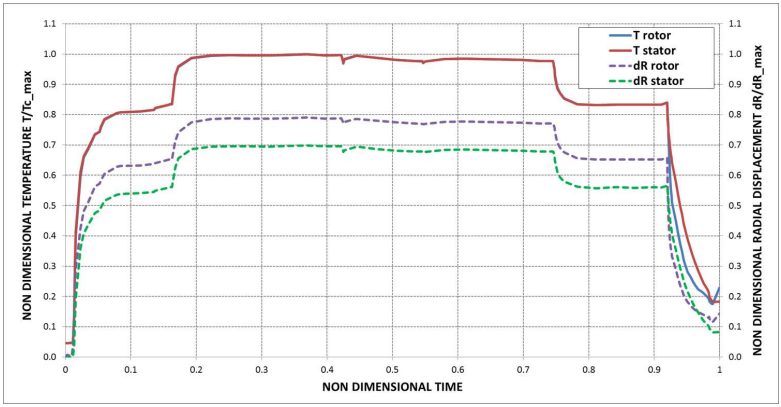

(a) Non dimensional temperature and displacement at seal C.

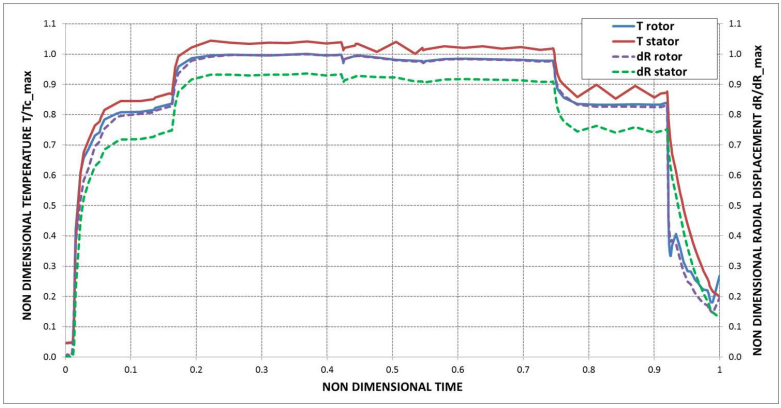

(b) Non dimensional temperature and displacement at seal D.

Figure 4.13: Temperature and displacement predictions on the rotor and stator walls normalized by maximum levels of outlet compressor temperature ($T_{c,max}$) and maximum radial displacements in seals (dR), respectively at inlet of the inner seal C (a) and at inlet of seal D (b).

startup phase), $t_{nd} = 0.5$ (base load), $t_{nd} = 0.7$ (minimum load, shutdown phase) respectively. On the other side, as mentioned, decelerations induce the opposite behaviour, with a fast over/undershot followed by a slow opening due to the rotor cooling. The response of each component occurs on a time scale related to several factors, such as rotation, thermal mass and heat-transfer coefficient, which explains the shift in picks of the gaps trends.

Model seals share the same trends, but seals C and D tend to assume values lower than those of the cold condition for almost the whole duration of the operation. In particular seals C and D reopen with values of gap higher then that of cold built condition only in the last descending ramp of the cycle, maintaining lower values for the rest of the operation. This leads to the reduction of the mass flow actually flowing in the plenum between shaft and cover shaft and feeding the rim cavity.

The reader is referred to Fig. 4.14 for a better visualization of the transient response and to appreciate the induced effect on the mass flow rates flowing through the seals. As shown, the flow is nearly a function of the corresponding seal radial clearance. The mass flow level increases or decreases with an augmentation or a reduction of the seal radial gap. In particular for the simulated cycle inspired by realistic conditions, the effect of the radial variations of the seal gaps is a reduction of the mass flow flowing through the seals for approximately all the operation, while the circuit around is quite insensible to these variations.

In Fig. 4.15 the induced effect on the mass flow rates flowing through the fluid network branches feeding the rim cavity and the vane and blade rows of the first stage of the turbine, is reported for stabilized conditions of the minimum load in startup phase, base load and minimum load in shutdown phase. The trend shown in the diagrams for the fluid branches providing coolant to vanes and blades, is characteristic not only of the chosen time points, but of the entire duration of the cycle. Indeed, approximatively the same negligible variations characterize the mass flows in branches feeding vanes and blades during the entire simulation, and the discrete three instants have been chosen for reasons of synthesis as a

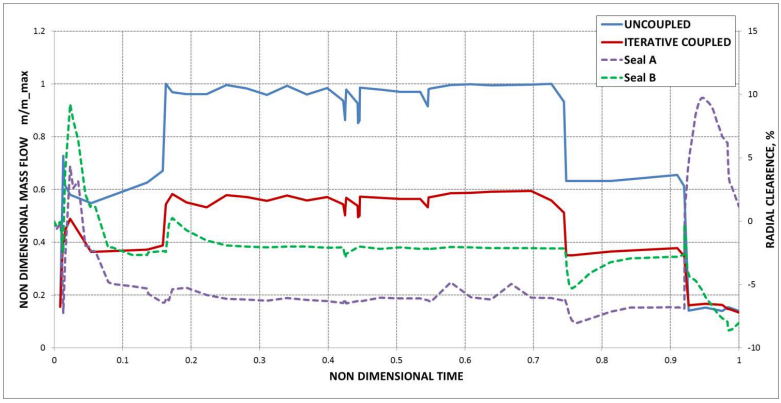

(a) Non dimensional mass flow rates and displacements at seal A and B.

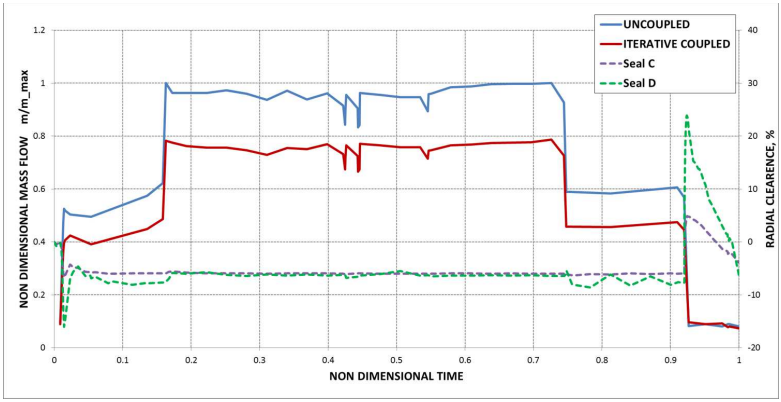

(b) Non dimensional mass flow rates and displacements at seal C and D.

Figure 4.14: Comparison of coolant flow rate through the labyrinth seal A, B, C, D. The flows are normalized by the respective value m_{max} corresponding to the steady state level of the uncoupled model. Radial seal clearance evolution as a percentage of the cold built levels are also shown for reference.

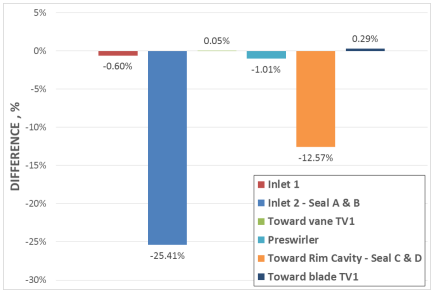

(a) Mass flow rates in the main fluid network branches at steady state minimum load - startup phase ($T_{nd} = 0.16$).

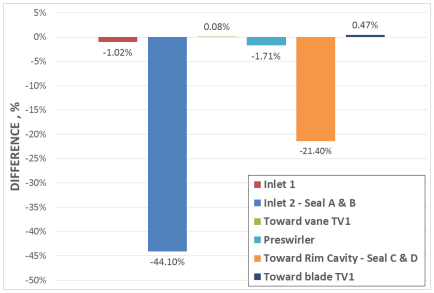

(b) Mass flow rates in the main fluid network branches at steady state base load ($T_{nd} = 0.72$).

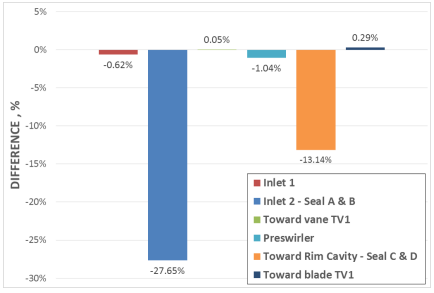

(c) Mass flow rates in the main fluid network branches at steady state minimum load - shutdown phase ($T_{nd} = 0.90$).

Figure 4.15: Comparison of coolant flow rate through the main fluid network branches. The differences ($m_{coupled} - m_{uncoupled}$) are normalized by the respective value m_{max} corresponding to the steady state level of the single branch in the uncoupled model.

demonstration of the very slight variations to which these sections of the fluid network are subjected.

This result can find its reason in the robustness of the machine in this part of the engine, and the efficient insulation from the thermal load of the hot part of the engine, shall ensure that the cooling flows toward blade and vanes are not actually influenced by the effect of the displacements of the seals of this region.

On the contrary, a significant effect of gaps variations is present on the cooling and purge flow toward the rim cavity, as a consequence of the approximatively continuous settlement on lower levels of seals gaps respect to the cold conditions.

The mass flow reduction affects the branch under the seals A and B for the whole transient operation, although an initial settlement of the corresponding gaps levels on higher values respect to the cold built one. This is a consequence of the downstream changes in gaps and pressure losses in the other parts of the circuit, causing an estimated cut of the mass flow rate under seals A and B of the 44% in steady state conditions (Fig. 4.15b). Anyway, the branch under seals A and B provides actually a little amount of air in all operating conditions, and therefore its variation on the overall system is of little impact.

Much more significant is the reduction of the mass flow rate toward the rim cavity which can reach the 21% in steady state conditions. Because of the modified pressure losses inside the circuit, a lower amount of mass flow is bleed from the compressor and this lack is transposed in the cut of the mass flow actually available for cooling and purging of the rotor stator cavity.

The variation in the mass flow to the rim cavity predicted by the iterative coupled approach, respect to the uncoupled model, could define two quite different scenarios in the definition of the lifespan of the adjacent hot components, according to the two different predictions. In particular the effect of the mass flow variation could be included in the blade flow function in order to determine if the corresponding variation in the pressure field around the blade, caused by the drop in the mass flow of

the rim cavity, could affect sensibly or not the hot component cooling. In addition, an other aspect to be evaluated should be the possible ingestion of hot gases due to the reduction of the purging flow, which could lead to a heavy detriment of the components lifespan.

Therefore, results provided by the iterative coupled approach potentially provide relevant information for deeper investigations about the most suitable design choices, in the specific case about efficiency characterizing the cooling system of the blade and the local phenomena of heat transfer in the cavity.

Regarding coupling effects on the transient metal temperature, predictions have been monitored and compared in particular at the seals passages and on the top of the turbine disk. The differences between time histories of the coupled and the uncoupled metal temperature predictions expressed as a percentage of the maximum level of the outlet compressor temperature ($T_{c,max}$) are given in Fig.s 4.16 and 4.17 for the labyrinth seals and in Fig. 4.18 for the blade anchoring region.

Throughout the cycle fairly coincident metal temperature histories are observed for uncoupled and iterative coupled approaches at seals locations. This is due to the fact that the driving parameter in the heat transfer in this part of the engine is the outlet compressor temperature which dominates almost the whole domain, heating and cooling model components. Due to the robustness of the machine in this region, variations in the mass flow rate feeding the rim cavity, produce slight metal temperature changes on seals components (Fig.s 4.16 and 4.17).

Only on the first turbine disk the effect of thermal gradients (result of the hot gas side thermal loads) is more significant, and in that region the effect of the change in the mass flow rate of coolant feeding the rim cavity produces an appreciable variation in the two predictions. The variation on the maximum value of the predicted temperature on the blade anchoring region is quite slight (around 1.5%, approximatively 8.5 K) but the general variation of the temperature on the base load phase can reach the 4.5% (Fig. 4.18).

Again these estimations could drive preliminary design choices and

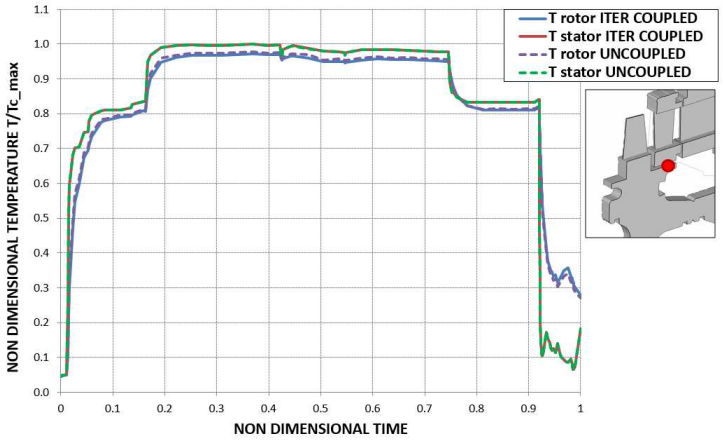

(a) Non dimensional temperature on seal A components.

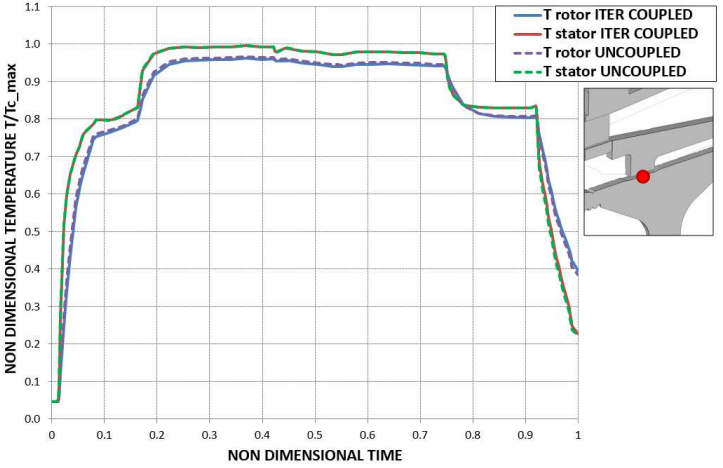

(b) Non dimensional temperature on seal B components.

Figure 4.16: Difference between the coupled and uncoupled analyses temperature predictions at seals A and B on rotor and stator components. Temperature are normalized respect to the maximum level of the outlet compressor temperature ($T_{c,max}$).

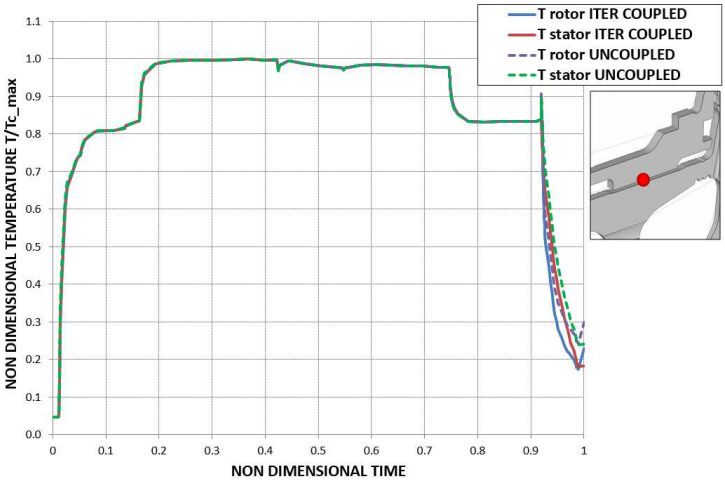

(a) Non dimensional temperature on seal C components.

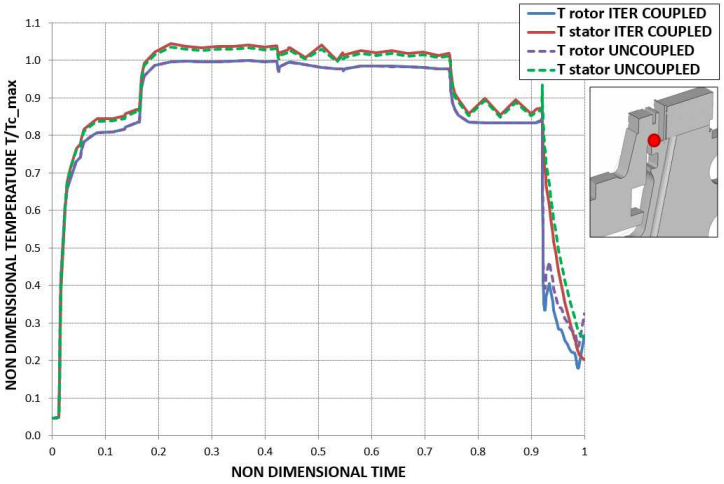

(b) Non dimensional temperature on seal D components.

Figure 4.17: Difference between the coupled and uncoupled analyses temperature predictions at seals C and D on rotor and stator components. Temperature are normalized respect to the maximum level of the outlet compressor temperature ($T_{c,max}$).

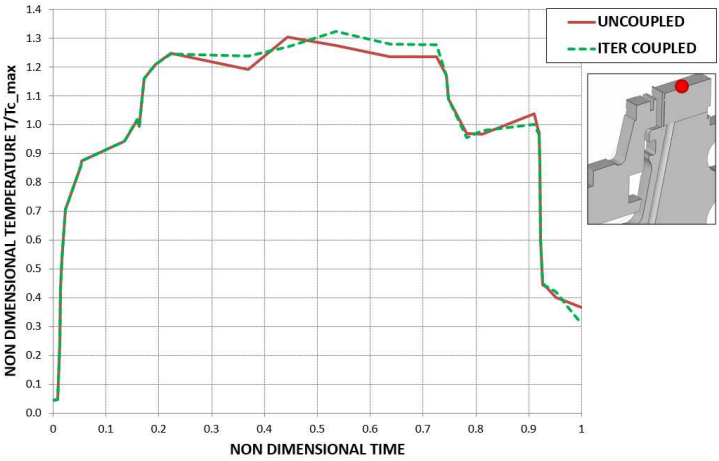

Figure 4.18: Difference between the coupled and uncoupled analyses temperature predictions at the blade anchoring region. Temperature are normalized respect to the maximum level of the outlet compressor temperature ($T_{c,max}$).

trace the path for more accurate investigations about the temperature variation in the seal cavity and at the blade anchoring, for the examined case. Further analyses could be performed with specific calculations addressed to catch those local phenomena, for instance the complex flow structures that can be generated in the cavity or around the blade due to the mass flow reduction, which can not be appreciated by the 1D fluid network model and which could lead to different levels of thermal loads (especially HTCs) hardly to predict with a simplified correlative approach.

Anyway, beyond the local level of accuracy not subject of the present assessment, the highlighted aspects of differentiations among the uncoupled approach and the iterative coupled methodology are a result of the strong interaction between aero-thermo-mechanical fields, which the new methodology demonstrated to be able to represent. Results prove the coupling capability of the procedure, able to capture the effect of running

clearances on the secondary air system properties and, more in general, on the thermo-mechanical state of the analysed domain, showing to be consistent with the involved physical phenomena.

Conclusions

Due to the changes in operating conditions, multi-physics investigations, typically adopted in aero-engines development, have become recently of great interest also for gas turbine engine manufacturers. Indeed, nowadays large power generation gas turbine have to face more and more frequent fast startups and shutdowns which are needed to satisfy the variability of the electricity demand, due to the introduction of renewable sources in the energy market. This imposes very frequent part load operations requiring the assessment of the transient thermo-mechanical status of the engine and its consequent effect on steady state conditions. Simulations able to account multiple coupled physics constraints and interactions between fluid network and solid domain in terms of thermal loads, seal running clearances and SAS properties, are need to properly satisfy the design and analysis goals, allow more accurate lifing predictions, and minimize efficiency impacts at part loads.

In particular the effect of running clearances in transient operations, with the consequent redefinition of the flow passages and gaps, can affect considerably the performance of the machine and the efficiency of the cooling system. Indeed the fluid-solid coupling in the properties evaluation of the engine internal SAS is strong, the structure may deform significantly between different operating regimes of the machine, and this interaction is thought to be fundamental to the prediction of the real behaviour of the engine in the transient areas. Thus, the effects of metal deformation due to centrifugal, pressure and thermal loads on aero-thermal state must be included in a the thermo-mechanical analysis. All

the major cooling flows are reciprocally dependent and strongly affected by modifications in the SAS geometry such as the labyrinth seals clearances and the rim seal gaps. If this strong coupling is not considered, the final temperature distributions on the engine has to be accounted considering higher uncertainty, which traduces in the introduction of higher safety margins in the engine design, both for components life prediction and for cooling and purge air consumption.

This work deals with a numerical methodology for the evaluation of the transient aero-thermo-mechanical status of a whole engine, developed in collaboration with Ansaldo Energia. The new procedure is developed for the specific study of large power generation gas turbine, with the modelling of the entire cross section referred to the *Whole Engine Model* (*WEM* approach). The computational methodology consists of a coupled analysis of a 1D flow network model of air engine secondary air system and a 2D axisymmetric solid thermo-mechanical finite element model of engine components. Strong coupling is achieved through iterations over the transient cycle, based on the successive solutions of the fluid and the solid sub-problems. In particular, the one-dimensional aerodynamic calculations yielding mass flows and pressures, and the 2D axisymmetric thermo-mechanical analysis providing temperatures and displacements are performed separately, with the main purpose of maintaining distinct the levels of discretization and complexity of each network (aerodynamic and thermal) used in the solution of the SAS and themo-mechanical analyses. The iterative process aims at taking into consideration the mutual interaction of the different solutions, in a robust and modular design and analysis tool, combining secondary air system, thermal and mechanical analyses. The heat conduction in the solid and the fluid-solid heat transfer is estimated by a customized version of the open source CalculiX® FEM solver. The secondary air system is modeled by a customized version of the native CalculiX® one-dimensional fluid network solver. The unsteady heat transfer calculation over the solid domain is coupled to a sequence of structural static and steady flow problems using a quasi-steady state approach. In particular, due to the convective time scale

much lower than the solid diffusive one, it is possible to assume that the influence of unsteadiness in the fluid domain is negligible and as a result, the flow field may be considered as a sequence of steady states. Secondary air system aerodynamic solution is performed standalone starting from cold condition over the transient cycle, contrary to the standard industrial practice based indeed on the execution of the SAS analysis at base load conditions with a subsequent scaling of the mass flow rates and pressures obtained, as a function primarily of rotational speed and power. The new procedure allows for the determination of pressure and mass flow distributions (whose splits can change in transient operation respect to the steady conditions) as a function of the heat transfer and geometry deformations encountered by the model in each considered time step. Main flow thermal loads and SAS fluid properties are imposed as boundary conditions in the whole engine CalculiX® FEM model containing solid and fluid meshes. Metal-fluid temperatures and structural deformations are computed in the thermo-mechanical calculation, post-processed and then used to update the geometries and temperature levels in the secondary air system fluid network. The iterative loop involving SAS and thermo-mechanical calculations is performed until a converged solution is reached.

The development of the procedure first has implied a customization of both the FEM and 1D fluid network solvers of the open source code CalculiX® . The code has been specifically tailored for turbo-machinery applications, and provides a wide range of specialist thermal modelling capabilities introduced through dedicated implementations. Modifications introduced aimed primary at the improvement of original capabilities of the solvers, at the introduction of new features and models need for WEM applications, and at the customisation of the code to meet the requirements of the industrial practice. The new capabilities have been assessed in a summary test cases included in the present work. The simplified geometry representative of a real engine compressor arrangement have been tested under transient conditions for the evaluation of the physical coherence of the new features implemented for the thermal transient modelling, and results have been compared with a reference FEM solver. The customized

code proved to be coherent with the physics of the problem and in good agreement with the reference FEM code. Also some of the more general new capabilities have been shared with the CalculiX® developers. Deemed of common utility, some new implementations have been included in the official releases. The idea in the code development is to share the more general aspects of innovation and remain aligned as much as possible with the official releases for a profitable overall improvement of the code.

Downstream the additional implementations for the transient thermal modelling and the respective assessment, efforts have been addressed to the definition of the strategy presented for the coupling of SAS and thermo-mechanical analyses, for a proper catching of boundary conditions variations in view of fluid-solid heat transfer and solid domain deformations.

The consistency of the coupled methodology described has been demonstrated in the present work with its application to a portion of the internal air system of a general arrangement of a large power generation gas turbine engine, extracted from a more large finite element model of the engine. The test case is composed of the part of the engine extending from the last stage of the compressor to the first stage rotor disk of the turbine, with the presence of the main typical SAS devices (seals, preswirl components, cavities, channels) and the complete flow path of cooling/sealing air, from compressor seal regions where the cooling flow is extracted, up to the first turbine stage. The model has been tested under a realistic transient operation cycle with two distinct regimes, minimum load and base load, separated by two couples of fast ramps of acceleration and deceleration. Two computations have been performed on the same model using the conventional uncoupled approach applying constant gaps definitions and one finalizing iteration, and the proposed methodology, with computation monitor nodes defined on seals, following the clearances variation and geometrical changes, used then to update the gaps values on the SAS model. Comparisons of the results of the two procedures reveal non negligible variations of the fluid properties detected by the proposed methodology respect to levels predicted by the uncoupled procedure, especially in terms

of cooling and purging mass flow feeding the rim cavity of the model for the analysed test case. These evidences attest the capability of the proposed methodology to catch coupling aero-thermo-mechanical interactions, showing its consistency with the involved physical phenomena.

A transient air system-thermomechanical WEM procedure and its thermal and aero-thermo-mechanical assessments are presented in this work, showing its physical coherence and consistence, and highlighting the need for an integrated coupled approach by presenting the effect of mutual interactions between the air system and the thermo-mechanical solution for WEM applications. Traditionally unmodelled interactions of solid and fluid domains in the conventional analysis techniques, can be catch with the proposed iterative coupled approach, for an efficient prediction of levels of local gaps, flow rates and temperatures during the transients in engine operation, whose variability was previously attributed to the modelling uncertainties. Coupled aero-thermo-mechanical analysis constitutes an improved multi-physics approach both for the design and the analysis of the Secondary Air System of gas turbine engines, as an instrument for the preliminary design choices and for the assessment of the behaviour of the engine in different ambient and off design operating conditions. Research novelty lies also in the application of such improved interdisciplinary approach to the industrial practice for large power generation gas turbines design and in the will of follows this path through the application of an open source code, whose improvements, beyond certain limits imposed by confidential reasons on some strategical aspects, can be shared with a scientific and user community for the pursuit of the development of a fast, reliable, multi-physics and multitasking code.

Future developments of the procedure will regard the improvement of some open issues of detail regarding a more flexible management of user boundary conditions, optimization of the solution strategy of the system of equations according to the boundary conditions assigned, and others. In addition further development will be aimed at performing a wide review and analysis of simulations results in which the procedure has been recently applied and still ongoing, performed on realistic industrial configurations,

for further assessments and improvements of the methodology capabilities. Future steps will be aimed at qualifying more broadly the new procedure for productive use, not only as an analysis tool but also as an instrument for the design and the respective optimization, thank to the information that an efficient modelling of aero-thermal-mechanical response in fluid-structure systems can add in simulating the transient engine behaviour.

List of Figures

List of Tables

Bibliography

[1] Garg, Vijay Kumar and Gaugler, Raymond E. "Effect of velocity and temperature distribution at the hole exit on film cooling of turbine blades." *Journal of Turbomachinery*, 119(2):343–351, 1997.

[2] Barringer, Michael, Coward, Andrew, Clark, Ken, Thole, Karen A, Schmitz, John, Wagner, Joel, Alvin, Mary Anne, Burke, Patcharin, and Dennis, Rich. "The design of a steady aero thermal research turbine (start) for studying secondary flow leakages and airfoil heat transfer." *ASME Paper No. GT2014-25570*, 2014.

[3] PW Power Systems and Pratt & Whitney . Internet websites www.pwps.com for PW Power Systems (a group company of mitsubishi heavy industries, ltd.) and www.pw.utc.com for Pratt & Whitney (a united technologies company)., 2014.

[4] Childs, Peter. "Gas turbine engine internal air systems." 2006.

[5] Błachnio, Józef and Pawlak, Wojciech Izydor. "Damageability of gas turbine blades–evaluation of exhaust gas temperature in front of the turbine using a non-linear observer." 2011.

[6] Reyhani, Majid Rezazadeh, Alizadeh, Mohammad, Fathi, Alireza, and Khaledi, Hiwa. "Turbine blade temperature calculation and life estimation-a sensitivity analysis." *Propulsion and power Research*, 2 (2):148–161, 2013.

[7] Mear, L Isobel, Owen, J Michael, and Lock, Gary D. "Theoretical model to determine effect of ingress on turbine disks." *Journal of Engineering for Gas Turbines and Power*, 138(3):032502, 2016.

[8] Micio, M. *Gas turbine secondary air system: experimental analysis and design tools developing.* PhD thesis, Università degli Studi di Firenze, Dipartimento di Energetica Sergio Stecco, 2009.

[9] Dixon, Jeffrey A, Valencia, Antonio Guijarro, Coren, Daniel, Eastwood, Daniel, and Long, Christopher. "Main annulus gas path interactions—turbine stator well heat transfer." *ASME Turbo Expo, No. GT2012-68588*, 2012.

[10] Young, C. "Fluid flow and heat transfer within the rotating internal cooling air system of gas turbines (icas-gt2)." *Rolls-Royce document*, 2002.

[11] Muller, Yannick. "Secondary Air System Model for Integrated Thermomechanical Analysis of a Jet Engine." *Proceedings of ASME Turbo Expo 2008: Power for Land, Sea, and Air*, Paper No. GT2008-50078, 2008.

[12] Chati, Yashovardhan S and Balakrishnan, Hamsa. Aircraft engine performance study using flight data recorder archives. In *Proceedings of the Aviation Technology, Integration, and Operations Conference*, 2013.

[13] Koli, Bharat R. *CFD investigation of a switched vortex valve for cooling air flow modulation in aeroengine.* PhD thesis, © Bharat Ramesh Koli, 2015.

[14] Lattime, Scott B and Steinetz, Bruce M. *Turbine engine clearance control systems: current practices and future directions.* National Aeronautics and Space Administration, Glenn Research Center, 2002.

[15] Hamed, Awatef A, Tabakoff, Widen, and Wenglarz, Richard. "Erosion, deposition, and their effect on performance." *Turbine Aerodynamics, Heat Transfer, Materials, and Mechanics*, page 585, 2014.

[16] Chapman, Jeffryes W, Kratz, Jonathan, Guo, Ten-Huei, and Litt, Jonathan. Integrated turbine tip clearance and gas turbine engine simulation. In *52nd AIAA/SAE/ASEE Joint Propulsion Conference*, page 5047, 2016.

[17] Melcher, Kevin J. "Controls considerations for turbine active clearance control." 2004.

[18] Balling, Lothar. "Fast cycling and rapid start-up: new generation of plants achieves impressive results." *Modern power systems. San Francisco CA*, 31(1):35–41, 2011.

[19] Sorce, A. Combined cycle flexibility solution, www.tpg.unige.it, 2016.

[20] IEA, International Energy Agency. www.iea.org, 2016.

[21] GE Power. www.gepower.com, 2017.

[22] IEEE Org. www.spectrum.ieee.org, 2012.

[23] Kim, JH, Song, TW, Kim, TS, and Ro, ST. "Model development and simulation of transient behavior of heavy duty gas turbines." *ASME Journal of engineering for gas turbines and power*, 123(3):589–594, 2001.

[24] Rolls-Royce. www.rolls-royce.com.

[25] Nielsen, Annette E, Moll, Christoph W, and Staudacher, Stephan. "Modeling and validation of the thermal effects on gas turbine transients." *ASME Journal of Engineering for Gas Turbines and Power*, 127(3):564–572, 2005.

[26] Chew, John W. and Hills, Nick. "Computational fluid dynamics and virtual aeroengine modelling." *Proceedings of the Institution of Mechanical Engineers, Part C: Journal of Mechanical Engineering Science*, 223(12):2821 – 2834, 2009.

[27] Giuntini, Sabrina, Andreini, Antonio, Facchini, Bruno, Mantero, Marco, Pirotta, Marco, Olmes, Sven, and Zierer, Thomas. Transient thermal modelling of whole gt engine with a partly coupled fem-fluid network approach. In *ASME Turbo Expo 2017: Turbomachinery Technical Conference and Exposition*, pages V05BT15A026–V05BT15A026. American Society of Mechanical Engineers, 2017.

[28] Muller, Yannick. "Integrated Fluid Network-Thermomechanical Approach for the Coupled Analysis of a Jet Engine." *Proceedings of ASME Turbo Expo 2009: Power for Land, Sea, and Air*, Paper No. GT2009-59104, 2009.

[29] Andrei, Luca, Andreini, Antonio, Facchini, Bruno, and Winchler, Lorenzo. "A decoupled cht procedure: application and validation on a gas turbine vane with different cooling configurations." *Energy Procedia*, 45:1087–1096, 2014.

[30] Sun, Zixiang, Chew, John W, Hills, Nicholas J, Volkov, Konstantin N, and Barnes, Christopher J. "Efficient Finite Element Analysis/-Computational Fluid Dynamics Thermal Coupling for Engineering Applications." *ASME Journal of turbomachinery*, 132(3):031016, 2010.

[31] Bohn, Dieter, Ren, Jing, and Kusterer, Karsten. "Conjugate Heat Transfer Analysis for Film Cooling Configurations With Different Hole Geometries." *Proceedings of ASME Turbo Expo 2003: Power for Land, Sea, and Air*, Paper No. GT2003-38369, 2003.

[32] Lin, Gang, Kusterer, Karsten, Ayed, Anis Haj, Bohn, Dieter, and Sugimoto, Takao. "Conjugate Heat Transfer Analysis of Convection-cooled Turbine Vanes Using γ-Reθ Transition Model." *International Journal of Gas Turbine, Propulsion and Power Systems*, 6(3), 2014.

[33] Okita, Yoji and Yamawaki, Shigemichi. "Conjugate Heat Transfer Analysis of Turbine Rotor-Stator System." *Proceedings of ASME*

Turbo Expo 2002: Power for Land, Sea, and Air, Paper No.GT2002-30615, 2002.

[34] Kassab, A., Divo, E., Heidmann, J., Steinthorsson, E., and Rodriguez, F. "BEM/FVM conjugate heat transfer analysis of a three-dimensional film cooled turbine blade." *International Journal of Numerical Methods for Heat & Fluid Flow*, 13(5):581–610, 2003.

[35] Ganine, Vlad, Hills, Nick, Miller, Matt, Barnes, Chris, Curzons, Steve, Turner, Lynne, and Smout, Peter. "Implicit Heterogeneous 1D/2D Coupling for Aero-Thermo-Mechanical Simulation of Secondary Air Systems." *Proceedings of ASME Turbo Expo 2015: Turbine Technical Conference and Exposition*, Paper No. GT2015-43406, 2015.

[36] Illingworth, Justin B, Hills, Nicholas J, and Barnes, Christopher J. "3D Fluid-Solid Heat Transfer Coupling of an Aero Engine Pre-Swirl System." *Proceedings of ASME Turbo Expo 2005: Power for Land, Sea, and Air*, Paper No. GT2005-68939, 2005.

[37] Javiya, Umesh, Chew, John, Hills, Nick, Dullenkopf, Klaus, and Scanlon, Timothy. "Validation of CFD and Coupled Fluid-Solid Modelling for a Direct Transfer Pre-Swirl System." *Proceedings of ASME Turbo Expo 2012: Turbine Technical Conference and Exposition*, Paper No. GT2012-69056, 2012.

[38] Kumar, BG Vinod, Chew, John W, and Hills, Nicholas J. "Rotating Flow and Heat Transfer in Cylindrical Cavities With Radial Inflow." *ASME Journal of Engineering for Gas Turbines and Power*, 135(3): 032502, 2013.

[39] May, David, Chew, John W, and Scanlon, Timothy J. "Prediction of Deswirled Radial Inflow in Rotating Cavities With Hysteresis." *ASME Journal of Turbomachinery*, 135(4):041025, 2013.

[40] Sun, Zixiang, Chew, John W, Hills, Nicholas J, Barnes, Christopher J, and Valencia, Antonio Guijarro. "3D Coupled Fluid-Solid Thermal

Simulation of a Turbine Disc Through a Transient Cycle." *Proceedings of ASME Turbo Expo 2012: Power for Land, Sea, and Air*, Paper No. GT2012-68430, 2012.

[41] Ganine, Vlad, Javiya, Umesh, Hills, Nick, and Chew, John. "Coupled Fluid-Structure Transient Thermal Analysis of a Gas Turbine Internal Air System With Multiple Cavities." *ASME Journal of Engineering for Gas turbines and Power*, 134(10):102508, 2012.

[42] Javiya, Umesh, Chew, John, Hills, Nick, and Scanlon, Timothy. "Coupled FE–CFD thermal analysis for a cooled turbine disk." *Proceedings of the Institution of Mechanical Engineers, Part C: Journal of Mechanical Engineering Science*, 229(18):3417 – 3432, 2015.

[43] Altuna, Arnau, Chaquet, Jose M, Corral, Roque, Gisbert, Fernando, and Pastor, Guillermo. "Application of a Fast Loosely Coupled Fluid/Solid Heat Transfer Method to the Transient Analysis of Low-Pressure-Turbine Disk Cavities." *Proceedings of ASME Turbo Expo 2013: Power for Land, Sea, and Air*, Paper No. GT2013-95426, 2013.

[44] Alizadeh, Mohammad, Izadi, Ali, and Fathi, Alireza. "Sensitivity analysis on turbine blade temperature distribution using conjugate heat transfer simulation." *Journal of Turbomachinery*, 136(1):011001, 2014.

[45] Nouri, B and Kuhhorn, A. Automated cae process for thermo-mechanical lifing prediction of a parameterized turbine blade with internal cooling. In *Proceedings of 5th European Conference on Computational Fluid Dynamics ECFD VI*, 2014.

[46] Dixon, JA, Verdicchio, JA, Benito, D, Karl, A, and Tham, KM. "Recent developments in gas turbine component temperature prediction methods, using computational fluid dynamics and optimization tools, in conjunction with more conventional finite element analysis techniques." *Proceedings of the Institution of Mechanical Engineers, Part A: Journal of Power and Energy*, 218(4):241–255, 2004.

[47] Reddy, Vishnu Vardhan, Selvam, Kathiravan, and De Prosperis, Roberto. "Gas Turbine Shutdown Thermal Analysis and Results Compared With Experimental Data." *Proceedings of ASME Turbo Expo 2016: Power for Land, Sea, and Air*, Paper No. GT2016-56601, 2016.

[48] Ganine, Vlad, Amirante, Dario, and Hills, Nicholas J. "Aero-Thermo-Mechanical Modelling and Validation of Transient Effects in a High Pressure Turbine Internal Air System." *Proceedings of ASME Turbo Expo 2016: Power for Land, Sea*, Paper No. GT2016-57739, 2016.

[49] Lück, Hannes, Schäfer, Michael, and Schiffer, Heinz-Peter. "Simulation of Thermal Fluid-Structure Interaction in Blade-Disc Configuration of an Aircraft Turbine Model." *Proceedings of ASME Turbo Expo 2014: Power for Land, Sea, and Air*, Paper No. GT2014-26316, 2014.

[50] Peschiulli, Antonio, Coutandin, Daniele, Del Cioppo, Marco, and Damasio, Massimo. "Development of a Numerical Procedure for Integrated Multidisciplinary Thermal-Fluid-Structural Analysis of an Aeroengine Turbine." *Proceedings of ASME Turbo Expo 2009: Power for Land, Sea, and Air*, Paper No. GT2009-59875, 2009.

[51] Tondello, Guilherme, Boruszewski, Wolodymir, Mengele, Fernando, Assato, Marcelo, Shimizu, Silvio, and Ziegler, Shayne. Coupled simulation of the secondary air flow, heat transfer, and structural deflection of a gas turbine engine. In *Proceedings of ASME Turbo Expo*, 2012.

[52] Dhondt, Guido. "Calculix crunchix user's manual version 2.11." 2016.

[53] Royce, Rolls. *The jet engine*. John Wiley & Sons, 2015.

[54] El Ella, HM Abo, Sjolander, SA, and Praisner, TJ. "Effects of an upstream cavity on the secondary flow in a transonic turbine cascade." *Journal of Turbomachinery*, 134(5):051009, 2012.

[55] Dhondt, Guido. *The Finite Element Method for Three-Dimensional Thermomechanical Applications*. John Wiley & Sons, 2004.

[56] Gimenez, G, Errera, M, Baillis, D, Smith, Y, and Pardo, F. "A coupling numerical methodology for weakly transient conjugate heat transfer problems." *International Journal of Heat and Mass Transfer*, 97:975–989, 2016.

[57] Ganine, V, Hills, NJ, and Lapworth, BL. "Nonlinear acceleration of coupled fluid–structure transient thermal problems by anderson mixing." *International Journal for Numerical Methods in Fluids*, 71 (8):939–959, 2013.

[58] Bohn, Dieter and Gier, Jochen. "The effect of turbulence on the heat transfer in closed gas-filled rotating annuli." *ASME Journal of Engineering for Gas Turbines and Power*, 120(4):824–830, 1998.

[59] Giuntini, Sabrina, Andreini, Antonio, Cappuccini, Giulio, and Facchini, Bruno. "Finite element transient modelling for whole engine-secondary air system thermomechanical analysis." *Energy Procedia*, 126:746–753, 2017.